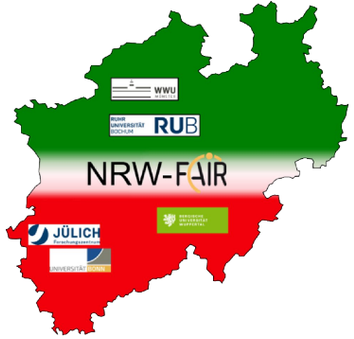

Production Mechanism Studies in pp → NNπ: Comparison with SMASH

VIII HADES physics analysis meeting 2026

***Saket Kumar Sahu*[1,2]**
[1]Ruhr University Bochum
[2]GSI Helmholtzzentrum für Schwerionenforschung GmbH

RUHR UNIVERSITÄT BOCHUM RUB

HADES

Why N* and Δ?

- “They are the simplest system to understand the **non-Abelian nature** of QCD”[1].

1.N. Isgur, in: V. Burkert, L. Elouadrhiri, J. Kelly, R.M. (eds.) (Eds.), NSTAR2000: Excited Nucleons and Hadronic Structure, Newport News, USA, 2000, pp. 422–445, arXiv:nucl-th/0007008.
2.Volker Burkert, Gernot Eichmann, Eberhard Klempt,Progress in Particle and Nuclear Physics, Volume 146, Part 2,2026, https://doi.org/10.1016/j.ppnp.2025.104214.

Why N* and Δ?

- "They are the simplest system to understand the **non-Abelian nature** of QCD"[1].
- Understanding **the production mechanisms and dynamical behavior** of these resonances is a key objective of this study.
- What is the relationship between **dynamically generated resonances** and **quark-model states**[2]?

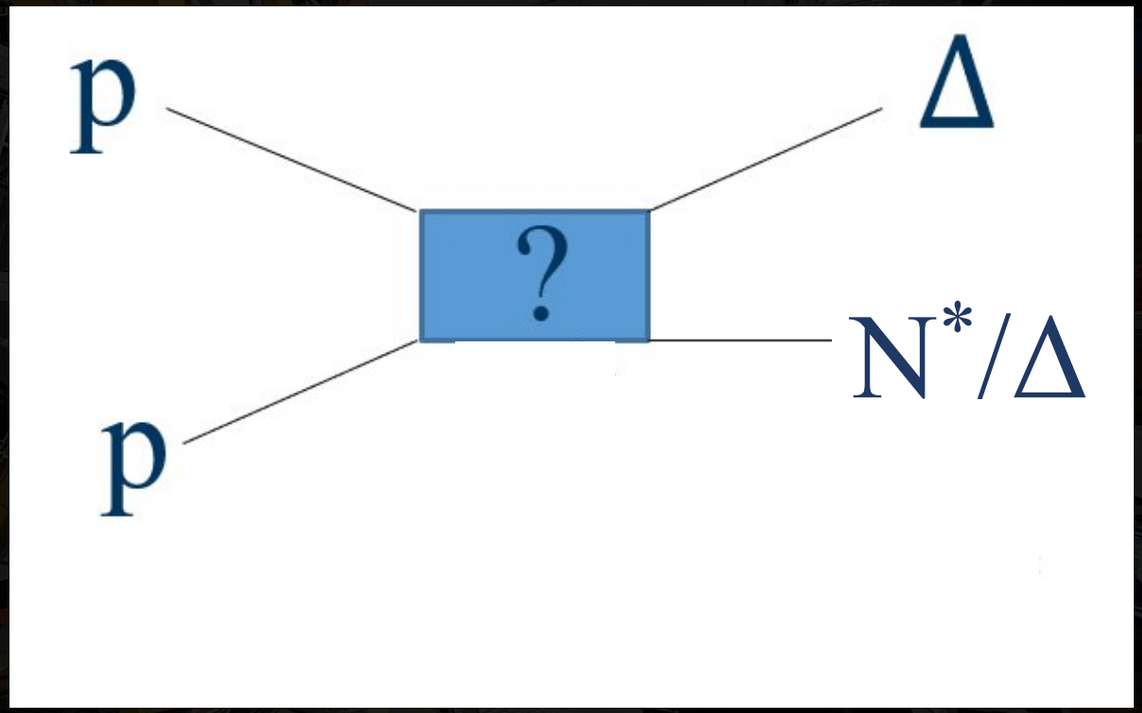

1.N. Isgur, in: V. Burkert, L. Elouadrhiri, J. Kelly, R.M. (eds.) (Eds.), NSTAR2000: Excited Nucleons and Hadronic Structure, Newport News, USA, 2000, pp. 422–445, arXiv:nucl-th/0007008.
2.Volker Burkert, Gernot Eichmann, Eberhard Klempt,Progress in Particle and Nuclear Physics, Volume 146, Part 2,2026, https://doi.org/10.1016/j.ppnp.2025.104214.

Towards Studying the Electromagnetic Properties of Light Baryons

- **Production mechanisms** and **reaction dynamics** of N* and Δ states in $pp \rightarrow NN\pi$ provide access to their **electromagnetic structure** through **dilepton decays**.

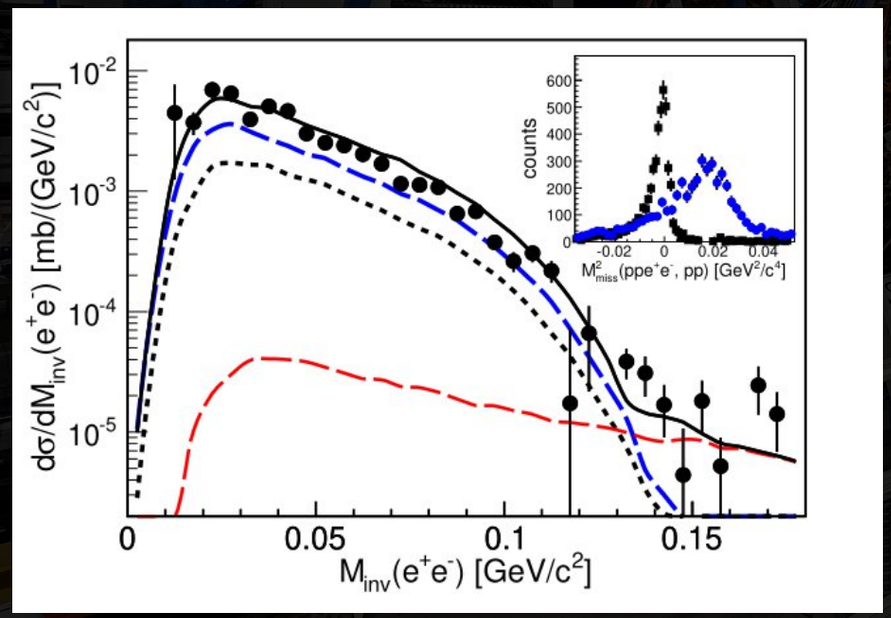

contribution of Δ and N(1440)[3]

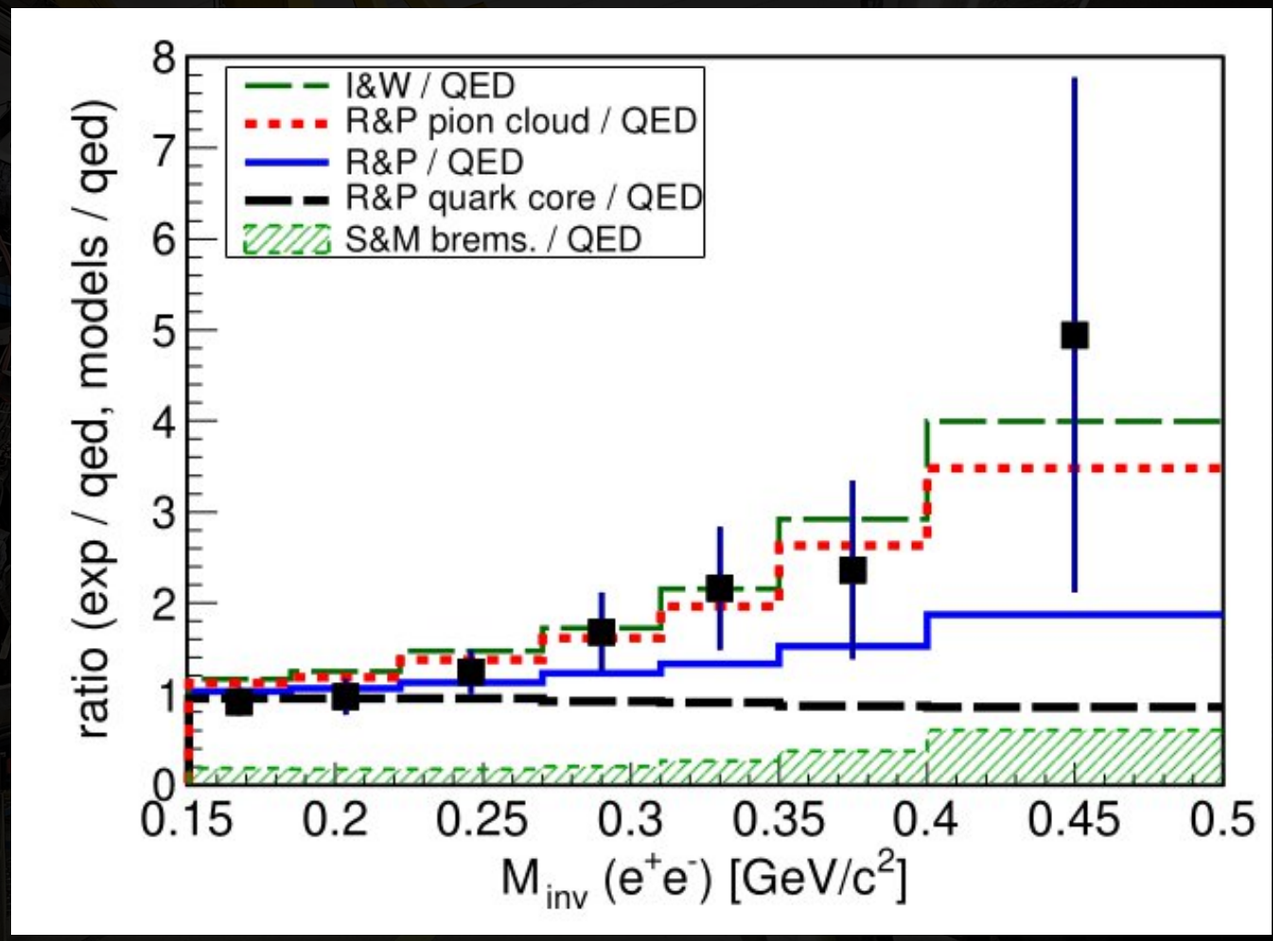

effective transition form factor for $\Delta \rightarrow pe^+e^-$ [3]

3.Adamczewski-Musch, J. *et al.* Δ(1232) Dalitz decay in proton-proton collisions at T=1.25 GeV measured with HADES at GSI. *Phys. Rev. C* **95**, 065205 (2017).

Towards Studying the Electromagnetic Properties of Light Baryons

- **Production mechanisms** and **reaction dynamics** of N* and Δ states in $pp \rightarrow NN\pi$ provide access to their **electromagnetic structure** through **dilepton decays**.
- Extract differential cross-sections and also the coupling strengths N^* and Δ resonances.
- How do these measurements improve the baseline for transport models and heavy-ion collisions?

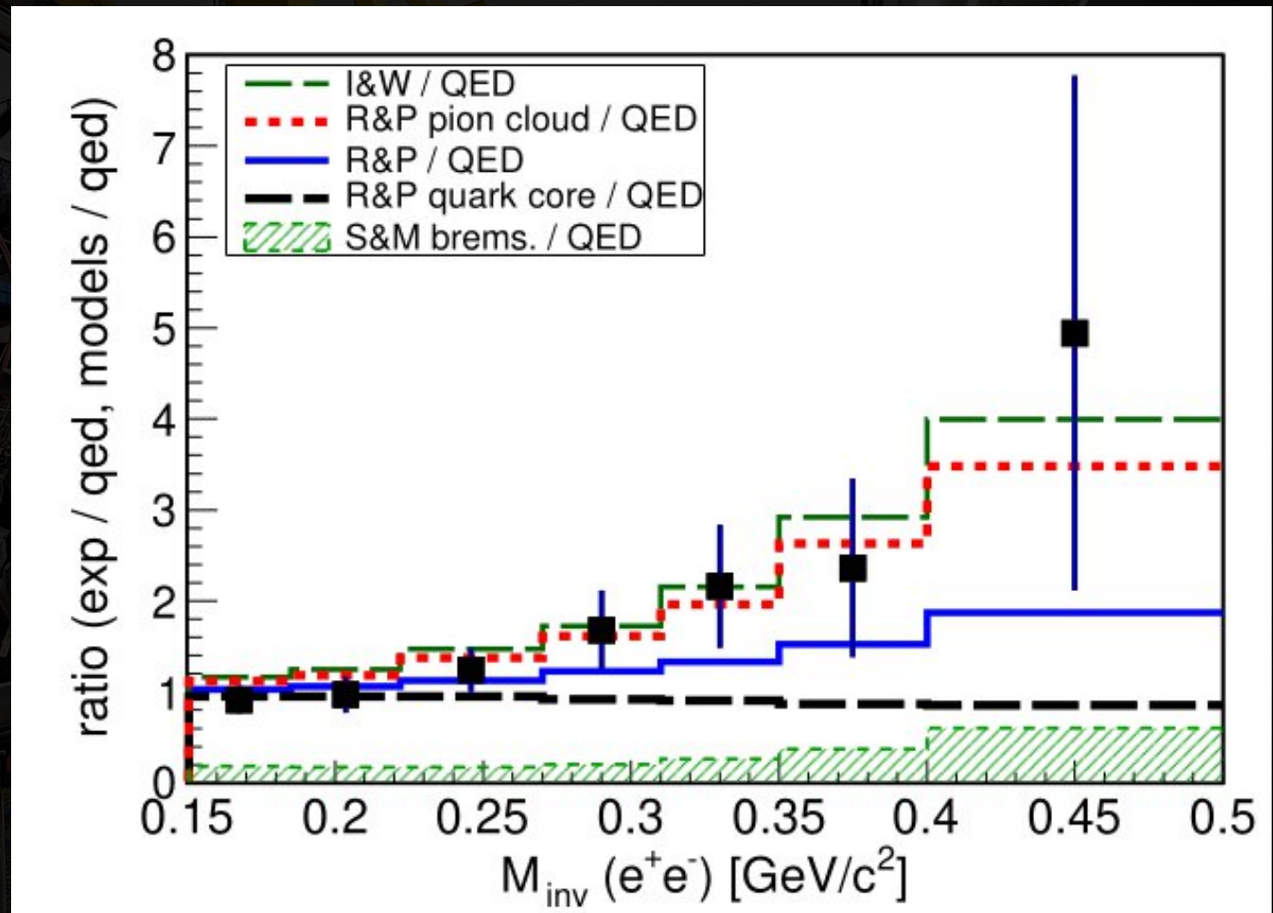

effective transition form factor for $\Delta \rightarrow pe^+e^-$ [3]

3.Adamczewski-Musch, J. *et al.* Δ(1232) Dalitz decay in proton-proton collisions at T=1.25 GeV measured with HADES at GSI. *Phys. Rev. C* **95**, 065205 (2017).

Particle Identification via TOF Residual χ^2

- For each event, four track PID hypotheses are evaluated:
  pp, pπ^+, π^+p, $\pi^+\pi^+$

- For each hypothesis Δt_i is calculated, where Δt_i = measured-expected TOF for track i.

- For each event, the four possible values of χ^2 are calculated corresponding to all four possible track combinations.

$$\chi^2 = (\Delta t_1)^2 + (\Delta t_2)^2$$

- The track PID hypothesis with the smallest χ^2 value is chosen to identify the PID of the two tracks.

Particle Identification via TOF Residual χ^2

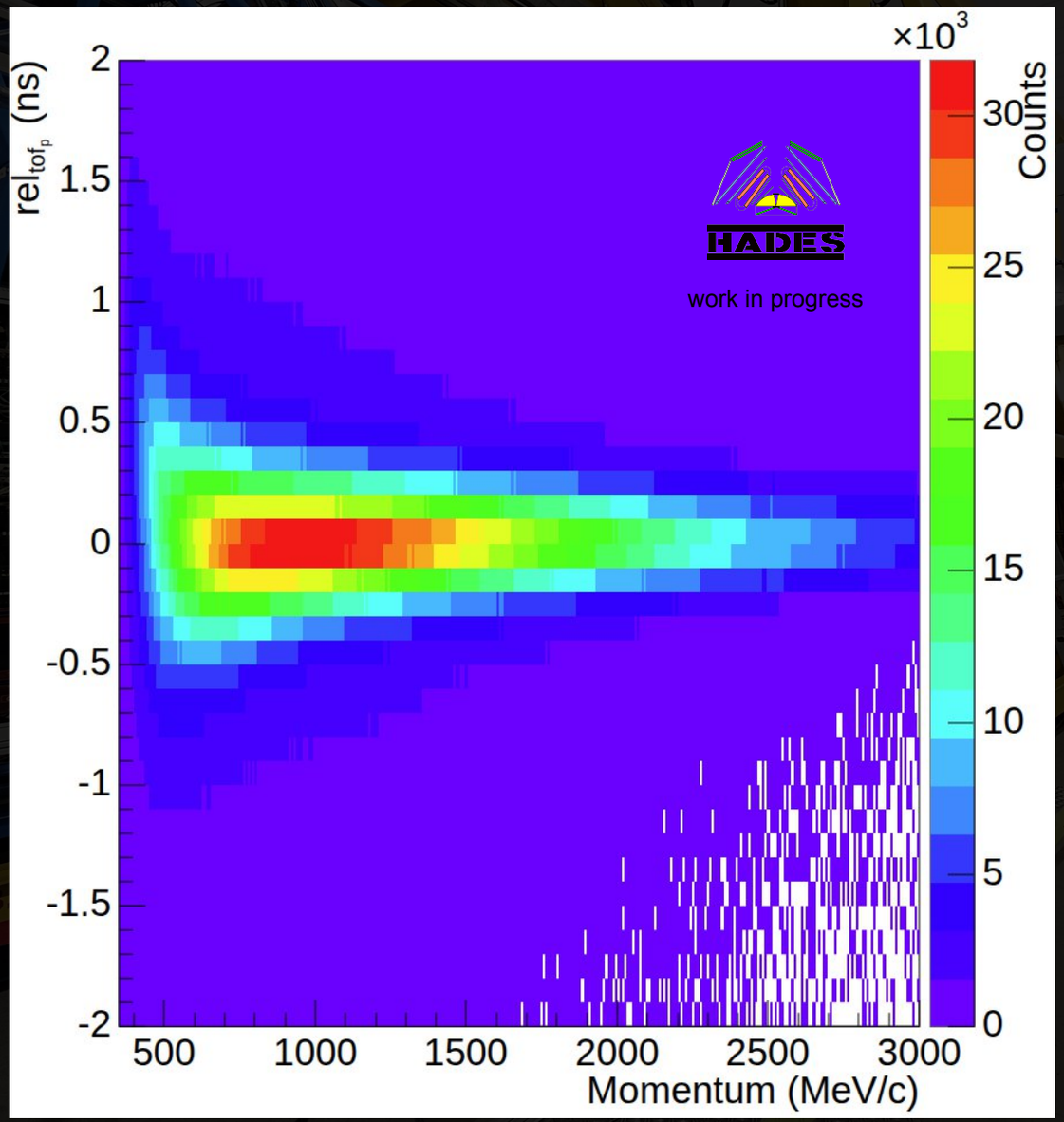

Missing Neutron Identification

- Select **missing neutron** by applying mass window for further analysis.
- Kinematic fit (Missing Mass Constraint) is applied to signal and sideband regions.

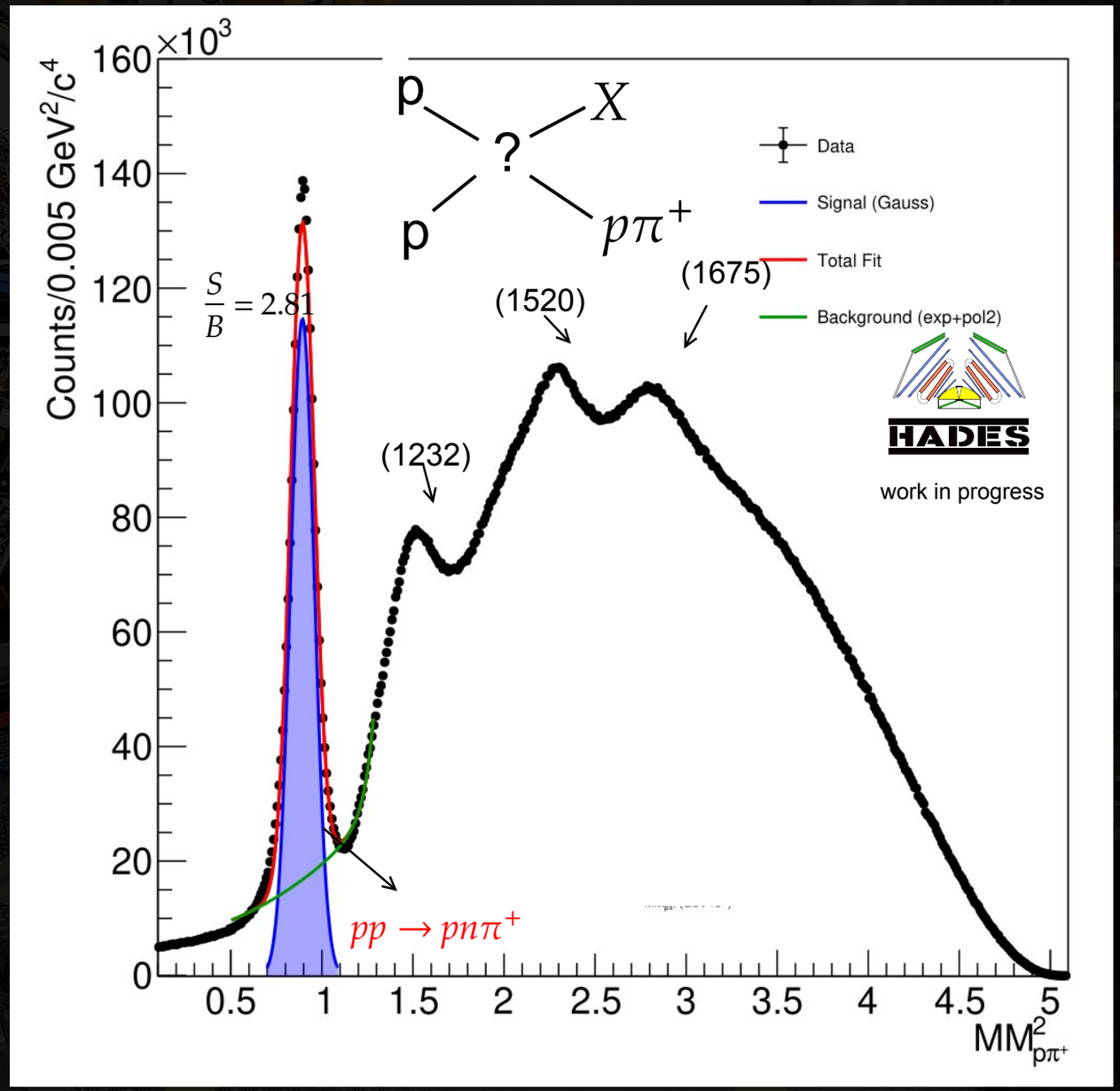

Missing Neutron Identification

- Select **missing neutron** by applying mass window for further analysis.
- Kinematic fit (Missing Mass Constraint) is applied to signal and sideband regions.

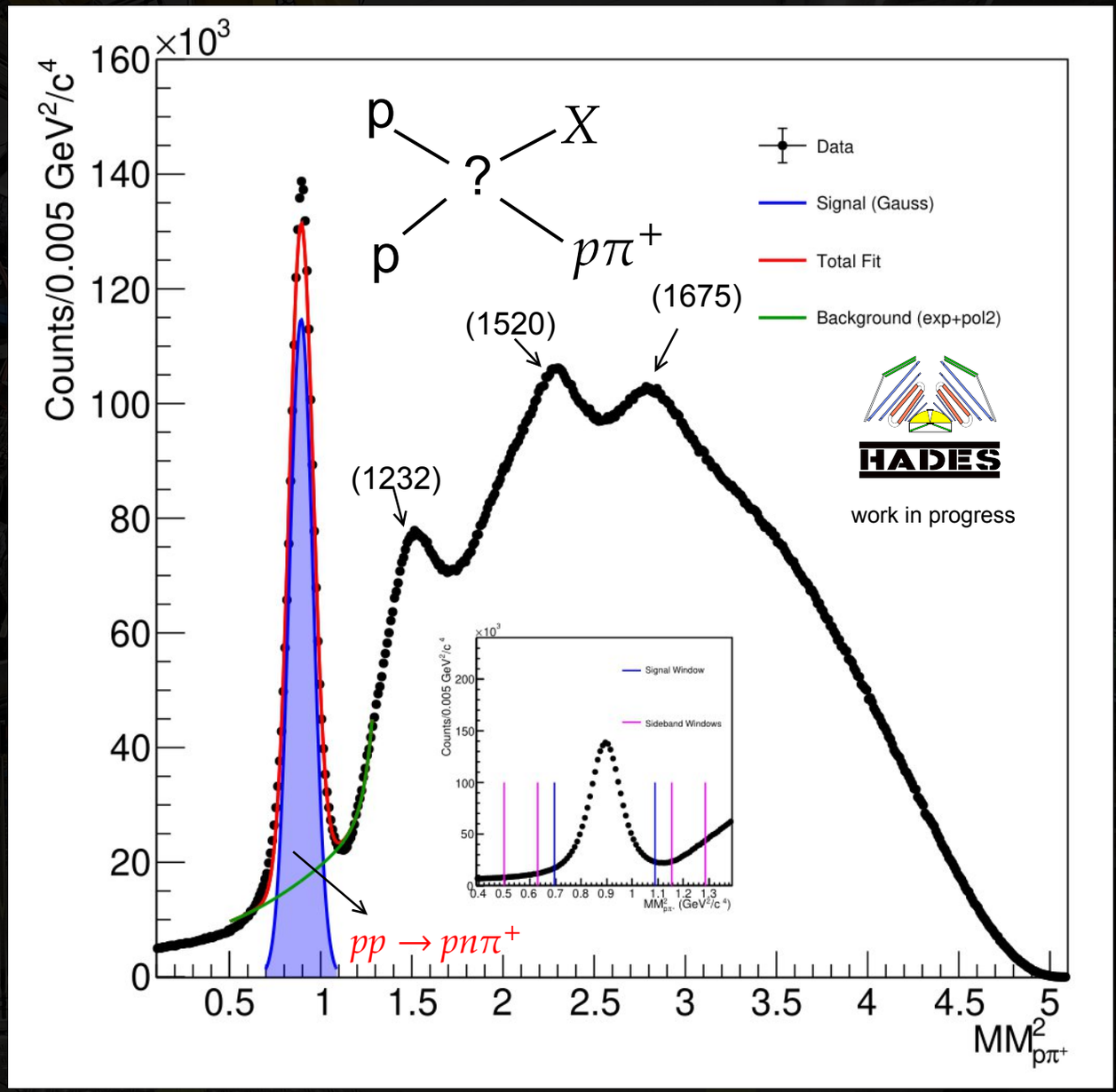

$pp \rightarrow pp\pi^0$

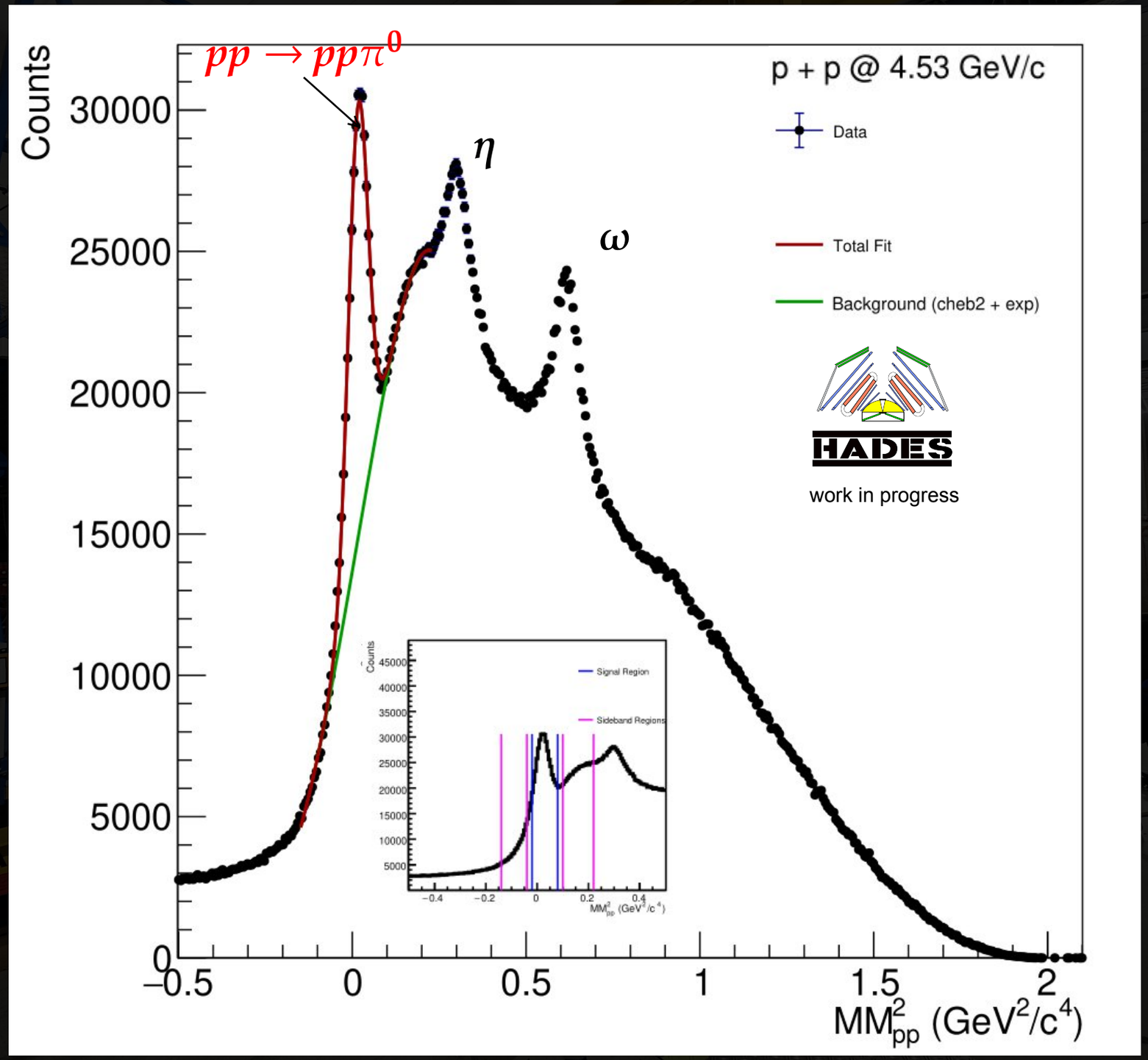

$pn\pi^+$ Vertex Selection

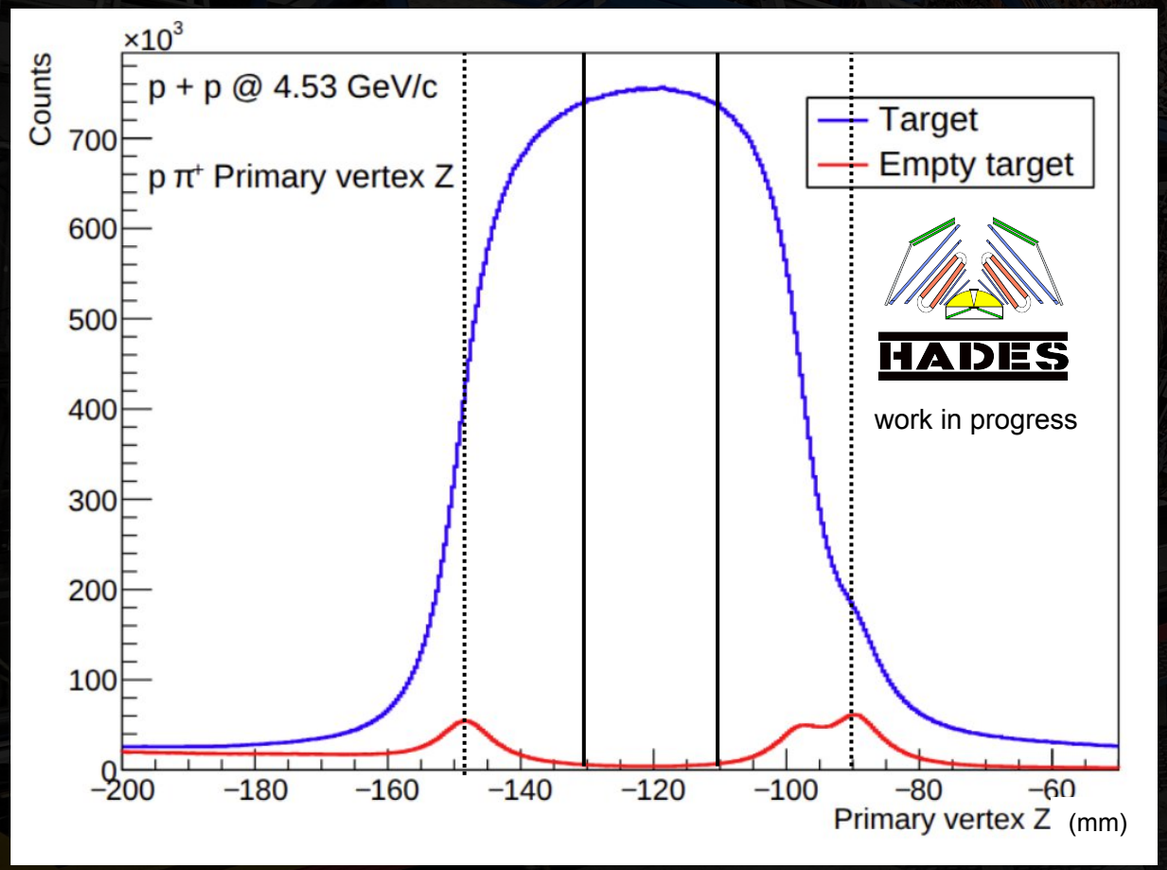

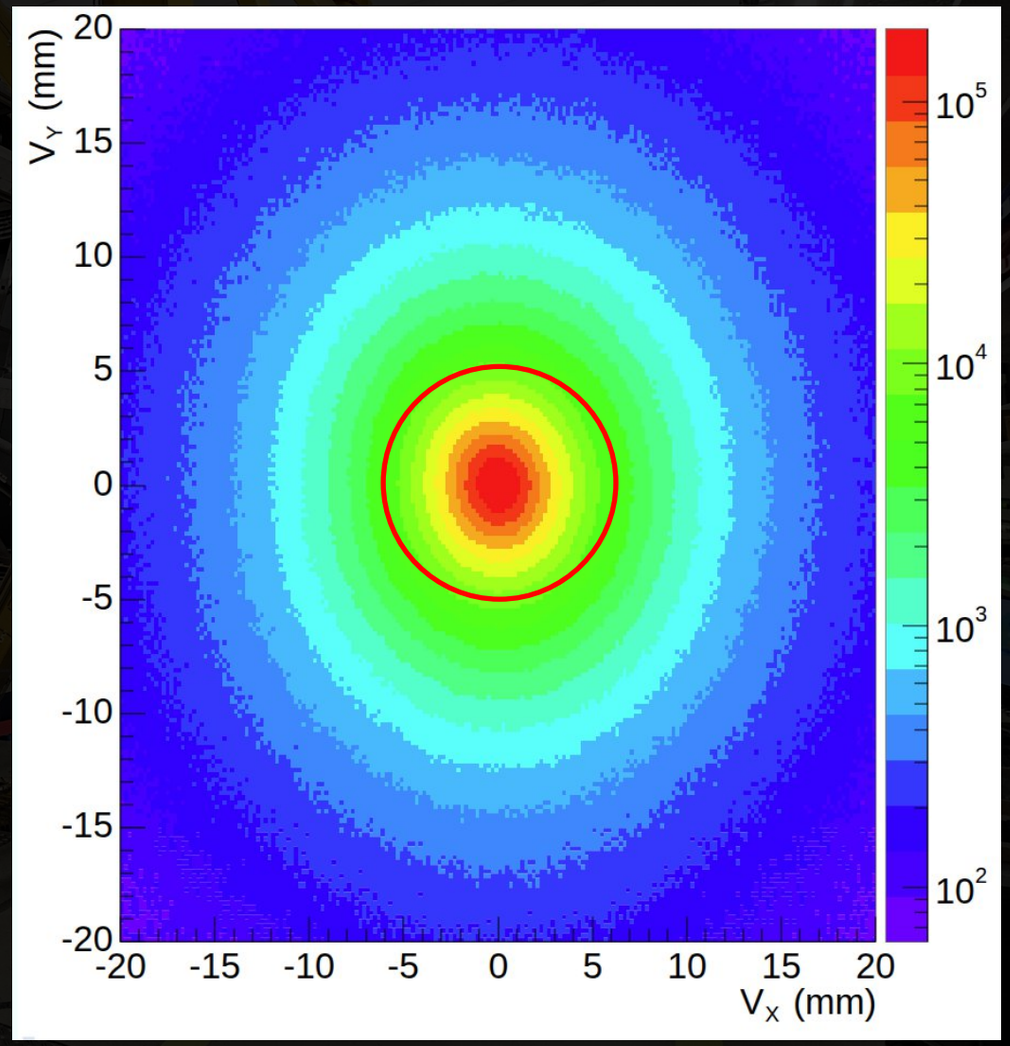

$pp \rightarrow pp\pi^0$ Vertex Selection

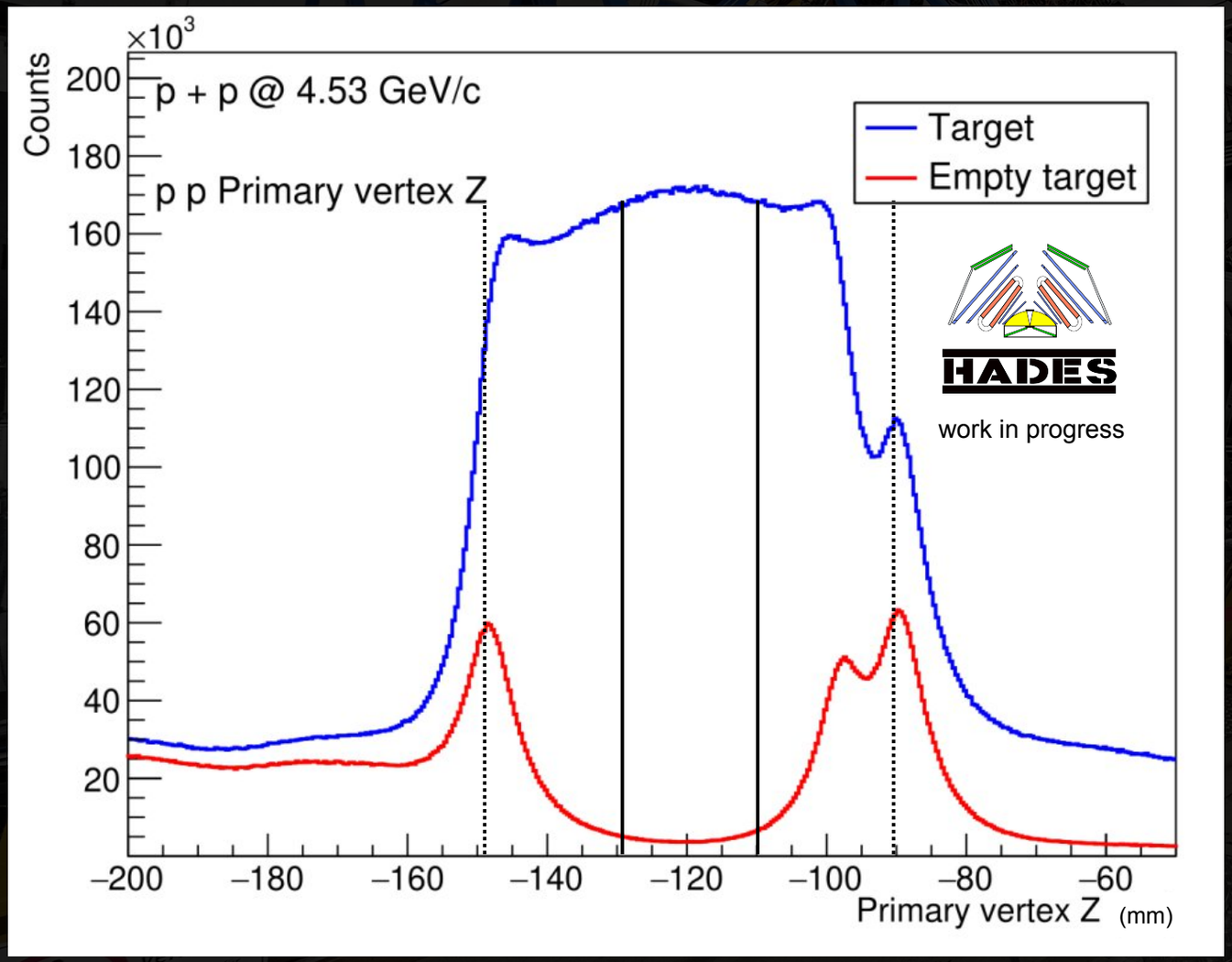

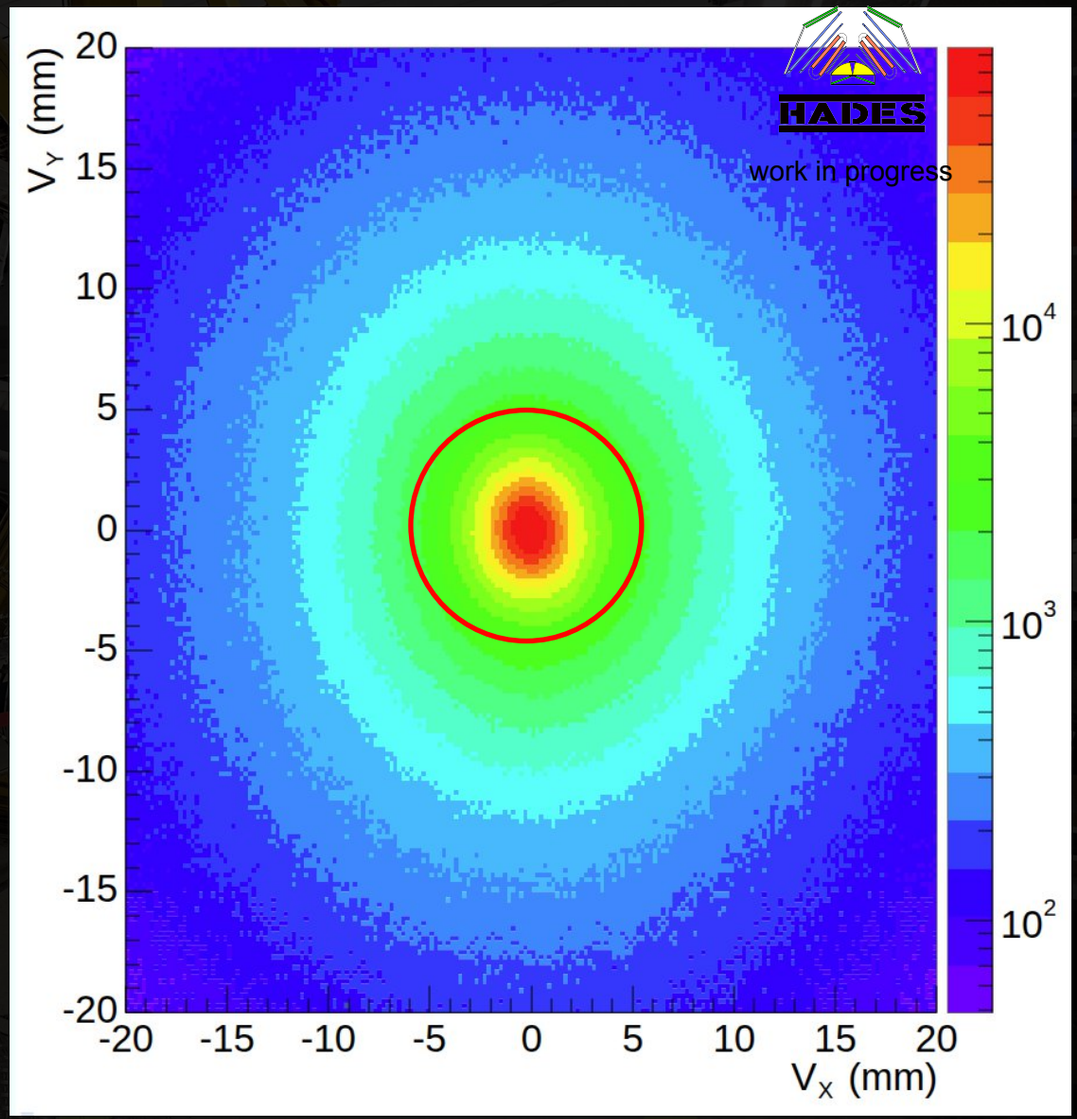

$pp \rightarrow pp\pi^0$ Vertex Selection

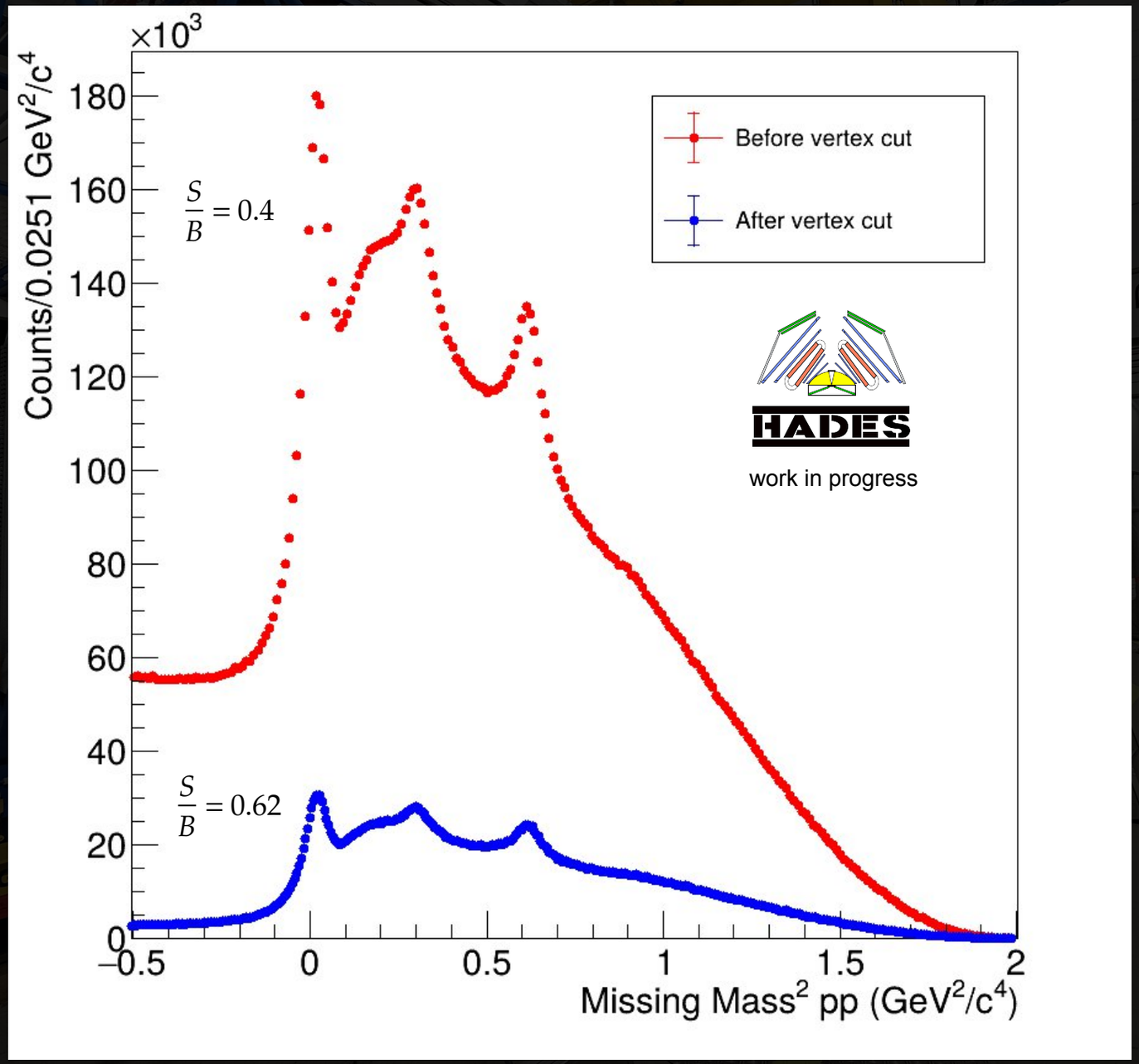

Sideband Subtracted Dalitz Plots

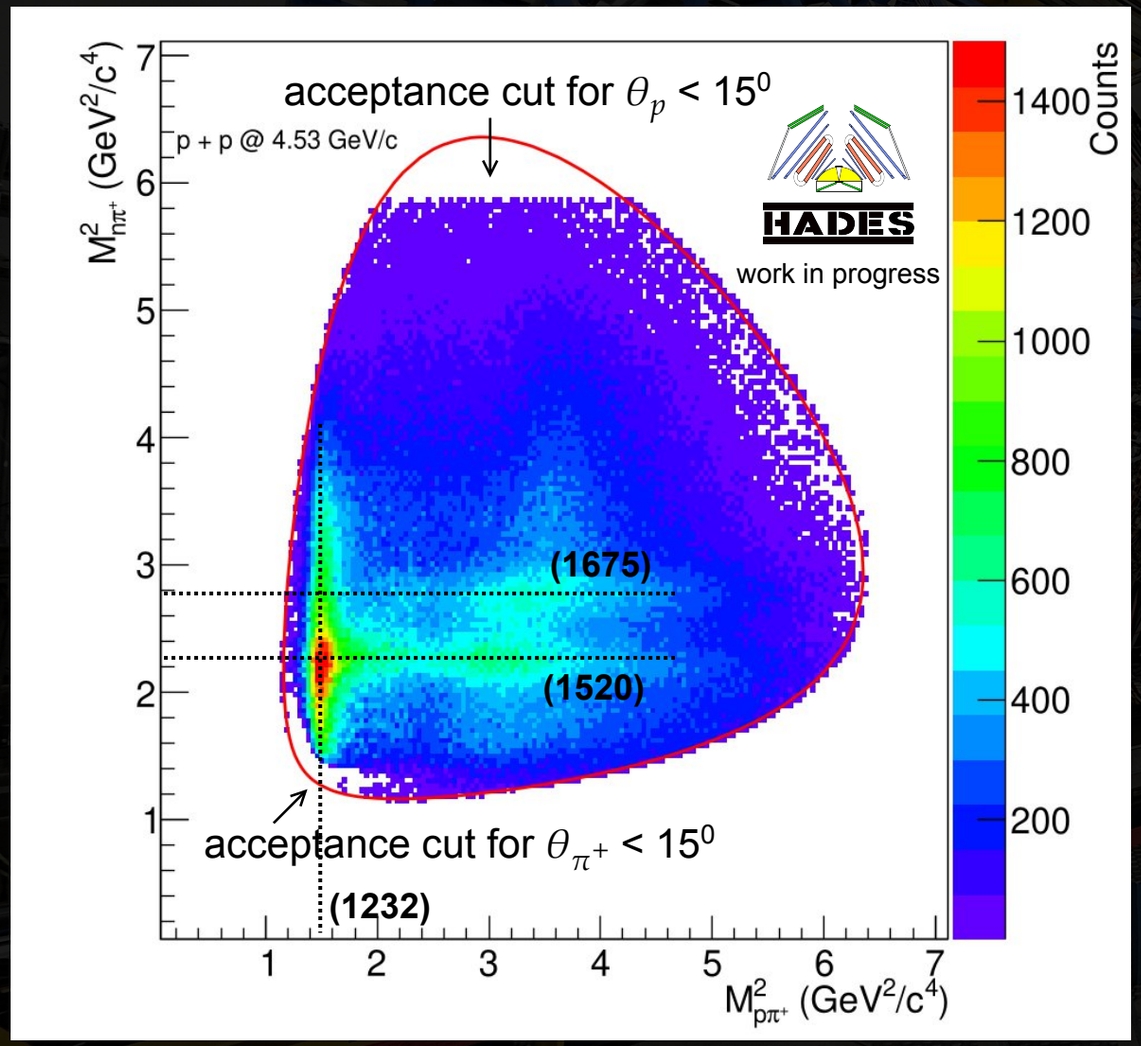

$pn\pi^+$

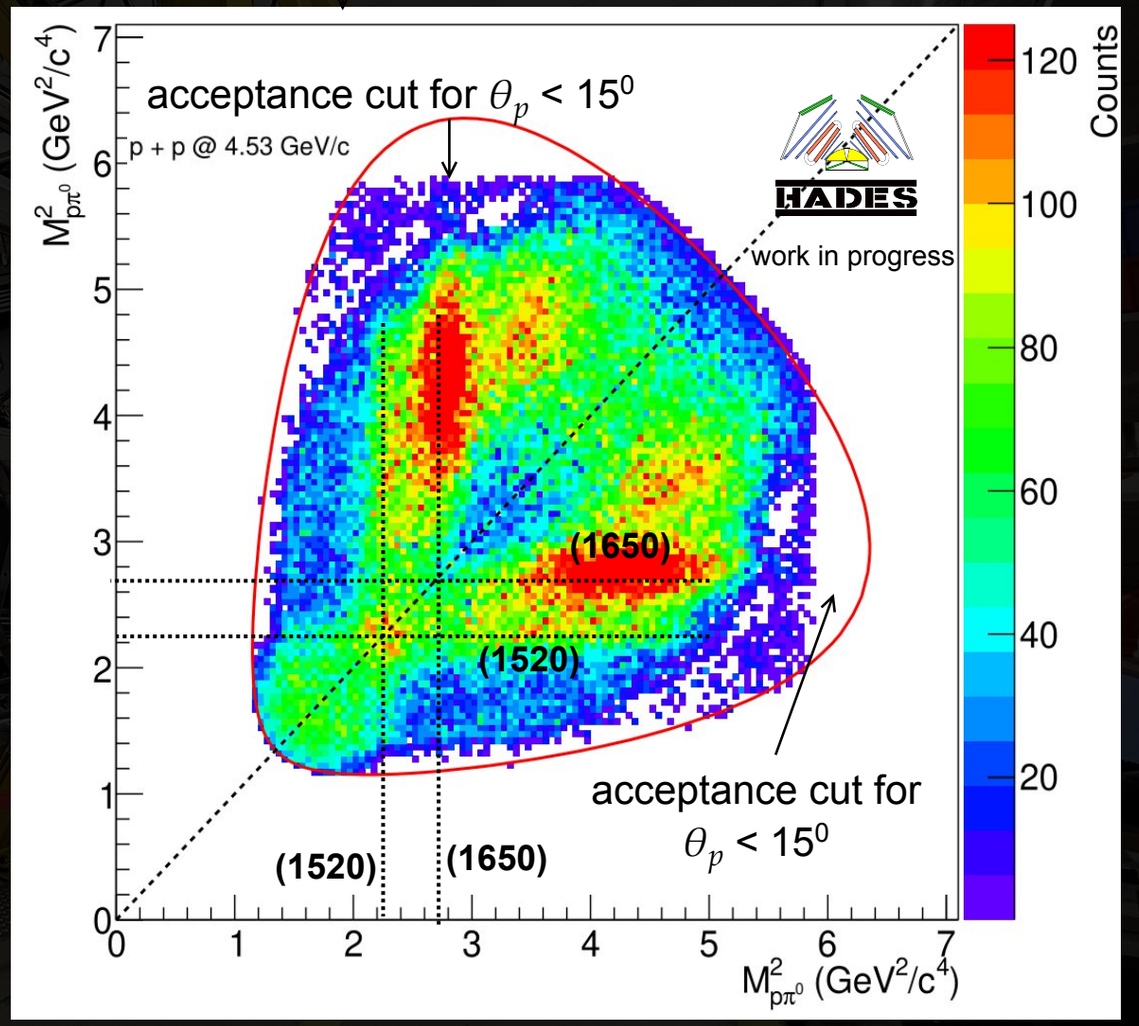

$pp\pi^0$

Comparision to Transport Model

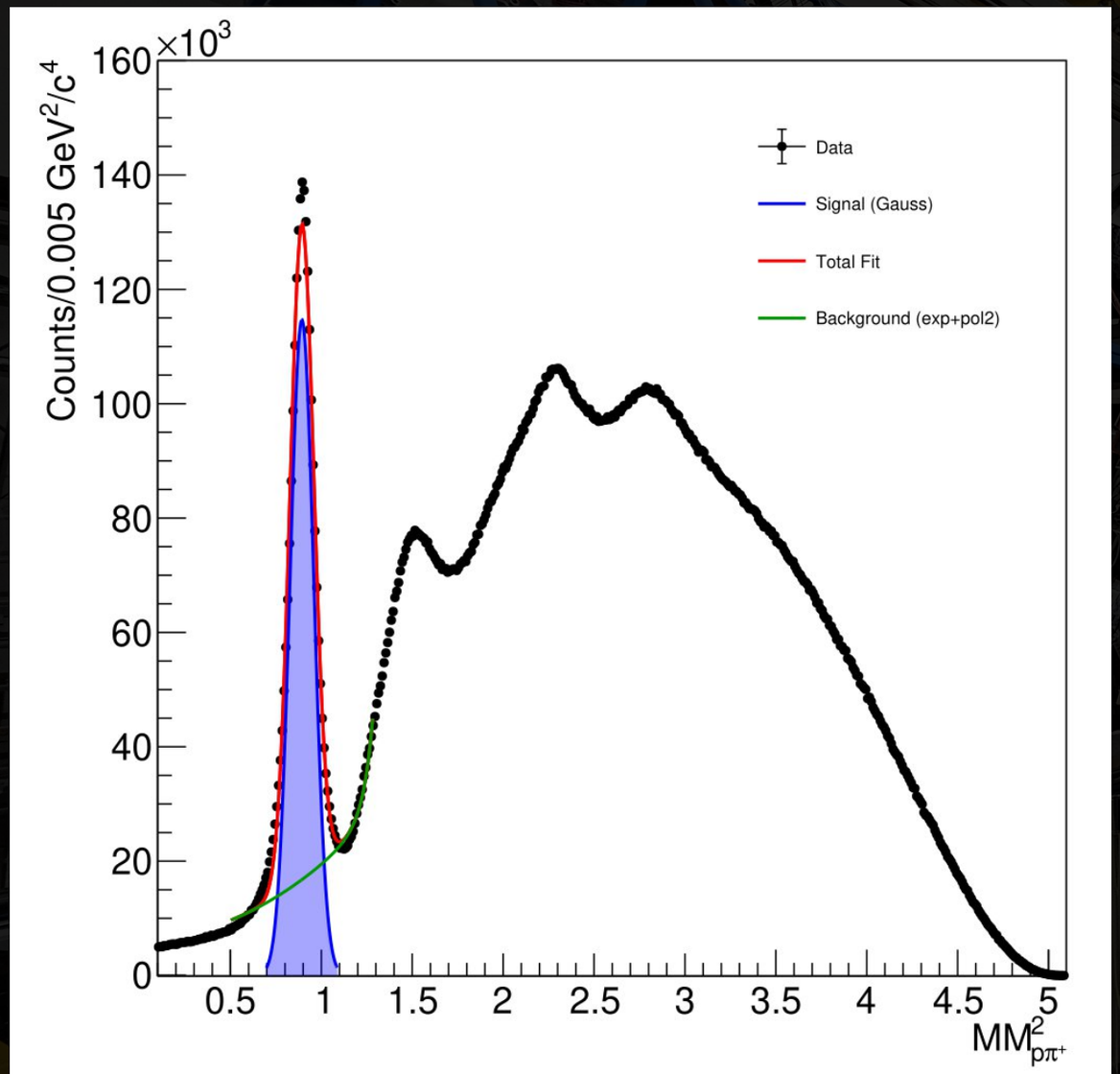

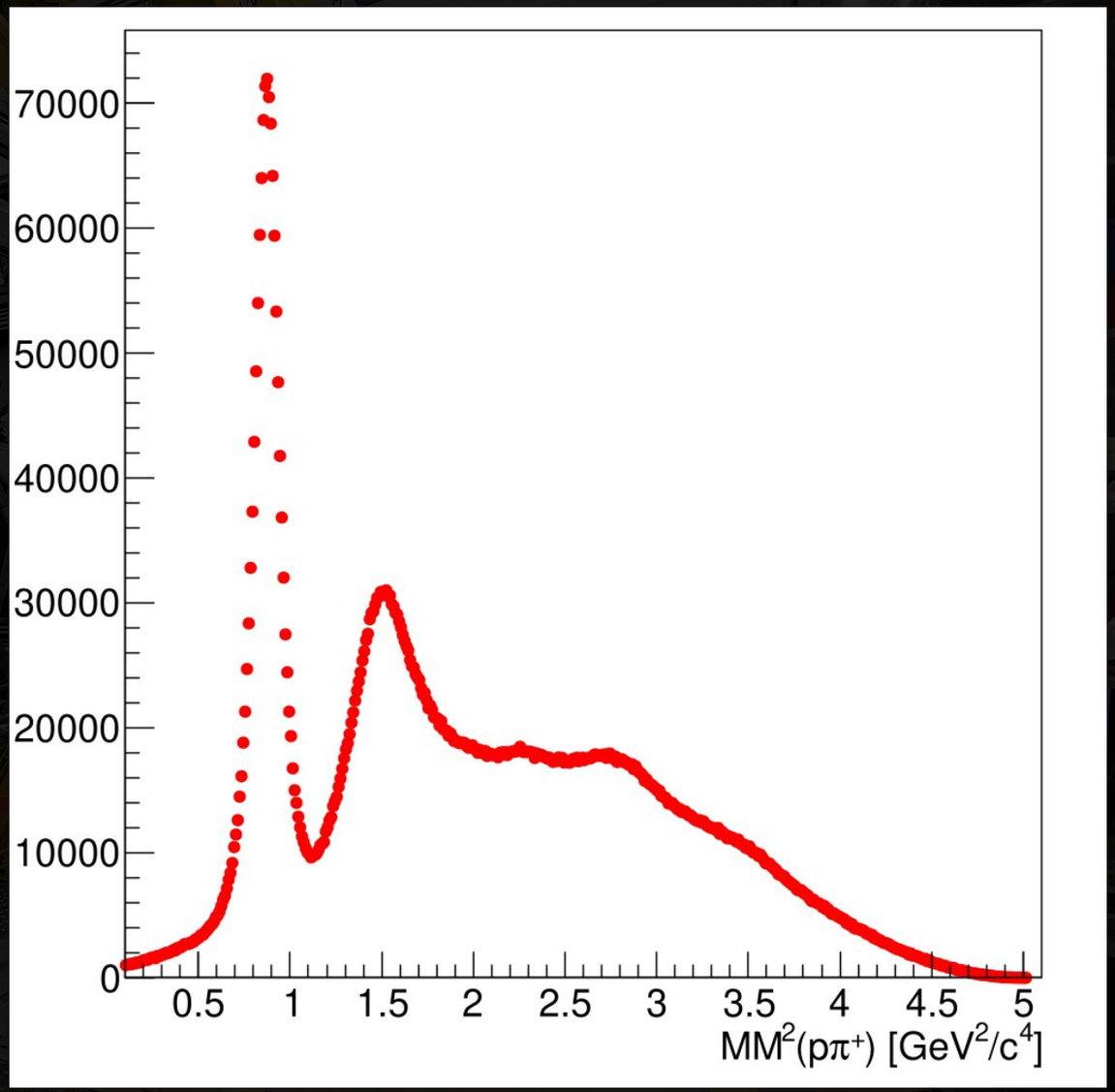

$pn\pi^+$

SMASH[6]

6. Weil, J., et al. Smash-transport/smash: SMASH-3.3. SMASH-3.3, Zenodo, 10 Dec. 2025, https://doi.org/10.5281/zenodo.17878251.

Comparision to Transport Model

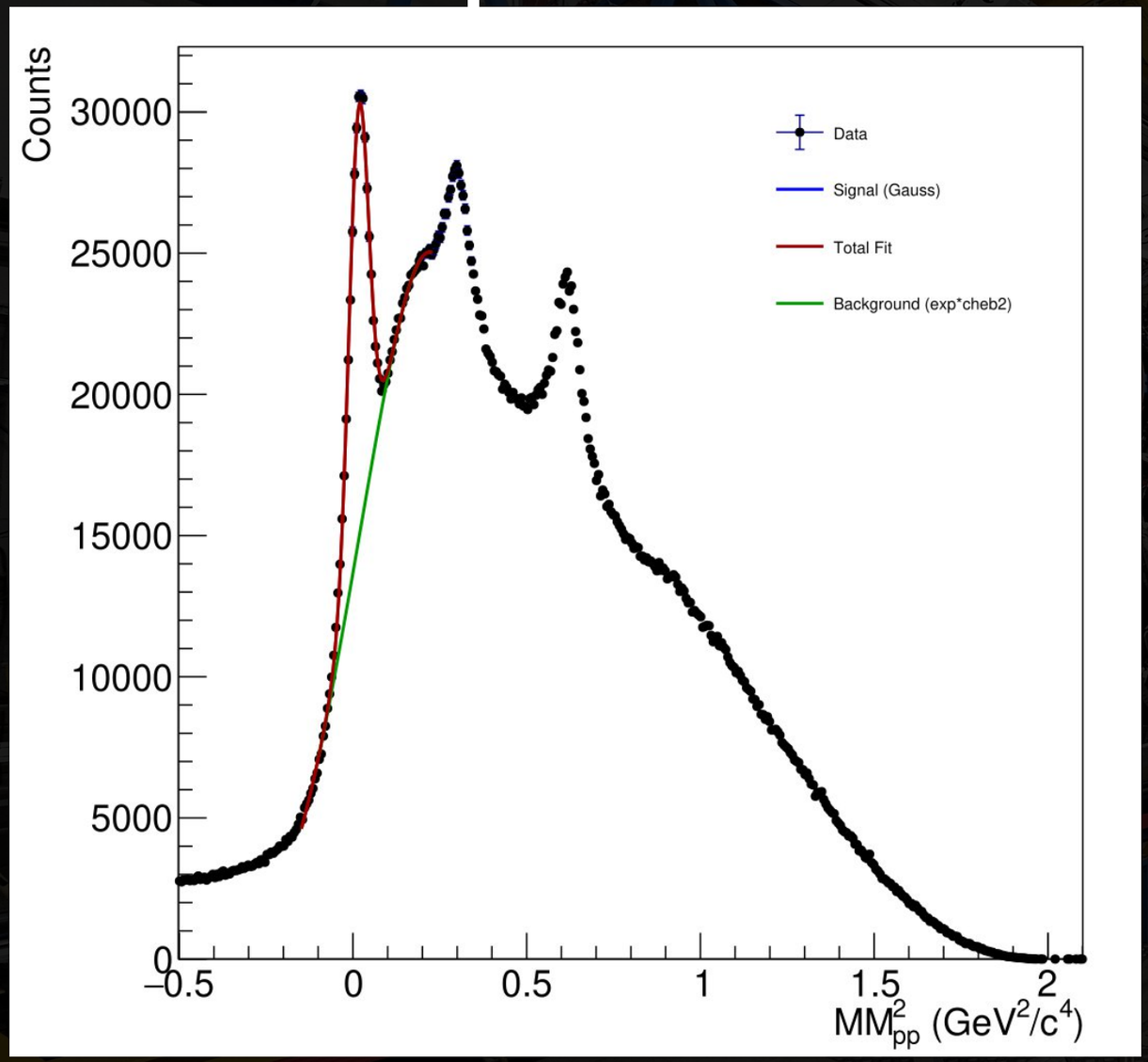

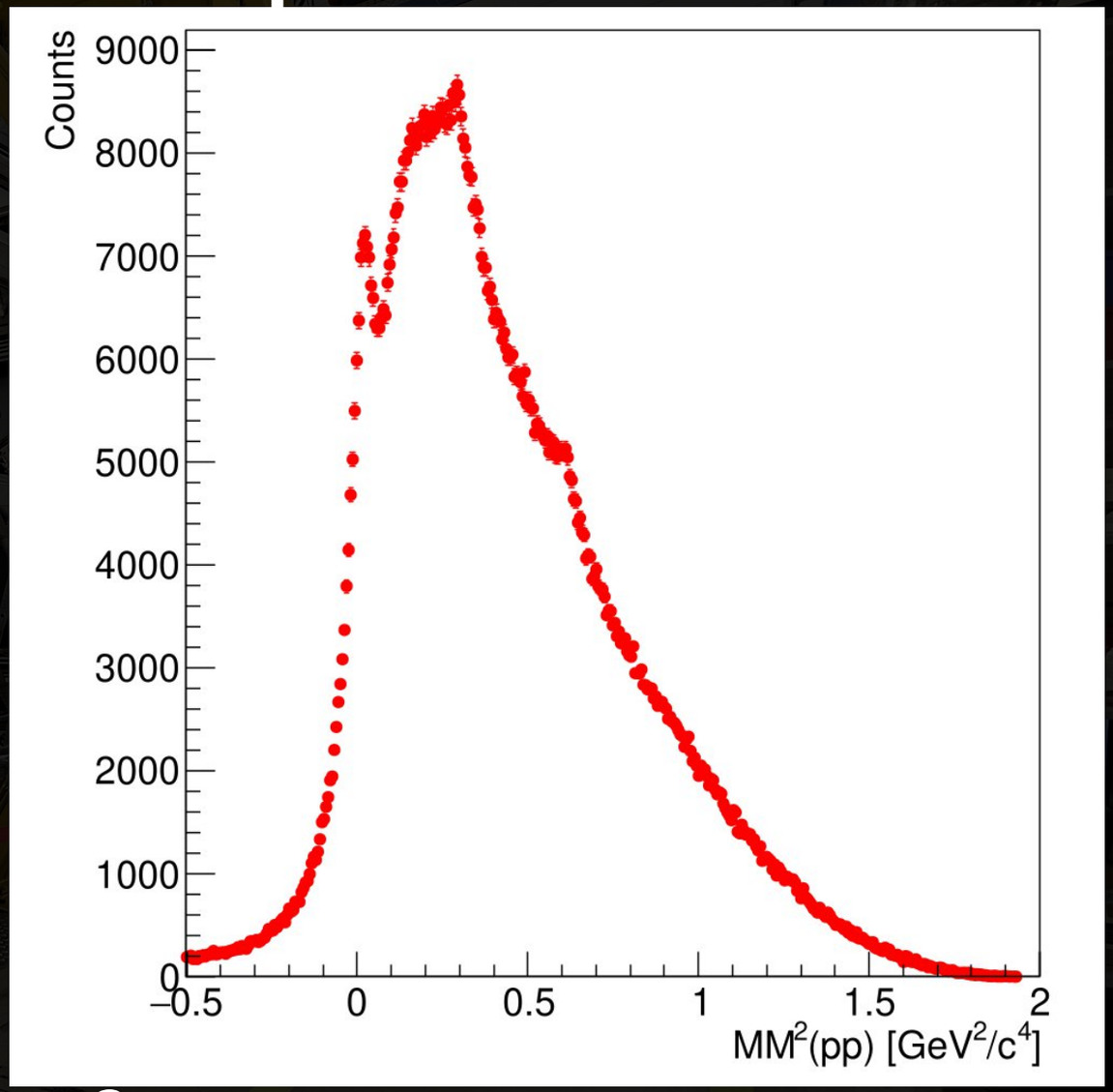

$pp\pi^0$ SMASH[6]

6. Weil, J., et al. Smash-transport/smash: SMASH-3.3. SMASH-3.3, Zenodo, 10 Dec. 2025, https://doi.org/10.5281/zenodo.17878251.

Comparision to Transport Models

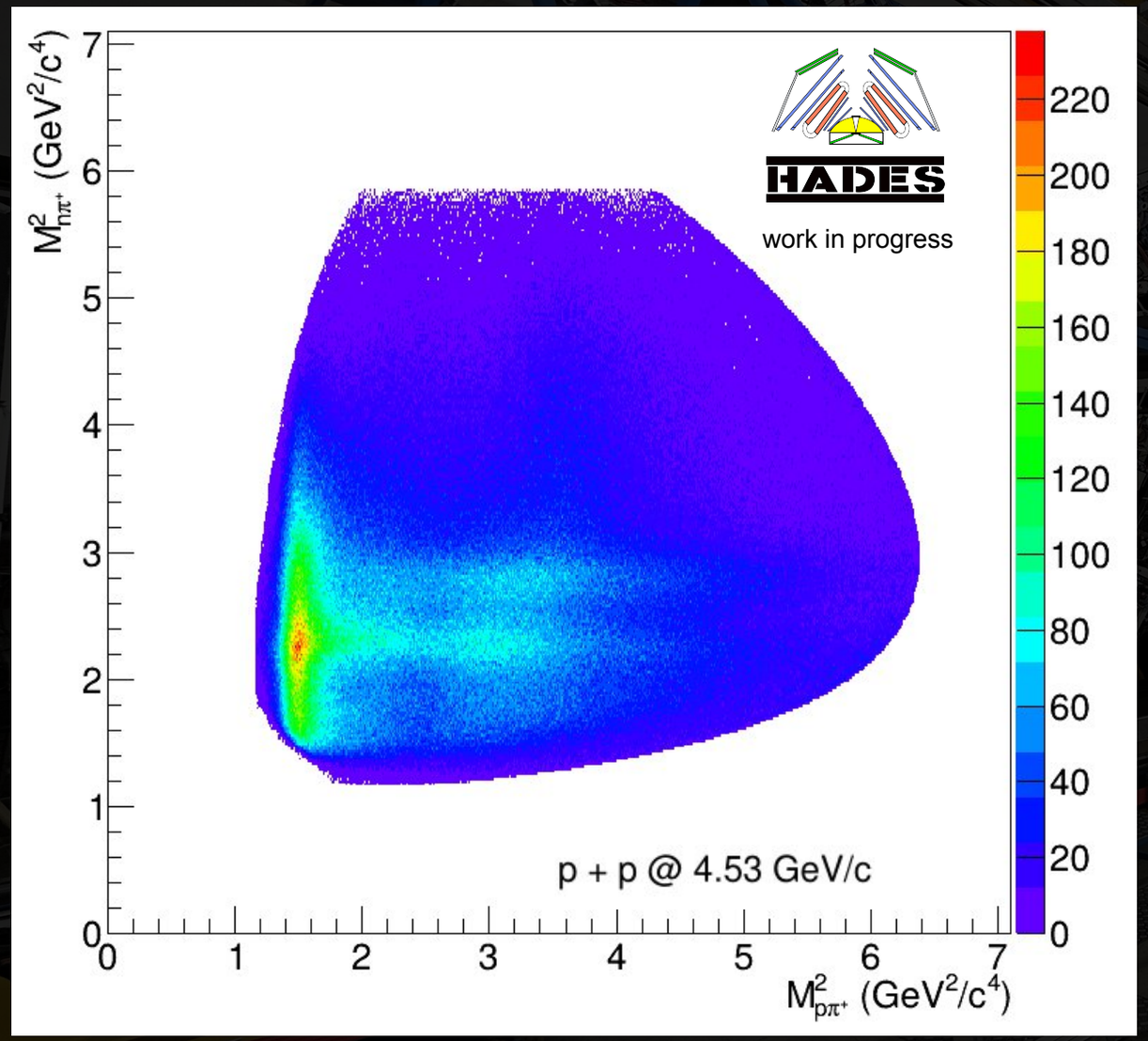

Data

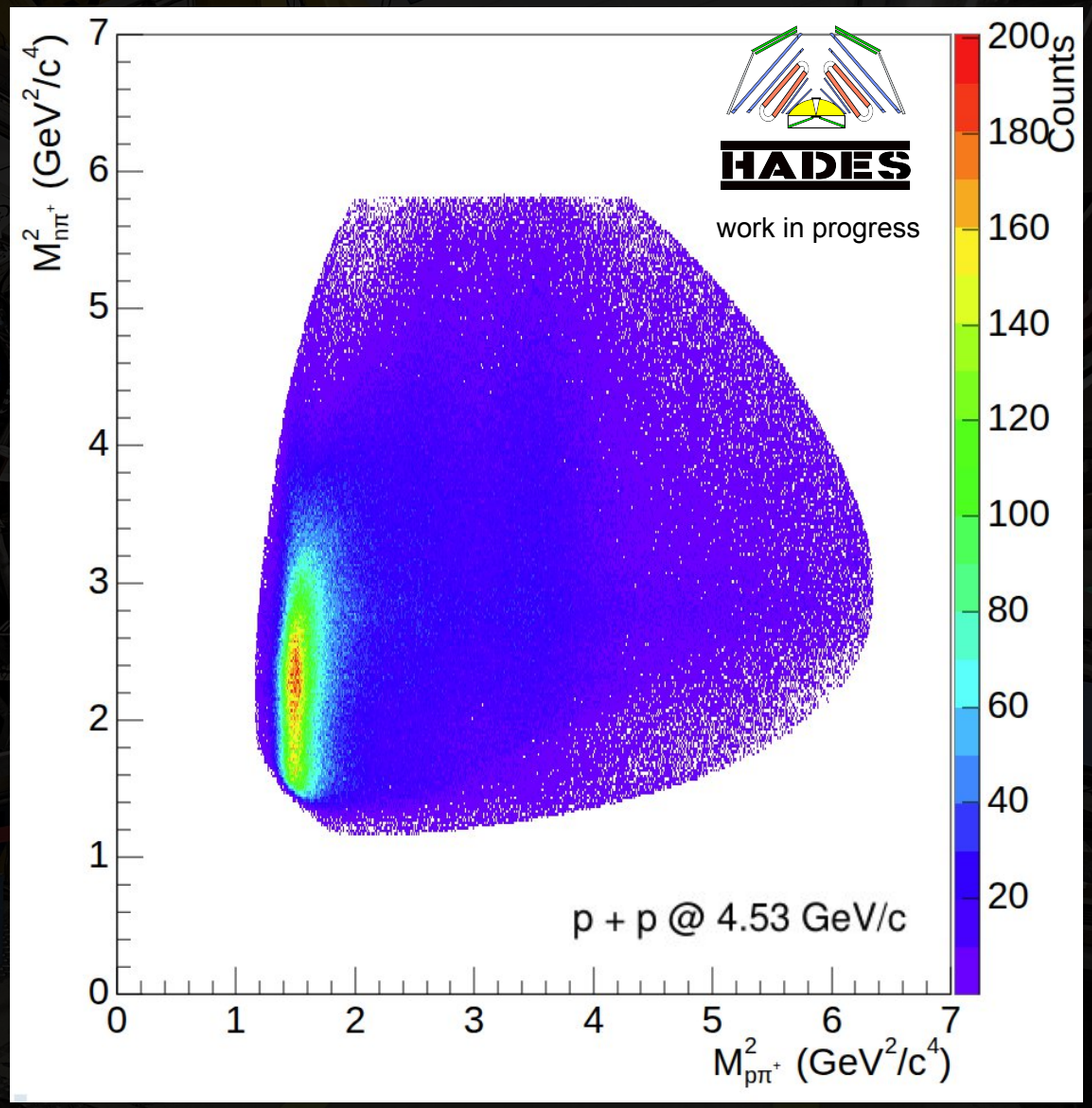

SMASH[6]

$pn\pi^+$

6. Weil, J., et al. Smash-transport/smash: SMASH-3.3. SMASH-3.3, Zenodo, 10 Dec. 2025, https://doi.org/10.5281/zenodo.17878251.

Comparision to Transport Models

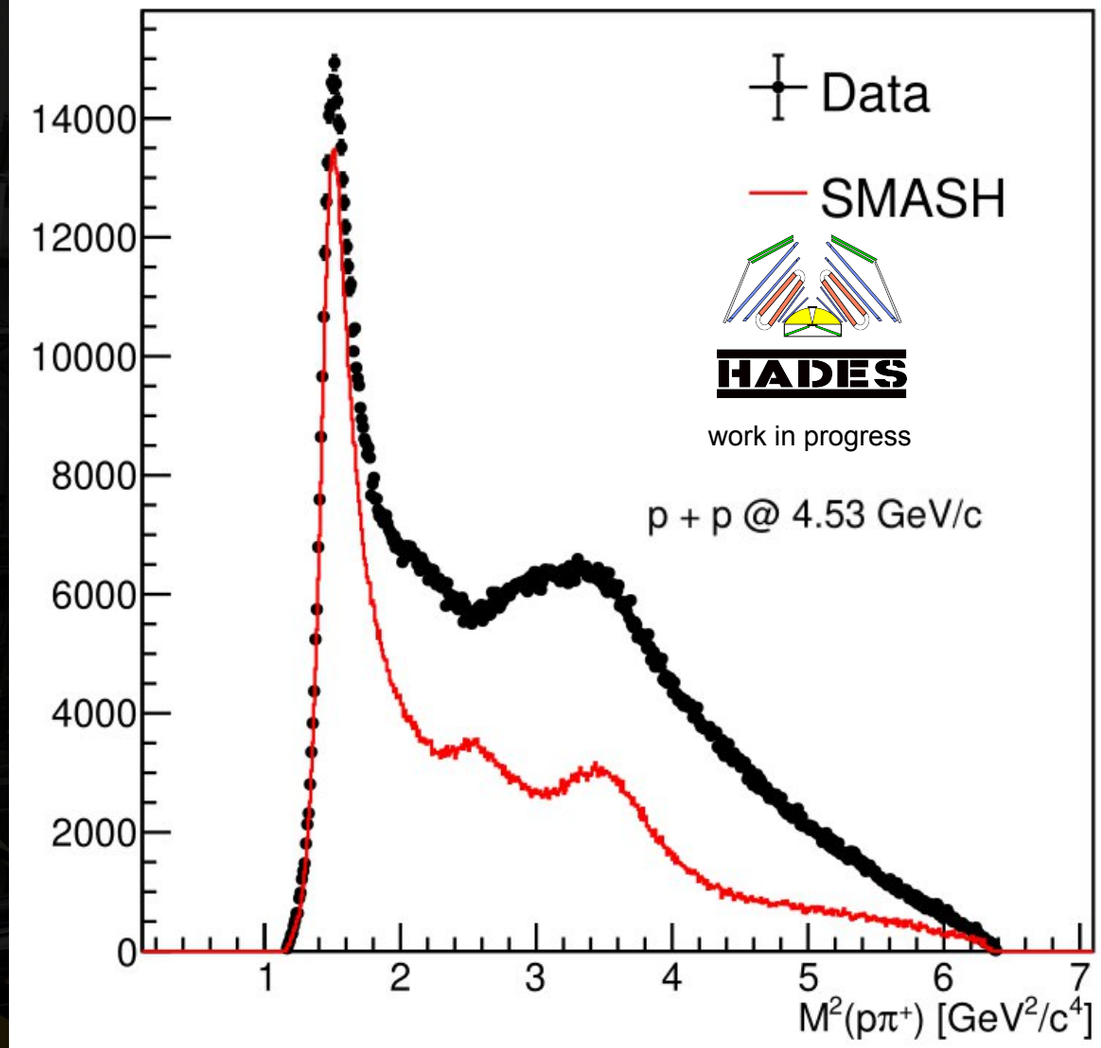

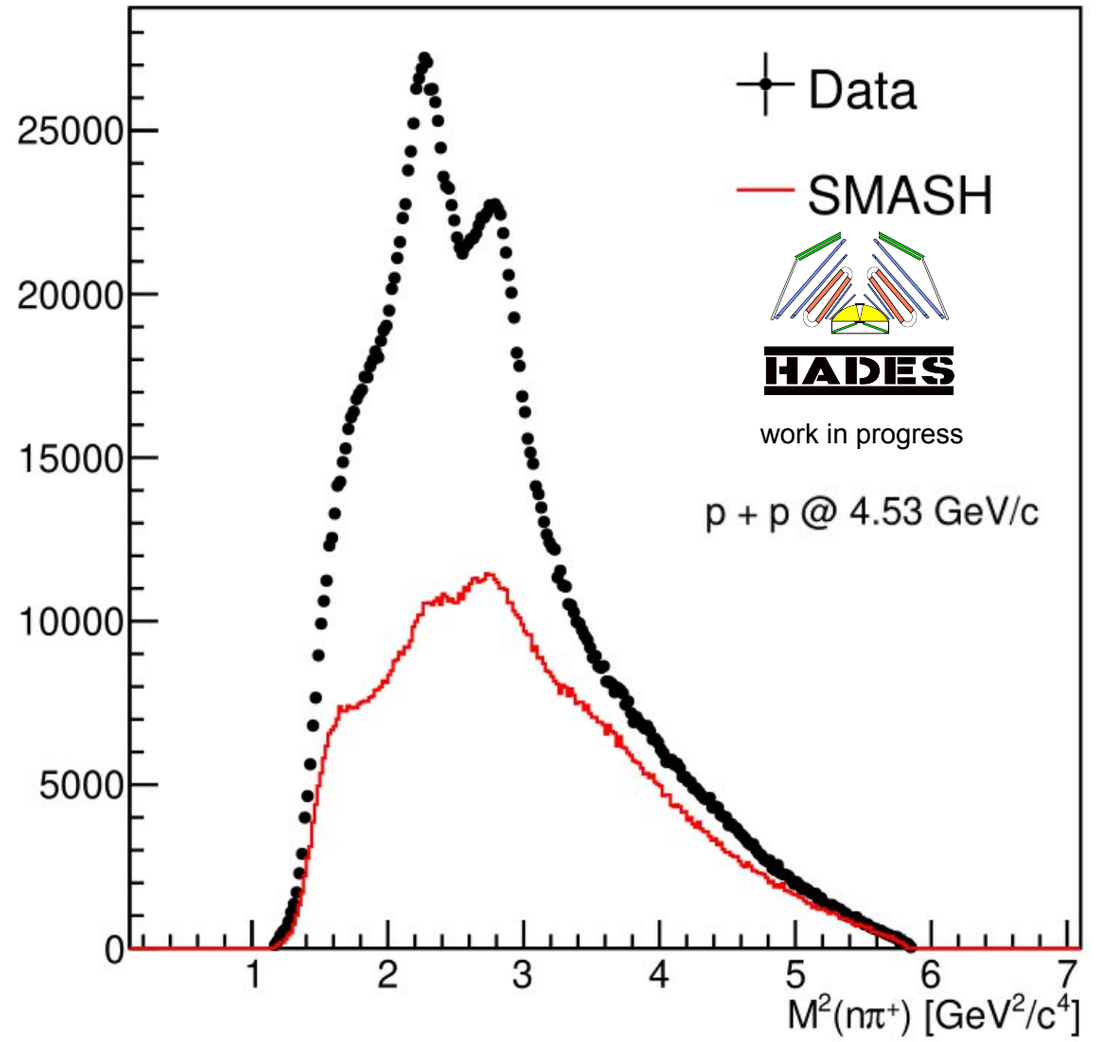

Data $pn\pi^+$ **SMASH**[6]

6. Weil, J., et al. Smash-transport/smash: SMASH-3.3. SMASH-3.3, Zenodo, 10 Dec. 2025, https://doi.org/10.5281/zenodo.17878251.

Comparision to Transport Models

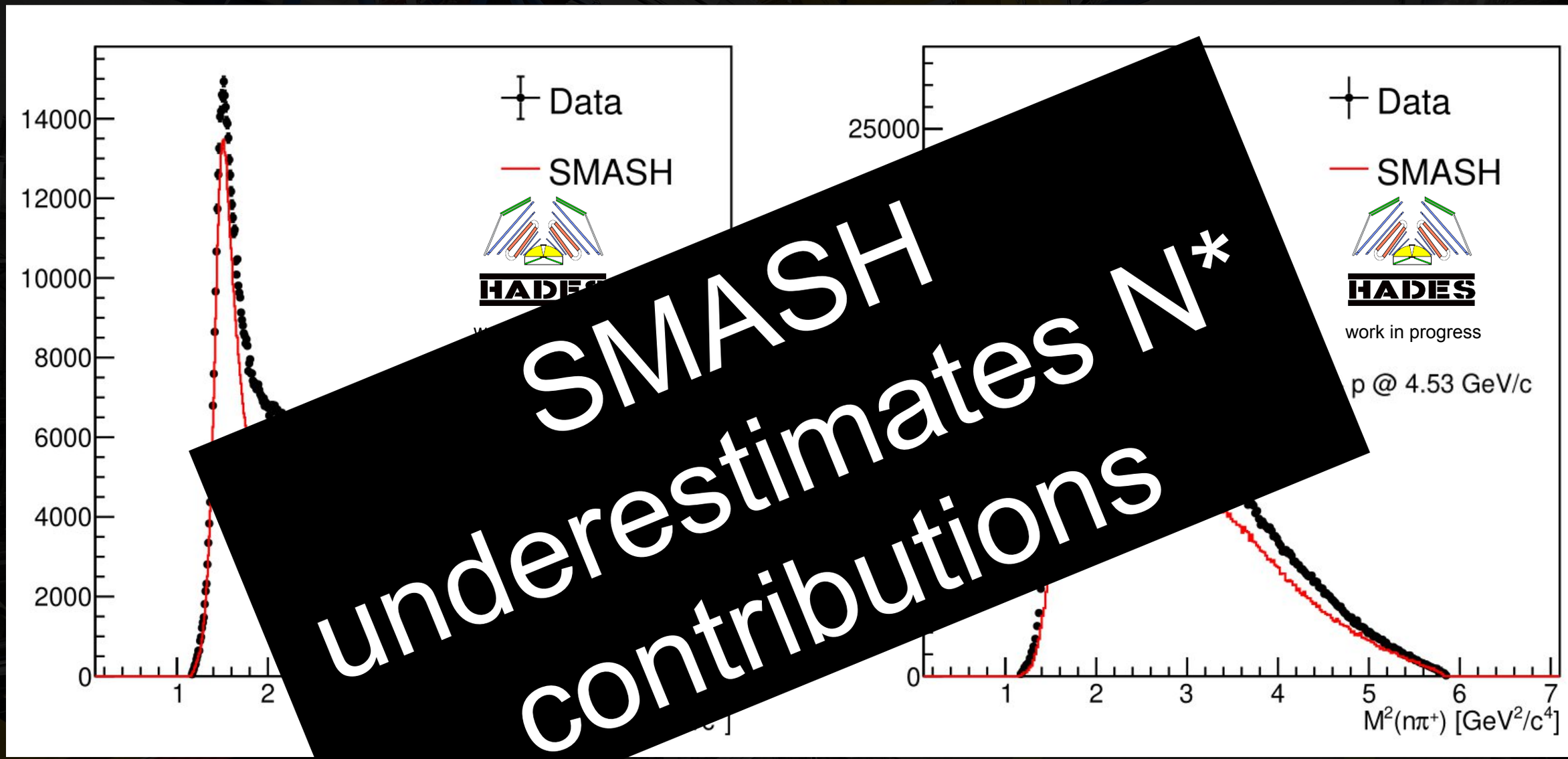

SMASH underestimates N* contributions

$pn\pi^+$

SMASH[6]

6. Weil, J., et al. Smash-transport/smash: SMASH-3.3. SMASH-3.3, Zenodo, 10 Dec. 2025, https://doi.org/10.5281/zenodo.17878251.

Comparision to Transport Models

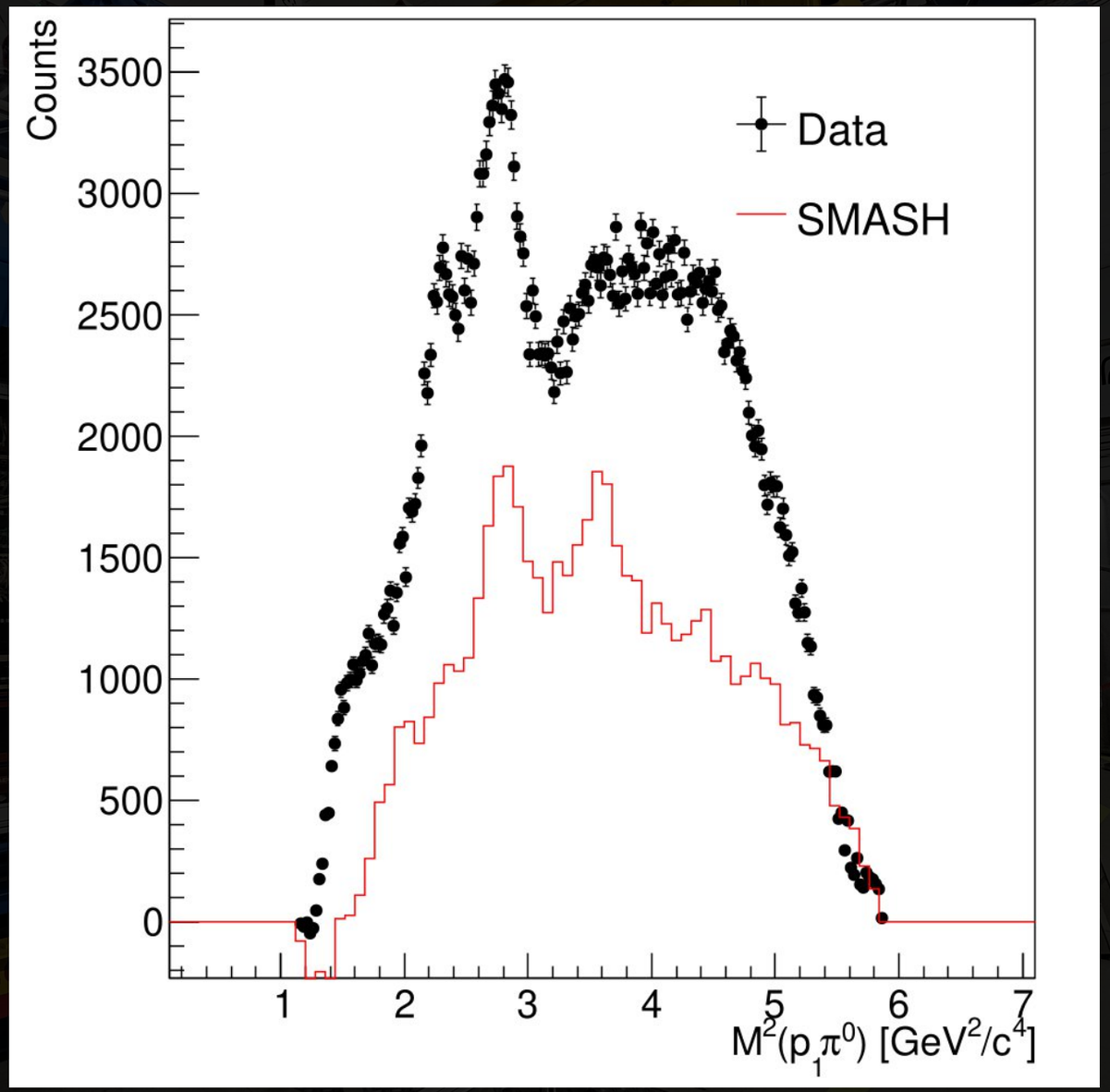

$pp\pi^0$

Preliminary JüBo Fit Results

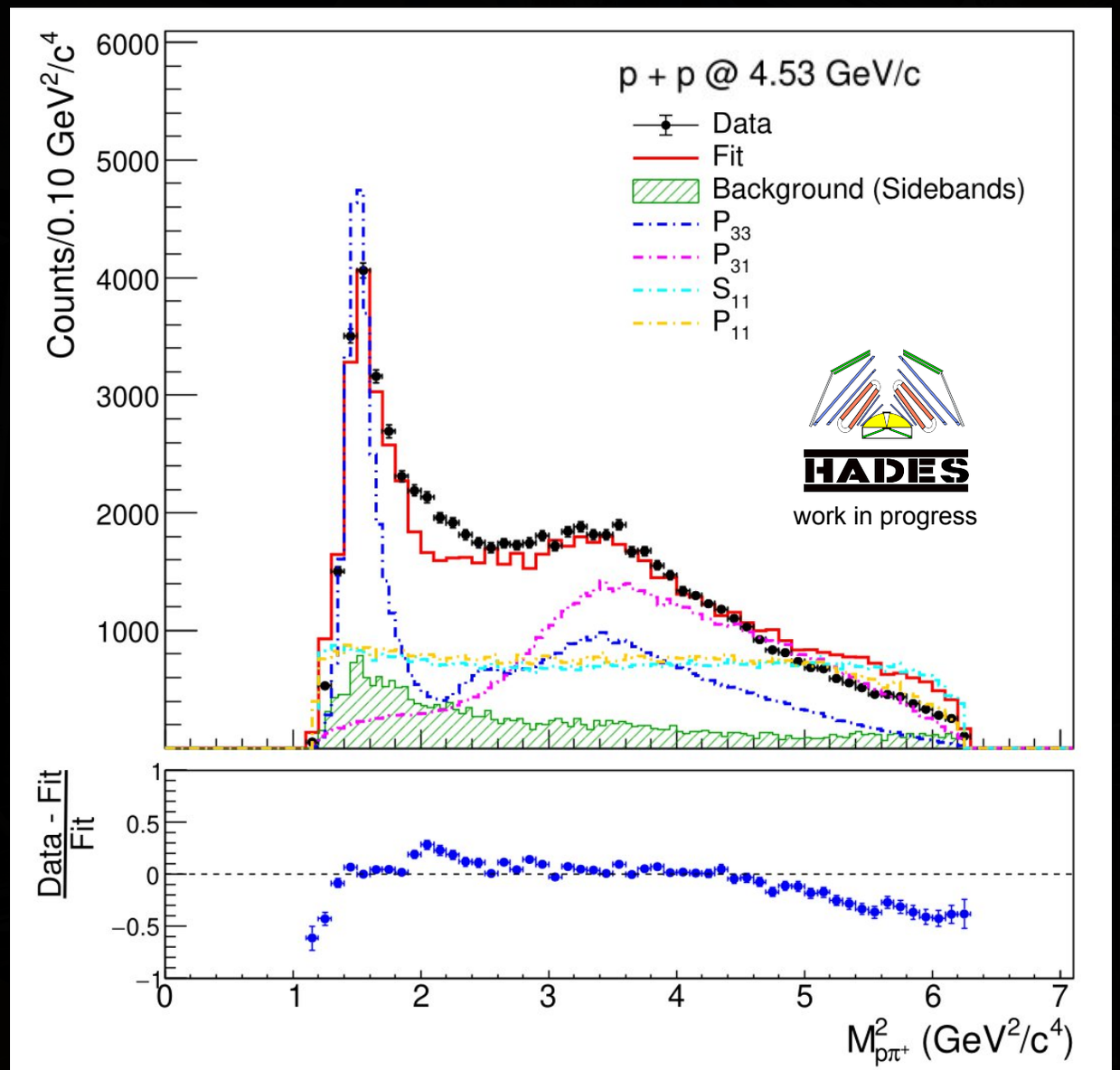

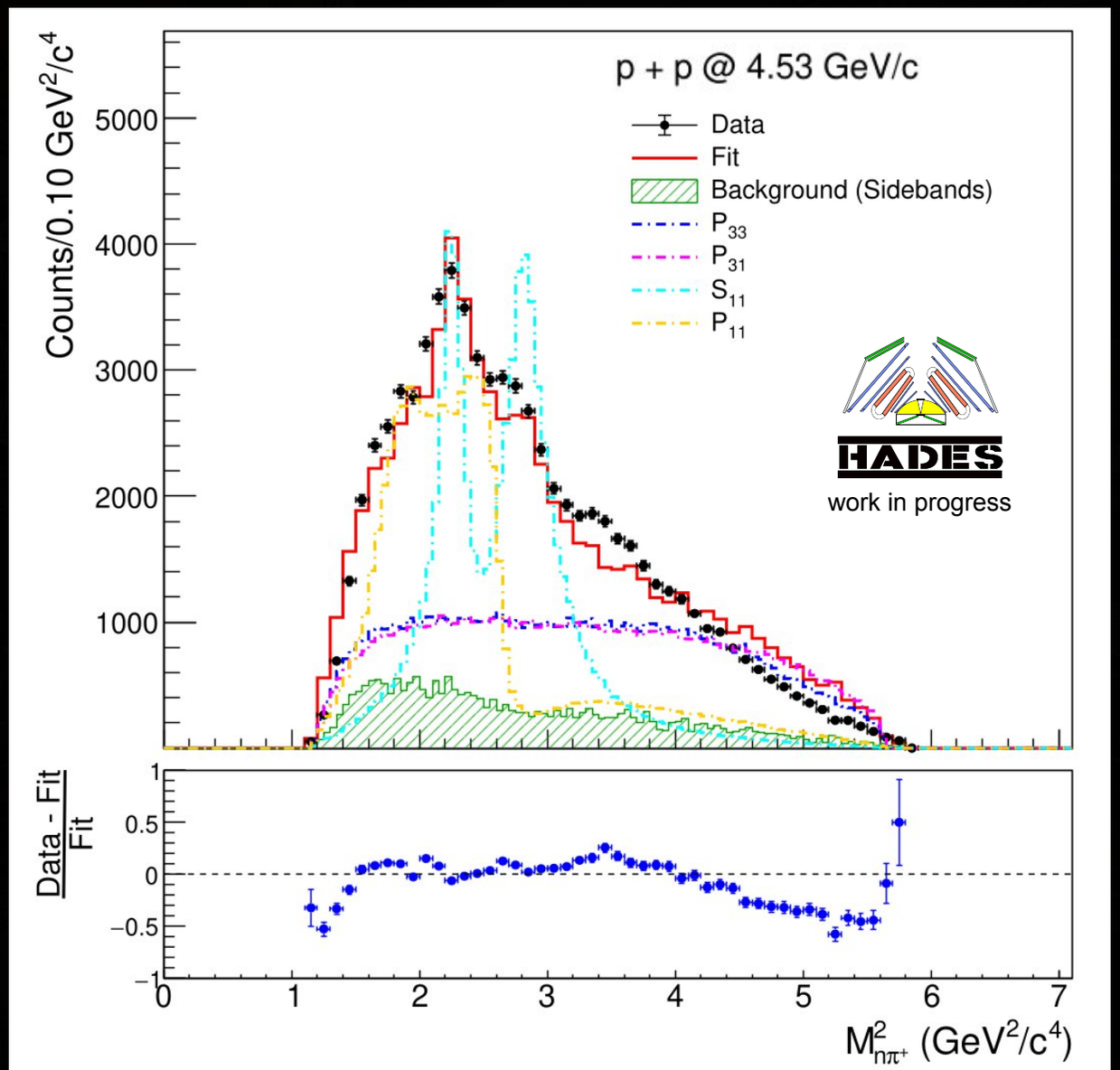

Fit Result (P33,P31,S11 and P11)

$$\frac{\sigma(pp \rightarrow pn\pi^{+})}{\sigma(pp \rightarrow pp\pi^{0})}$$

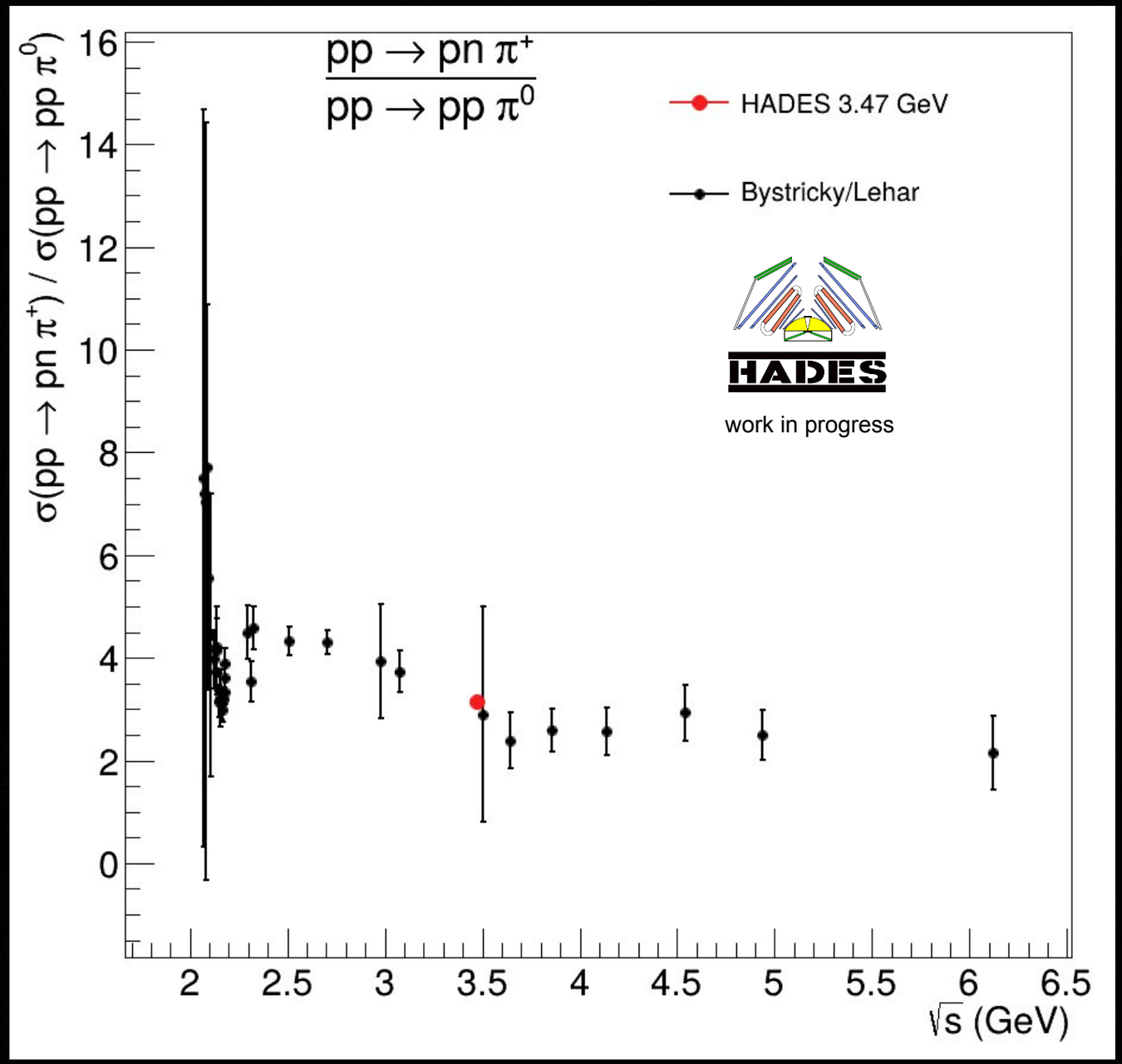

Efficiency Correction based on
$F(M^2_{p\pi^+}), F(M^2_{n\pi^+}), \cos(\theta^{cm}_n), \phi^{cm}_{plane}$

$\frac{\sigma(pp \to pn\pi^+)}{\sigma(pp \to pp\pi^0)}$

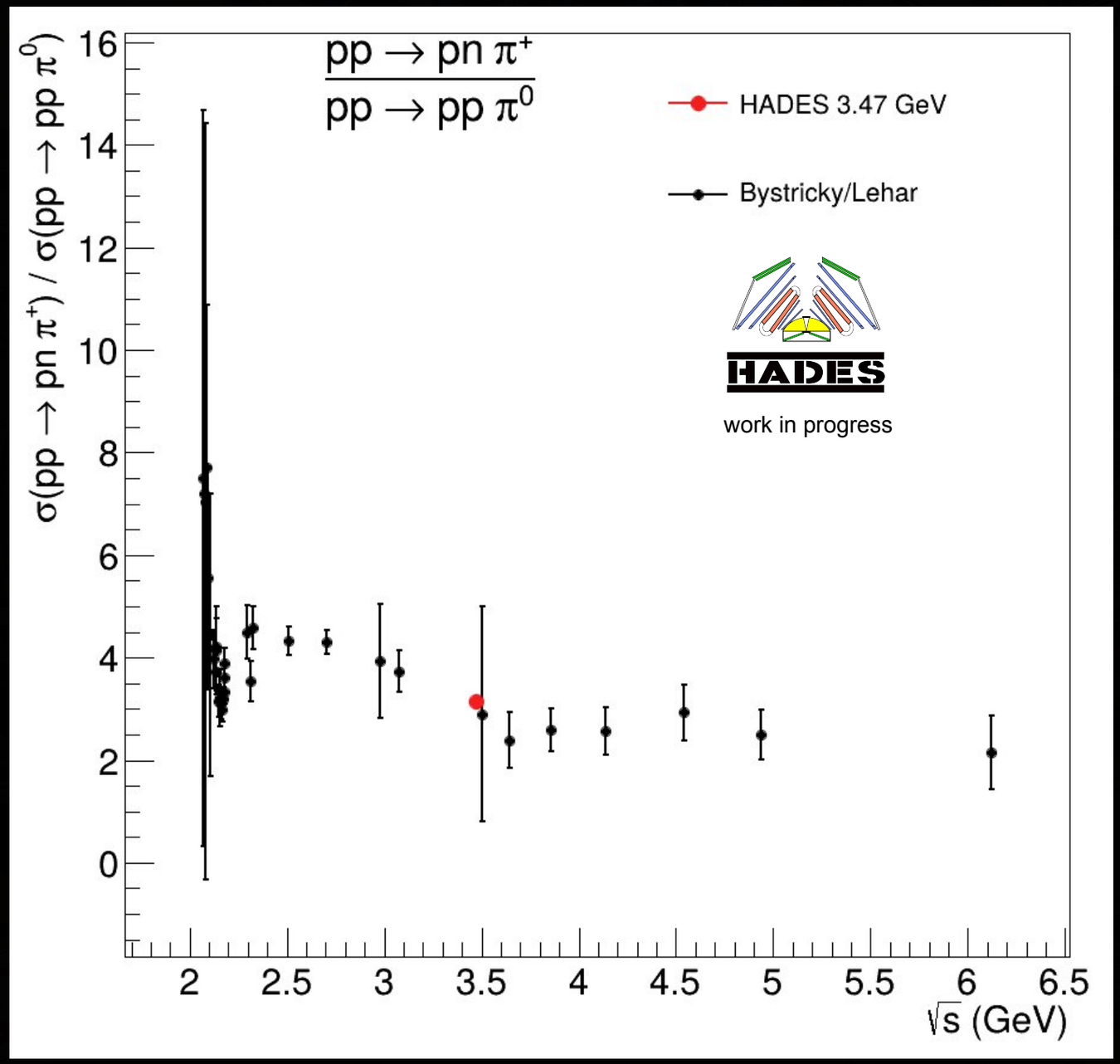

$$\frac{\sigma(pp\to pn\pi^+)}{\sigma(pp\to pp\pi^0)} = 3.1 \pm 0.005\ (stat)$$

The decreasing cross-section ratio reflects the transition from Δ(1232)-dominated pion production to increasing contributions from higher-mass baryon resonances.

Conclusion and Outlook

- The data provides valuable constraints for improving the implementation of baryon-resonance dynamics in transport models such as SMASH.
- Preliminary fit to the $pp \rightarrow pn\pi^+$ case shows the coupled channel machinery works.
- A good benchmark case to validate this machinery and assess whether it can be used to compute the FSI for other channels involving $\mathrm{K}\Lambda$ and $\mathrm{K}\Sigma$.
- Once the fit for $pp \rightarrow pn\pi^+$ case is finalised, quantify the different MB contribution.
- Also do a combined fit of the $pp \rightarrow pn\pi^+$ and $pp \rightarrow pp\pi^0$ channels.
- Extract cross-sections for $pp \rightarrow pn\pi^+$ and $pp \rightarrow pp\pi^0$ channels

Conclusion and Outlook

- The data provides valuable constraints for improving the implementation of baryon-resonance dynamics in transport models such as SMASH.
- Preliminary fit to the $pp \rightarrow pn\pi^+$ case shows the coupled channel machinery works.
- A good benchmark case to validate this machinery and assess whether it can be used to compute the FSI for other channels involving $\mathrm{K}\Lambda$ and $\mathrm{K}\Sigma$.
- Once the fit for $pp \rightarrow pn\pi^+$ case is finalised, quantify the different MB contribution.
- Also do a combined fit of the $pp \rightarrow pn\pi^+$ and $pp \rightarrow pp\pi^0$ channels.
- Extract cross-sections for $pp \rightarrow pn\pi^+$ and $pp \rightarrow pp\pi^0$ channels

Δ Thank You Δ

t_p vs t_n

$$t_p = (p_{beam} - p_{proton})^2$$

$$t_n = (p_{beam} - p_{neutron})^2$$

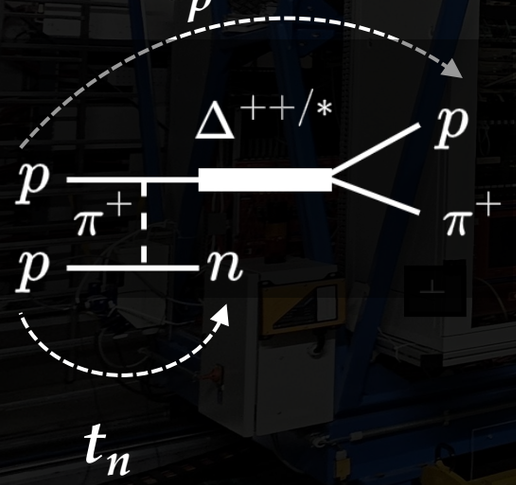

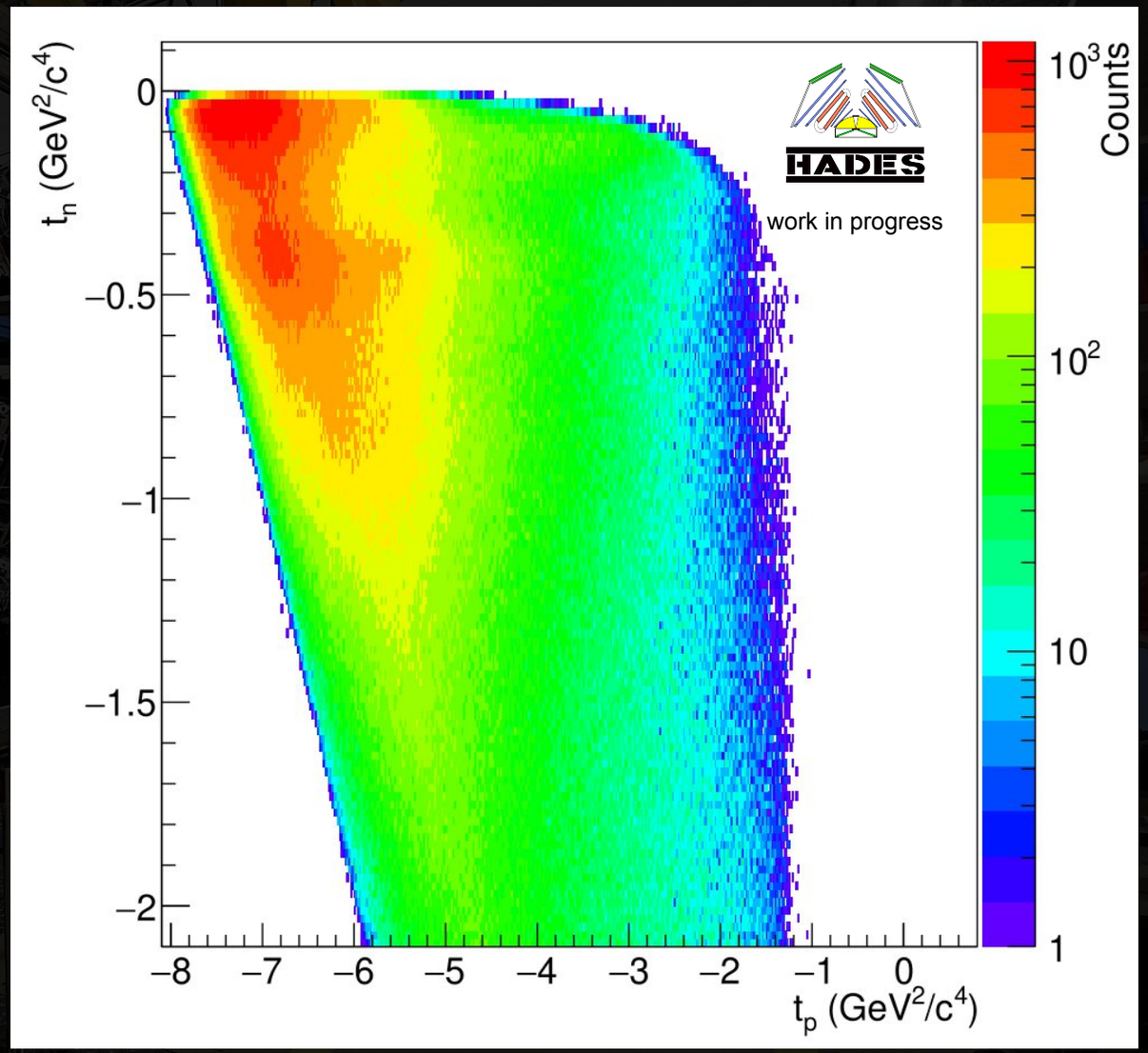

t Resolutions

$$t_2 = (p_{beam} - p_{neutron})^2$$

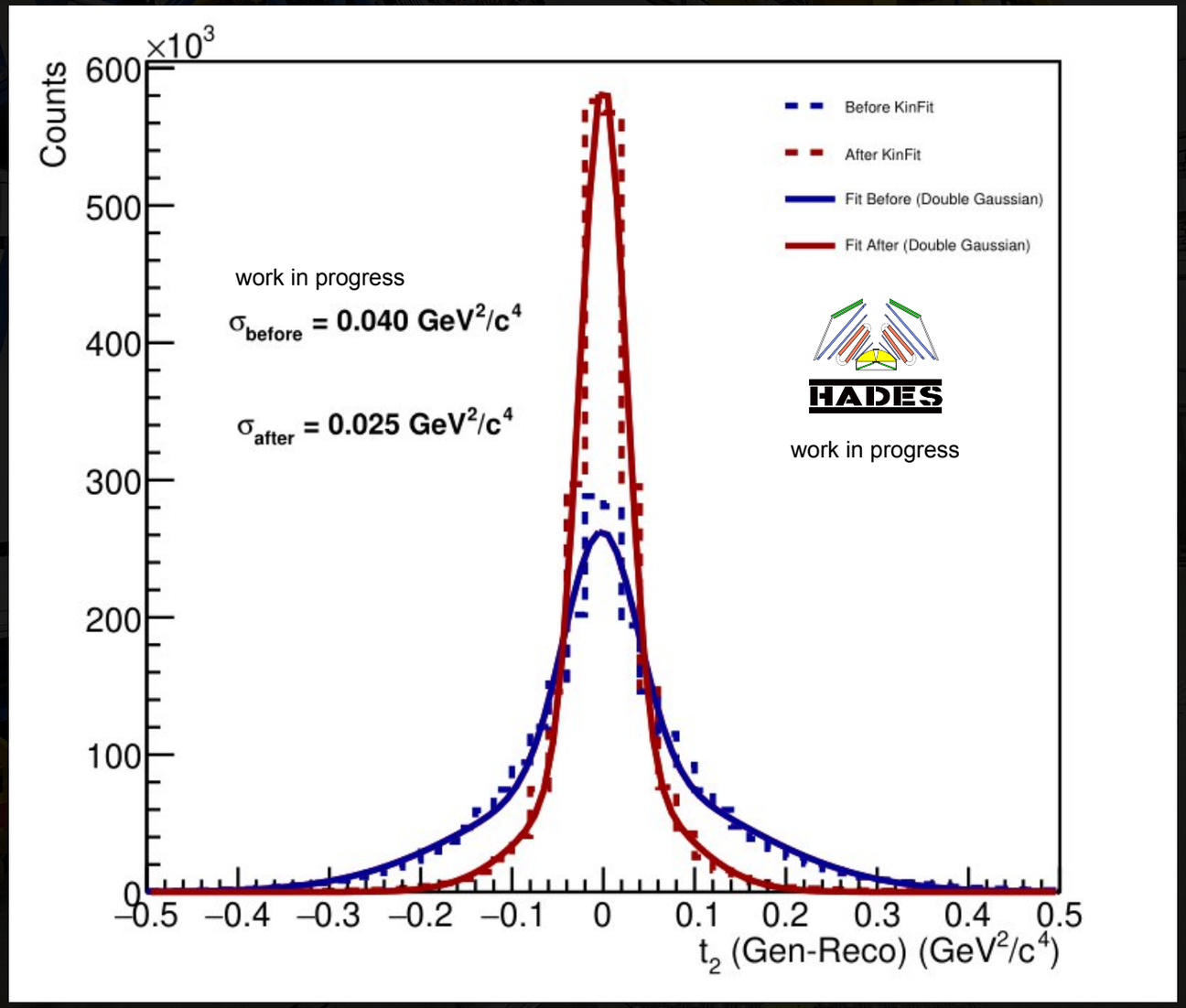

work in progress

$pp \rightarrow pn\pi^+$ with **Jülich-Bonn Dynamic Coupled Channel Approach**

- Dynamical Coupled Channel (DCC) [2] approach : simultaneous analysis of different reactions.
- Allows for extracting the coupling strength of the resonances to final states.

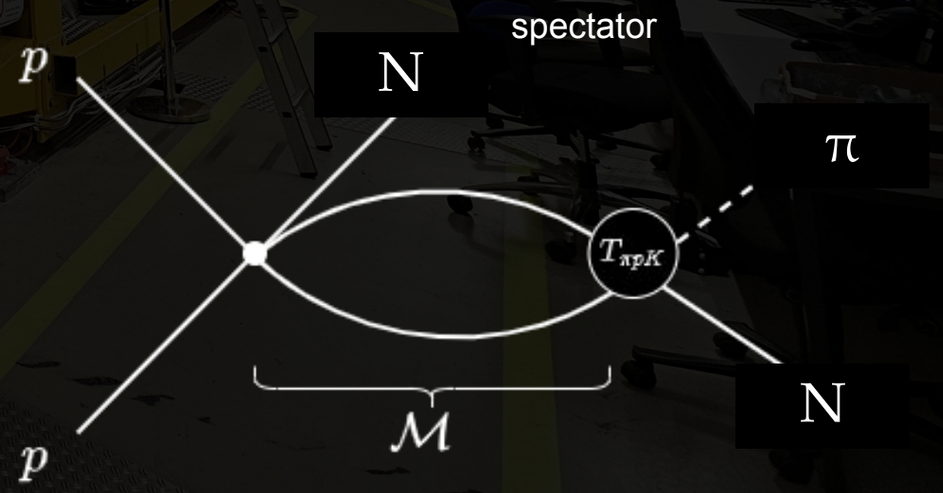

2. D. Rönchen *et al.*, Photocouplings at the pole from pion photoproduction. Eur. Phys. J. A 50 (6) 101 (2014) DOI: 10.1140/epja/i2014-14101-3

$pp \rightarrow pn\pi^+$ with **Jülich-Bonn Dynamic Coupled Channel Approach**

- Dynamical Coupled Channel (DCC) [2] approach : simultaneous analysis of different reactions.
- Allows for extracting the coupling strength of the resonances to final states.
- $\mathcal{M}$ is the invariant matrix element for calculating the invariant mass distribution and $T_{\pi pK}$ is the full JüBo T-Matrix for different channels ($\mathrm{K} \rightarrow \pi\mathrm{N}$), includes s-channel and dynamically generated resonances.

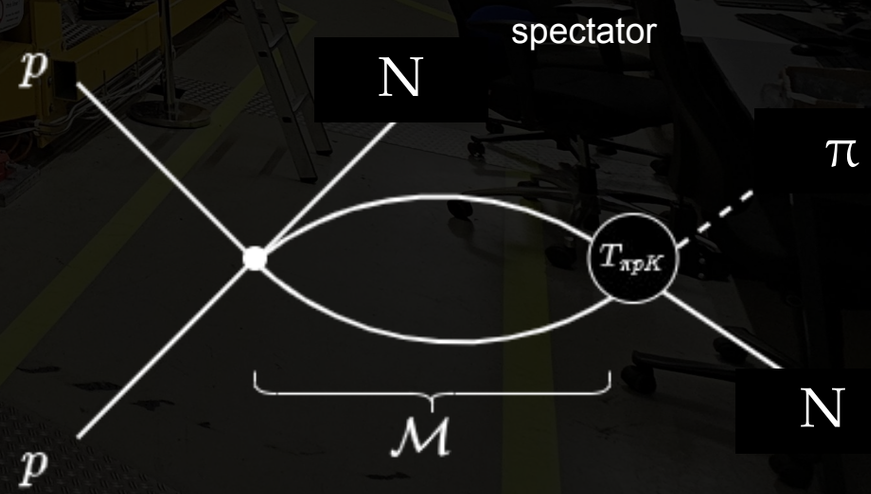

2. D. Rönchen *et al.*, Photocouplings at the pole from pion photoproduction. Eur. Phys. J. A 50 (6) 101 (2014) DOI: 10.1140/epja/i2014-14101-3

$pp \to pn\pi^+$ with **Jülich-Bonn Dynamic Coupled Channel Approach**

- Dynamical Coupled Channel (DCC) [2] approach : simultaneous analysis of different reactions.
- Allows for extracting the coupling strength of the resonances to final states.
- $\mathcal{M}$ is the invariant matrix element for calculating the invariant mass distribution and $T_{\pi pK}$ is the full JüBo T-Matrix for different channels ($\mathrm{K} \to \pi\mathrm{N}$), includes s-channel and dynamically generated resonances.

$$\mathcal{M}_{\mu\nu}(q,p',\epsilon) = V_{\mu\nu}(q,p',\epsilon) + \sum_{\hat{K}} \int_0^\infty dp\, p^2 T_{\mu\hat{K}}(q,p,\epsilon) G_{\hat{K}}(p,\epsilon) V_{\hat{K}\nu}(p,p',\epsilon)$$

Kernel which contains the coupling information of the resonances to the final state

all possible meson baryon channels

ϵ - C.M energy of $pp \to pn\pi^+$

- $\mathrm{MB} \to \mathrm{MB}$ interactions (e.g. FSI) are incorporated by Jülich-Bonn model (fitted through lots of data) within SU(3) dynamics.

2. D. Rönchen *et al.*, *Photocouplings at the pole from pion photoproduction. Eur. Phys. J. A 50 (6) 101 (2014) DOI: 10.1140/epja/i2014-14101-3*

$pp \to pn\pi^+$ with **Jülich-Bonn Dynamic Coupled Channel Approach**

- Dynamical Coupled Channel (DCC) [2] approach : simultaneous analysis of different reactions.
- Allows for extracting the coupling strength [illegible] final states.
- $\mathcal{M}$ is the invariant matrix [illegible] distribution and $T_{\pi N}$ [illegible] includes s-ch[illegible]

$$\mathcal{M}_{\mu\nu}(\quad \epsilon)G_K(p,\epsilon)V_{K\nu}(p,p',\epsilon)$$

all possible meson baryon channels

ϵ - C.M energy of $pp \to pn\pi^+$

Can we decouple final-state interactions from the production mechanism?

- MB → MB int[illegible]ctions (e.g. FSI) are incorporated by Jülich-Bonn model (fitted through lots of data) within SU(3) dynamics.

2. D. Rönchen *et al.*, *Photocouplings at the pole from pion photoproduction. Eur. Phys. J. A 50 (6) 101 (2014) DOI: 10.1140/epja/i2014-14101-3*

AmpTools – Framework for Amplitude Analysis

Purpose:

- Toolkit for performing Partial Wave Analysis (PWA)[3].
- Fits complex amplitudes for exclusive reactions.

Key Features:

- Flexible physics model definitions (resonances, backgrounds).
- Coherent and incoherent amplitude combinations.
- Event-based maximum likelihood fitting.

$$-2\ln\mathcal{L}(\theta) = -2\left(\sum_{i=1}^{N}\ln I(x_i;\theta) - \int I(x;\theta)\eta(x)\,dx\right) + c_1$$

- GPU acceleration for fast computations.
- Interfaces with ROOT.

3. doi.org/10.5281/zenodo.5039377

Normalization and Barrier Factors

- The amplitude is normalized and multiplied by a barrier factor:

$$A_{JuBo}(L,I,J) = B_L(q)\sqrt{\frac{\rho(s,m_1,m_2)\,K_f}{K_i}}A_{L,I,J}(\alpha,\gamma)$$

- $B_L(\mathrm{q})$ is the Blatt-Weisskopf barrier factor for a spectator with the orbital angular momentum L.
- K_i,K_f are initial and final momenta in the CM frame.
- ρ is the Meson-Baryon phase space volume.

Testing the Machinery

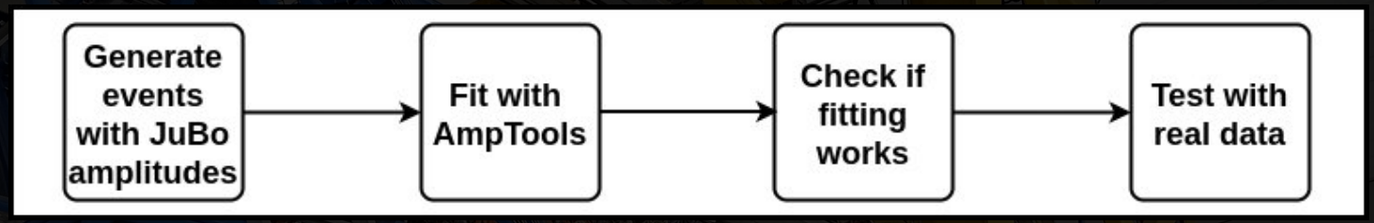

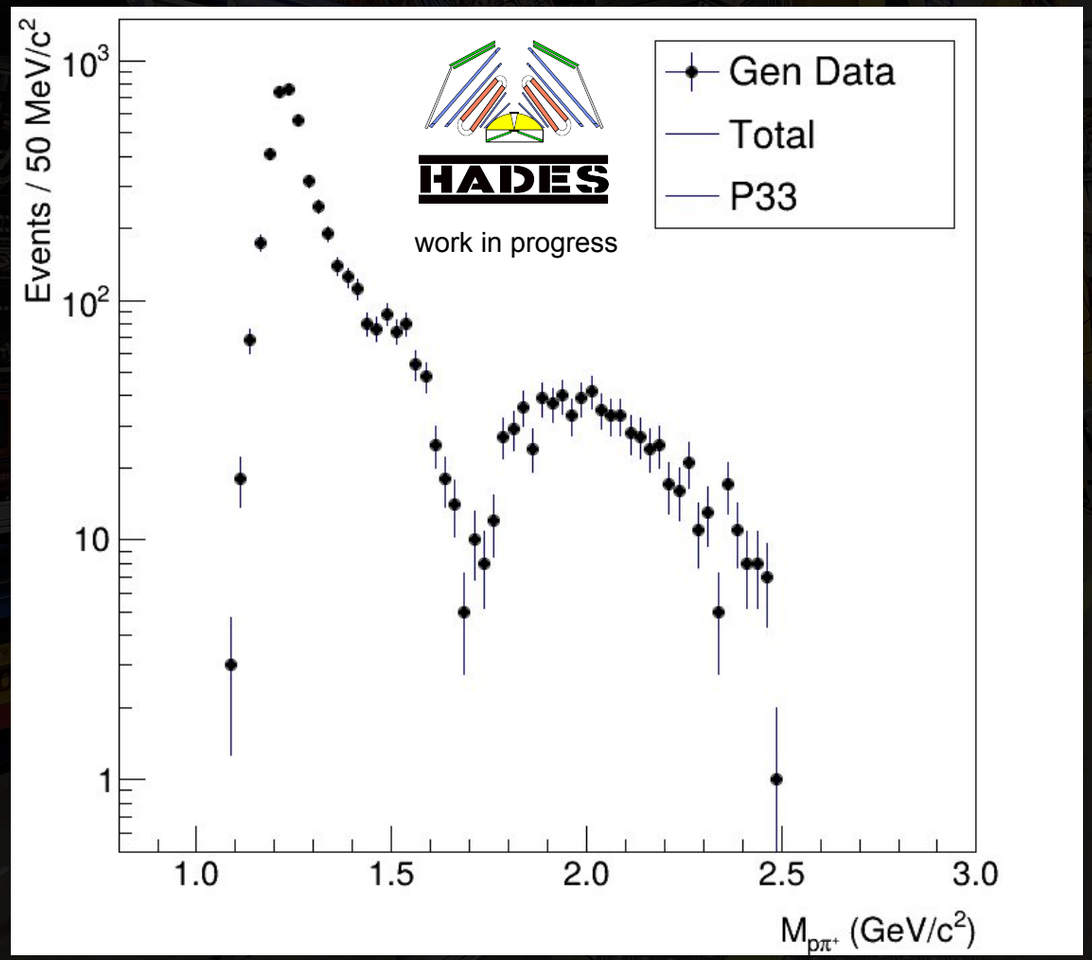

Testing the Machinery

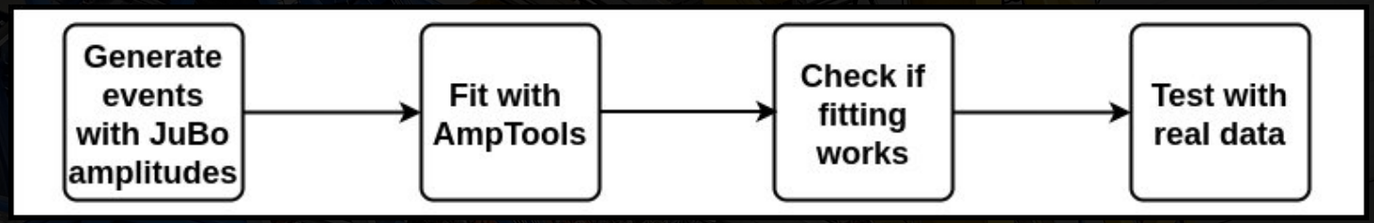

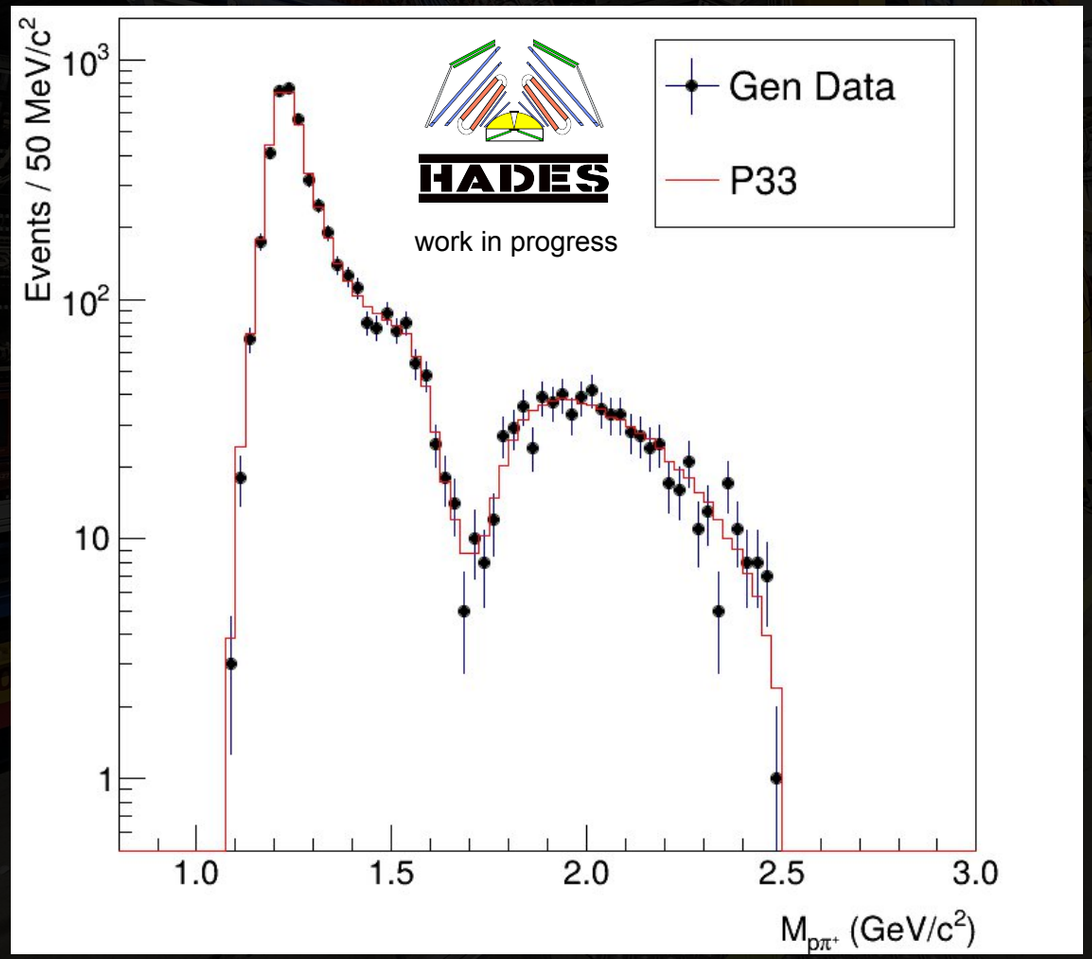

Testing the Machinery

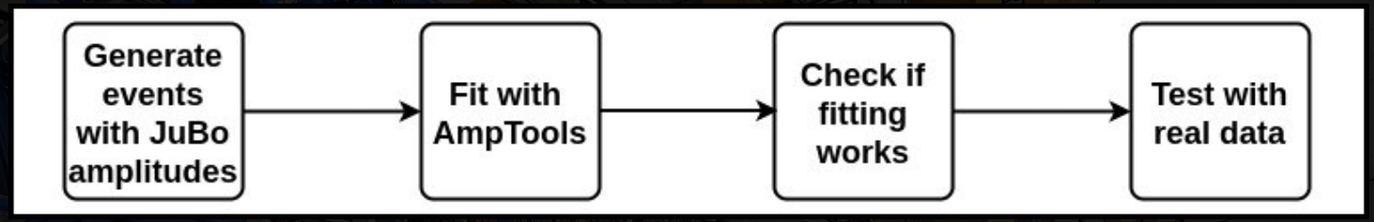

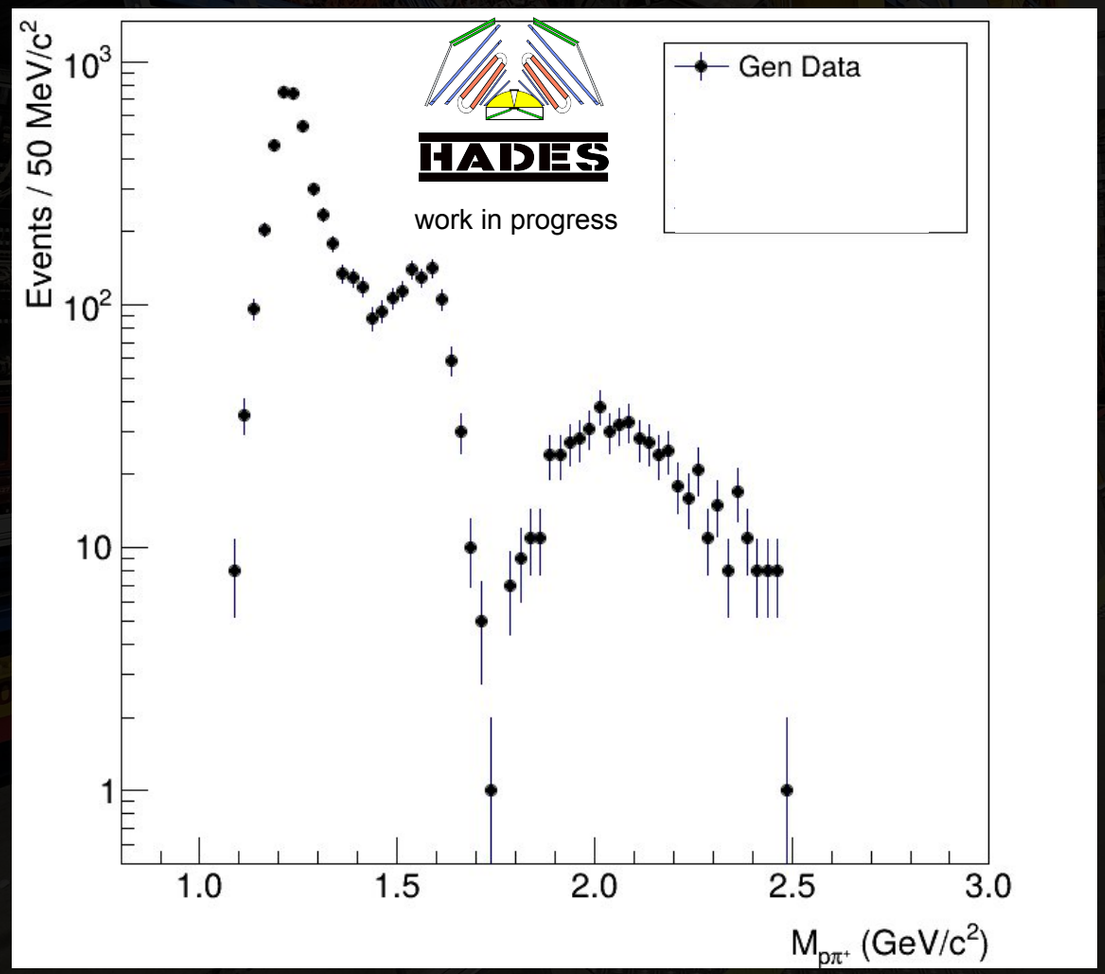

Testing the Machinery

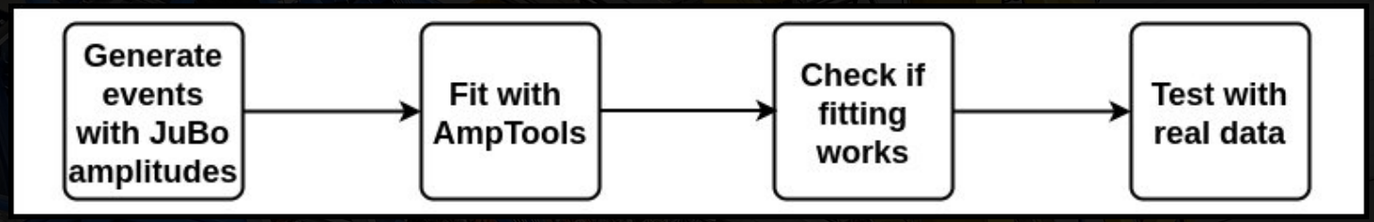

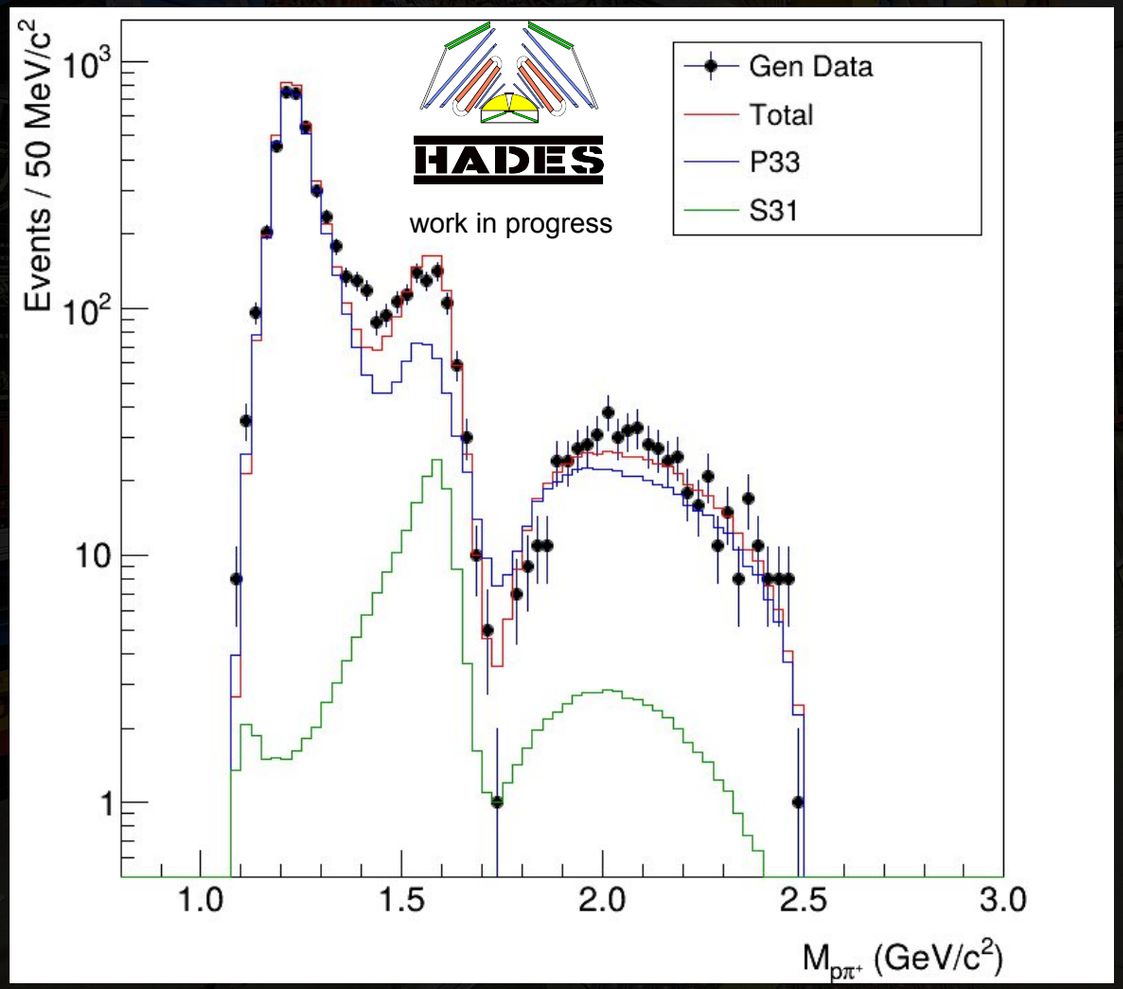

Preliminary Fit Results

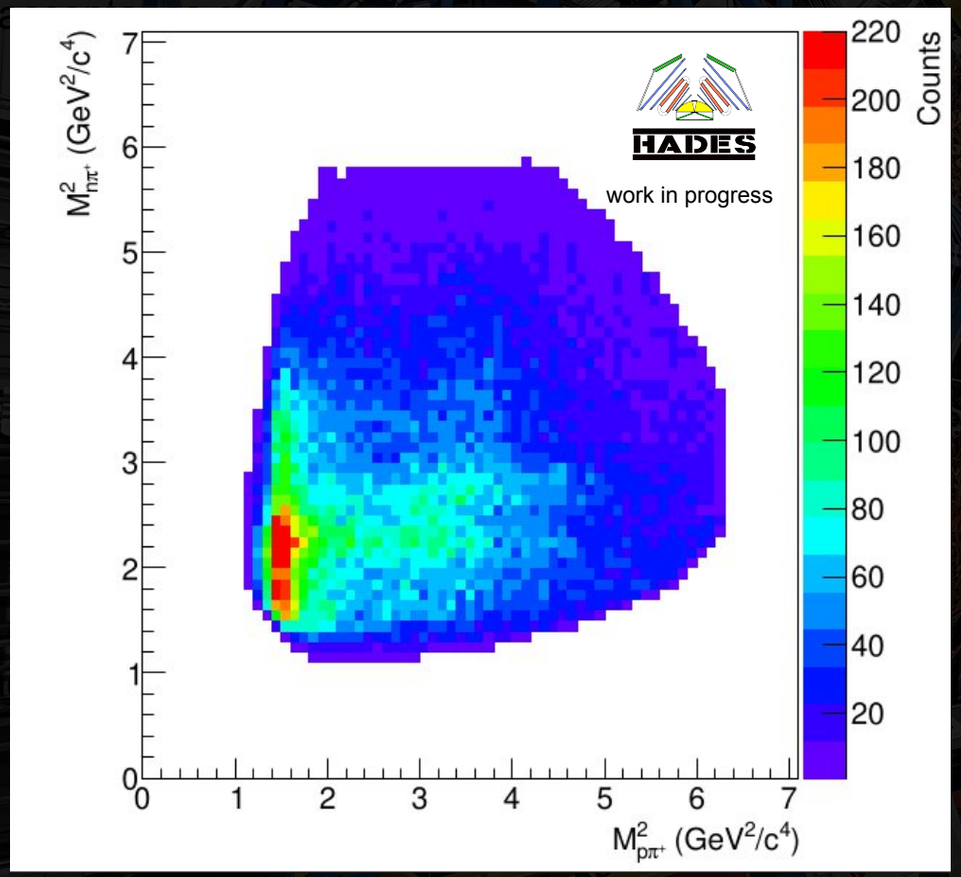

Data

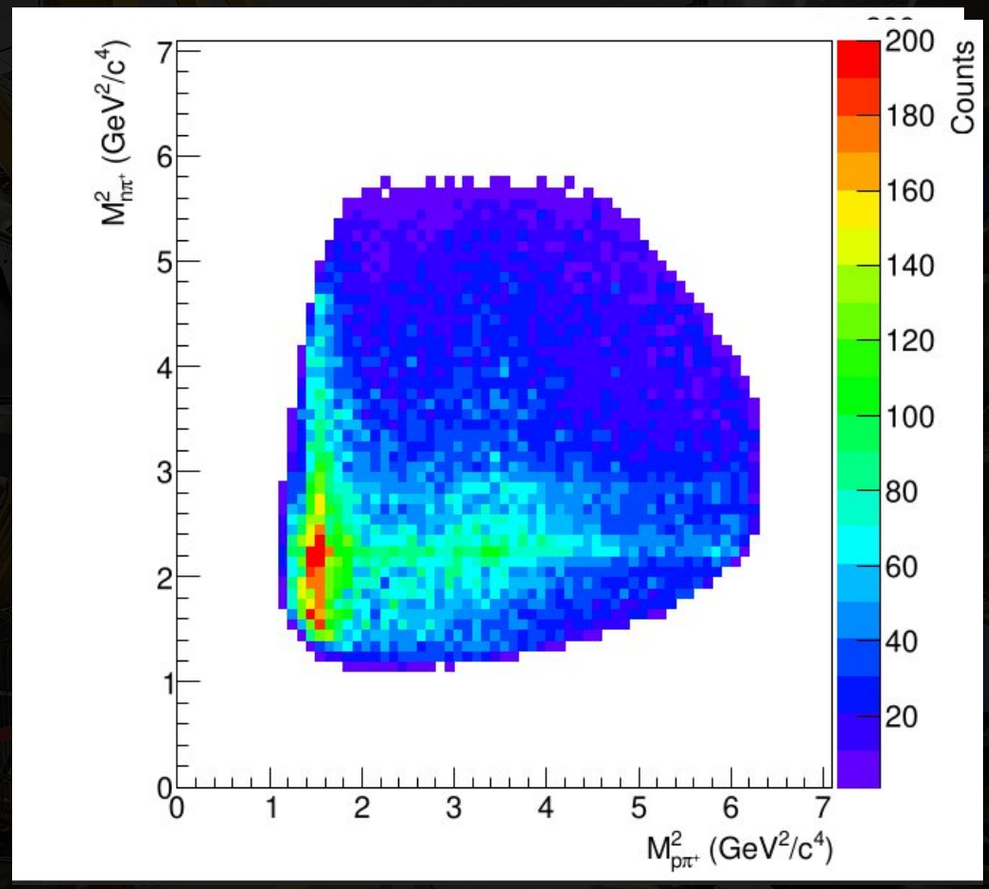

Fit Result (P33,P31,S11 and P11)

Preliminary Fit Results

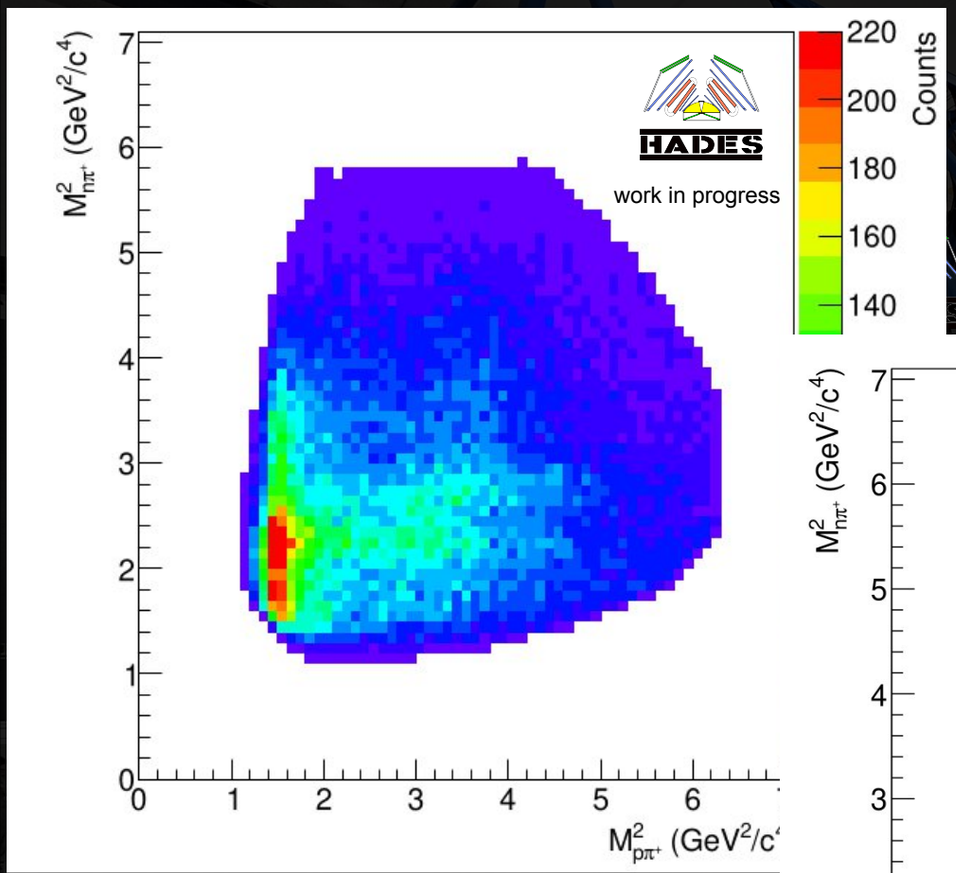

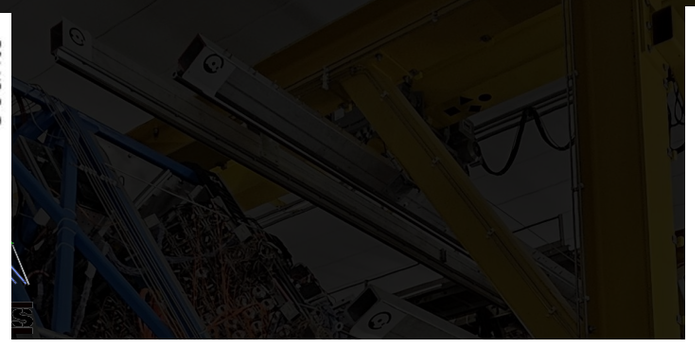

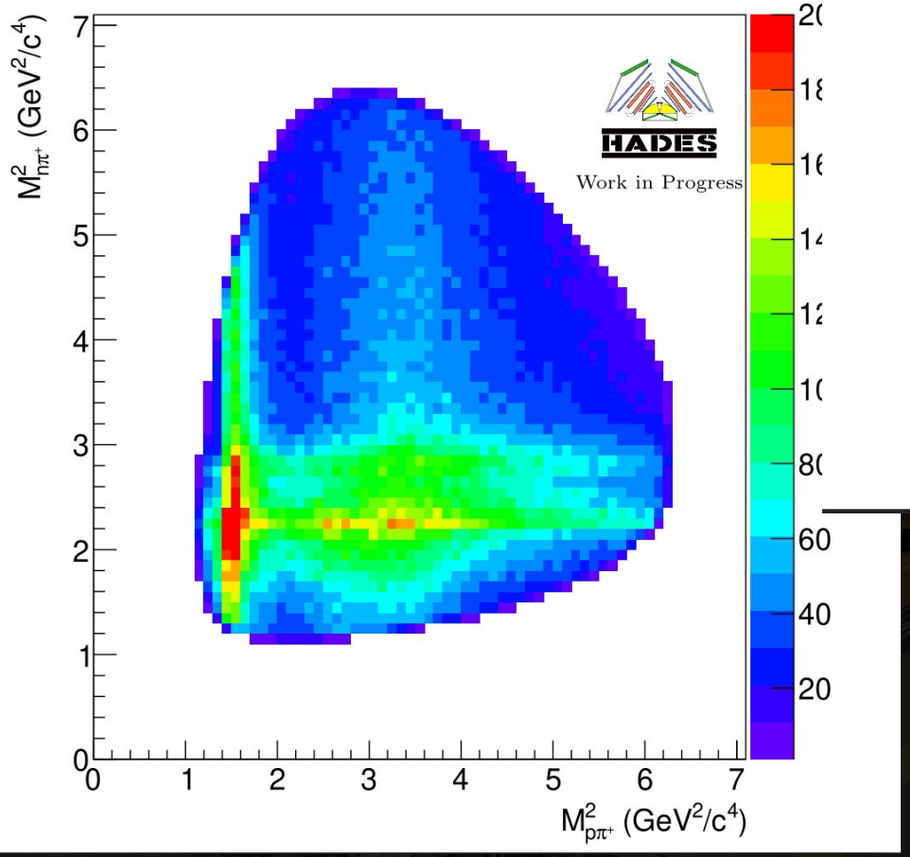

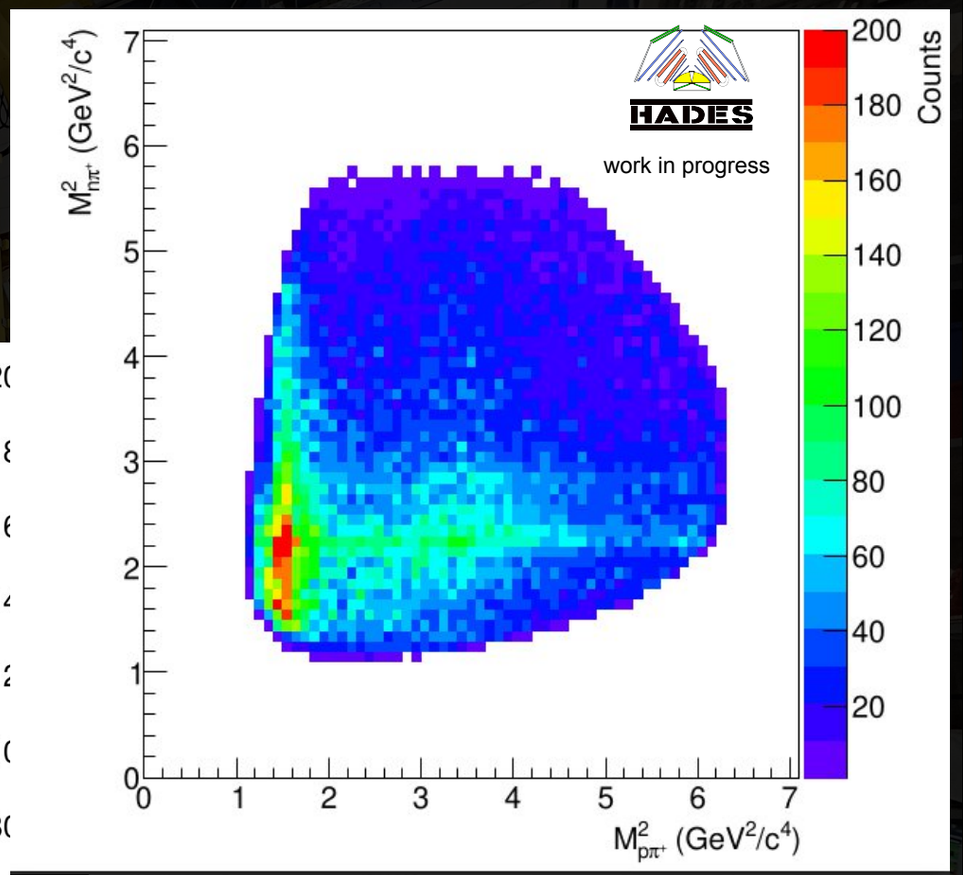

Data

Acceptance Corrected

Fit Result (P33,P31,S11 and P11)

Preliminary Fit Results

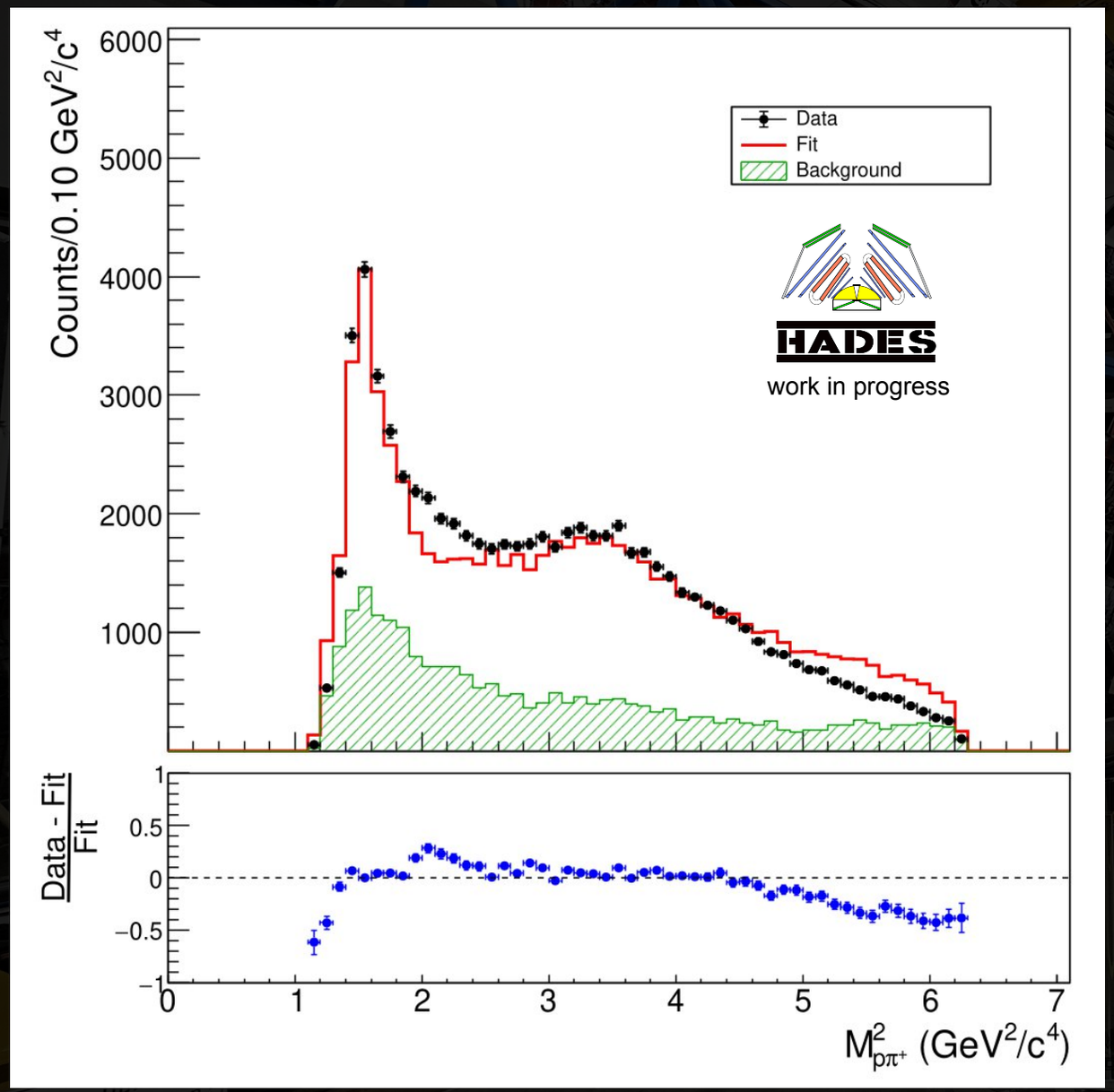

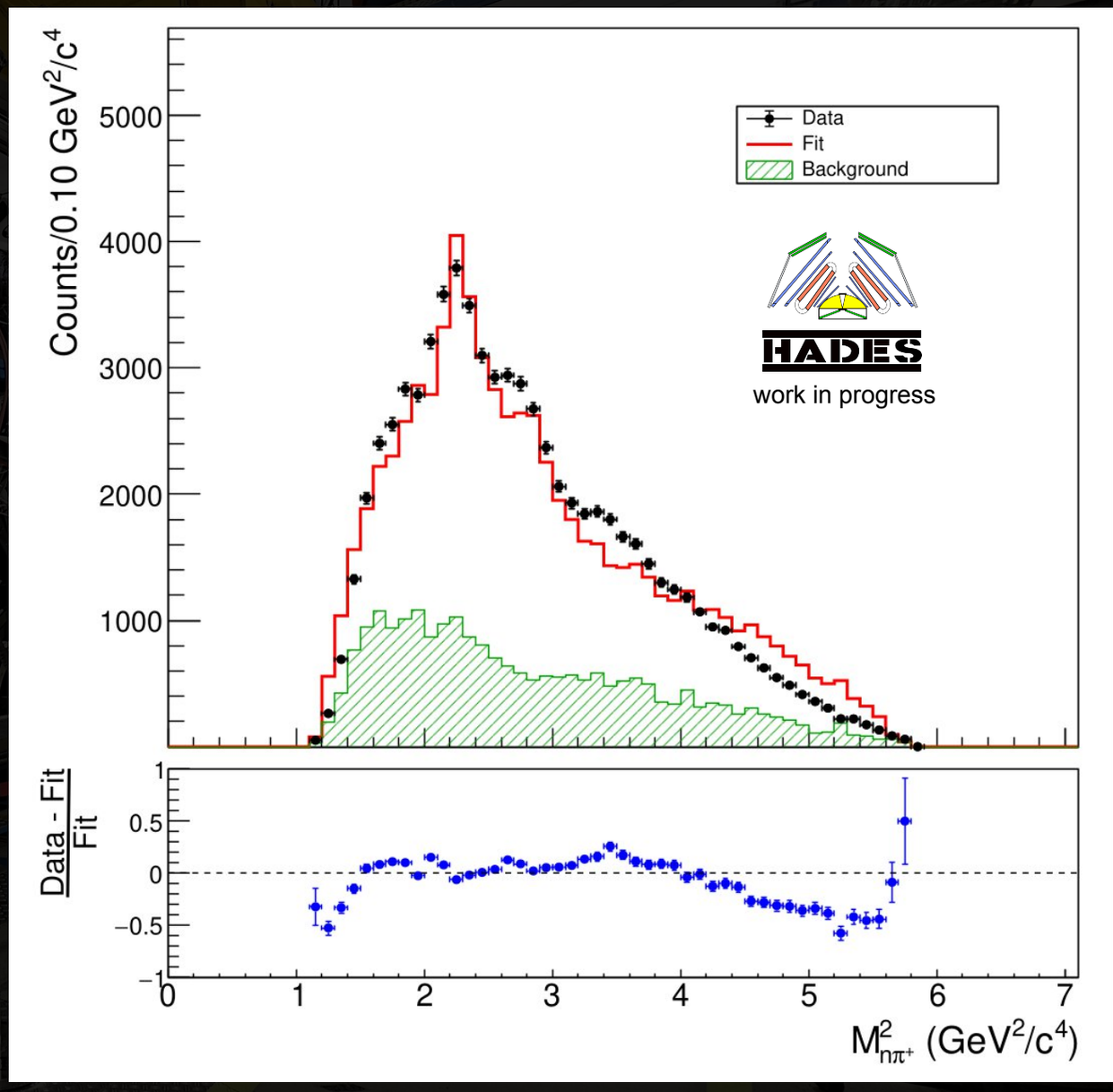

Fit Result (P33,P31,S11 and P11)

Comparision to Transport Models

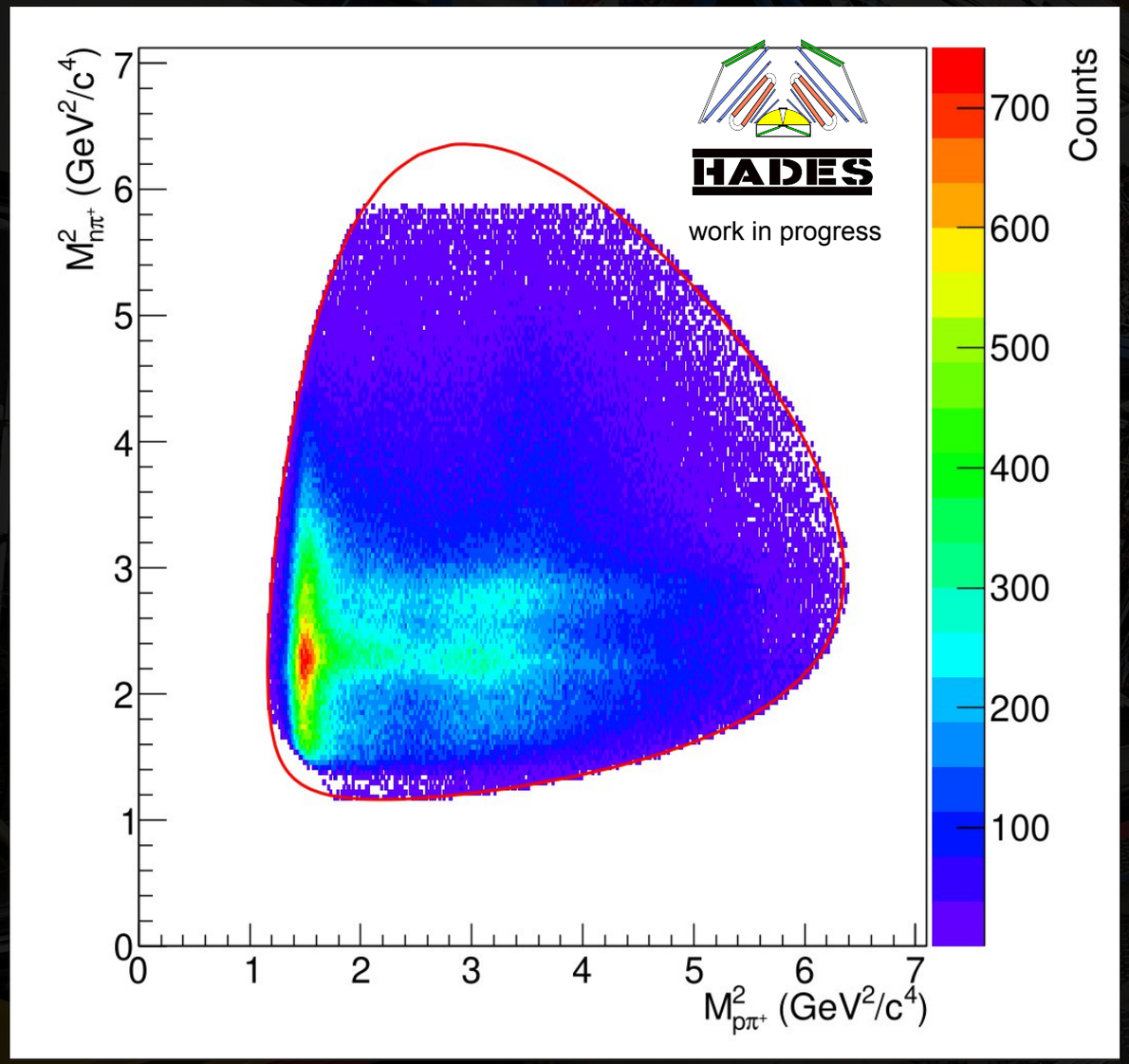

Data

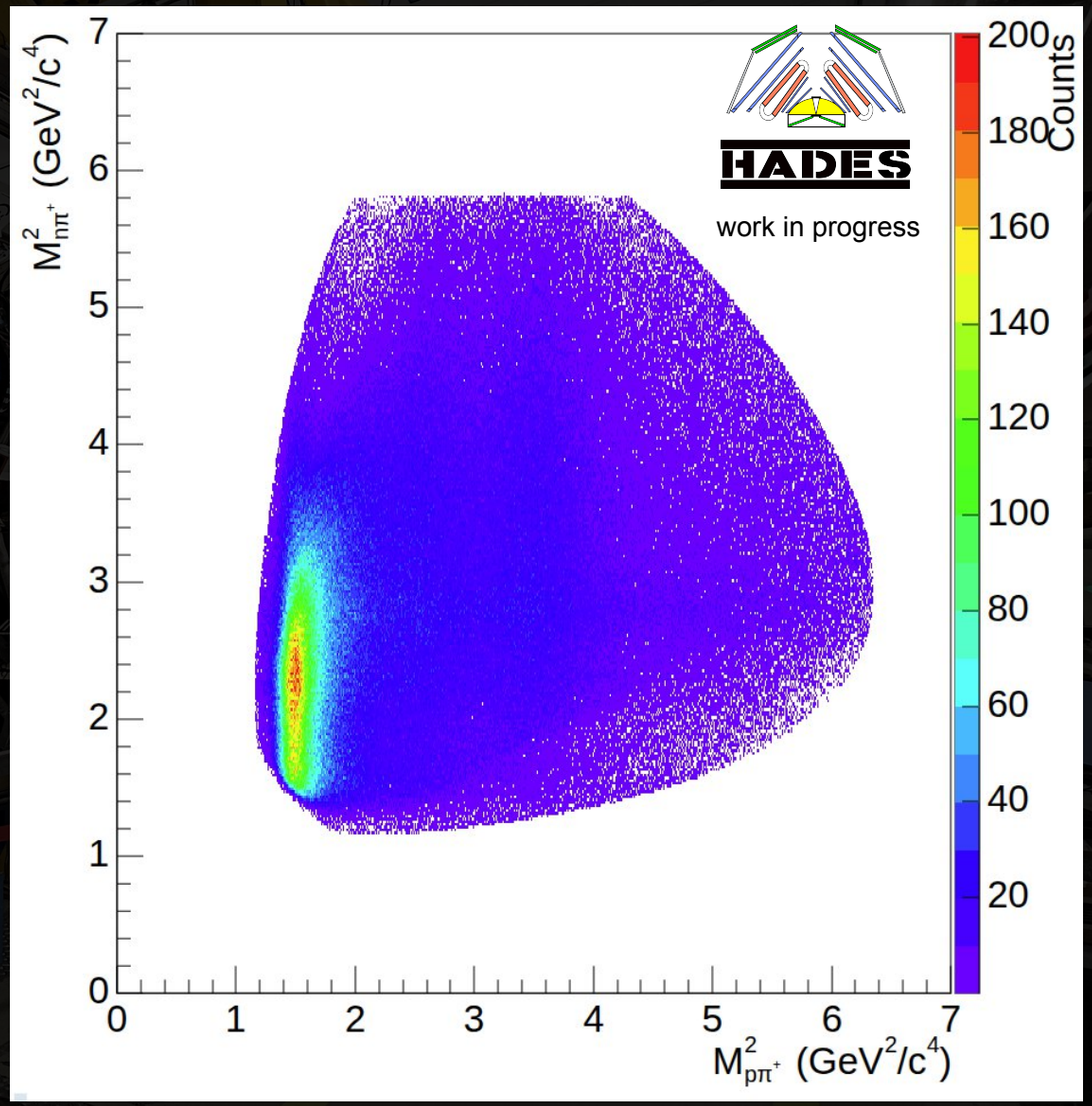

SMASH[4]

4. https://doi.org/10.5281/zenodo.17878251

Comparision to SMASH

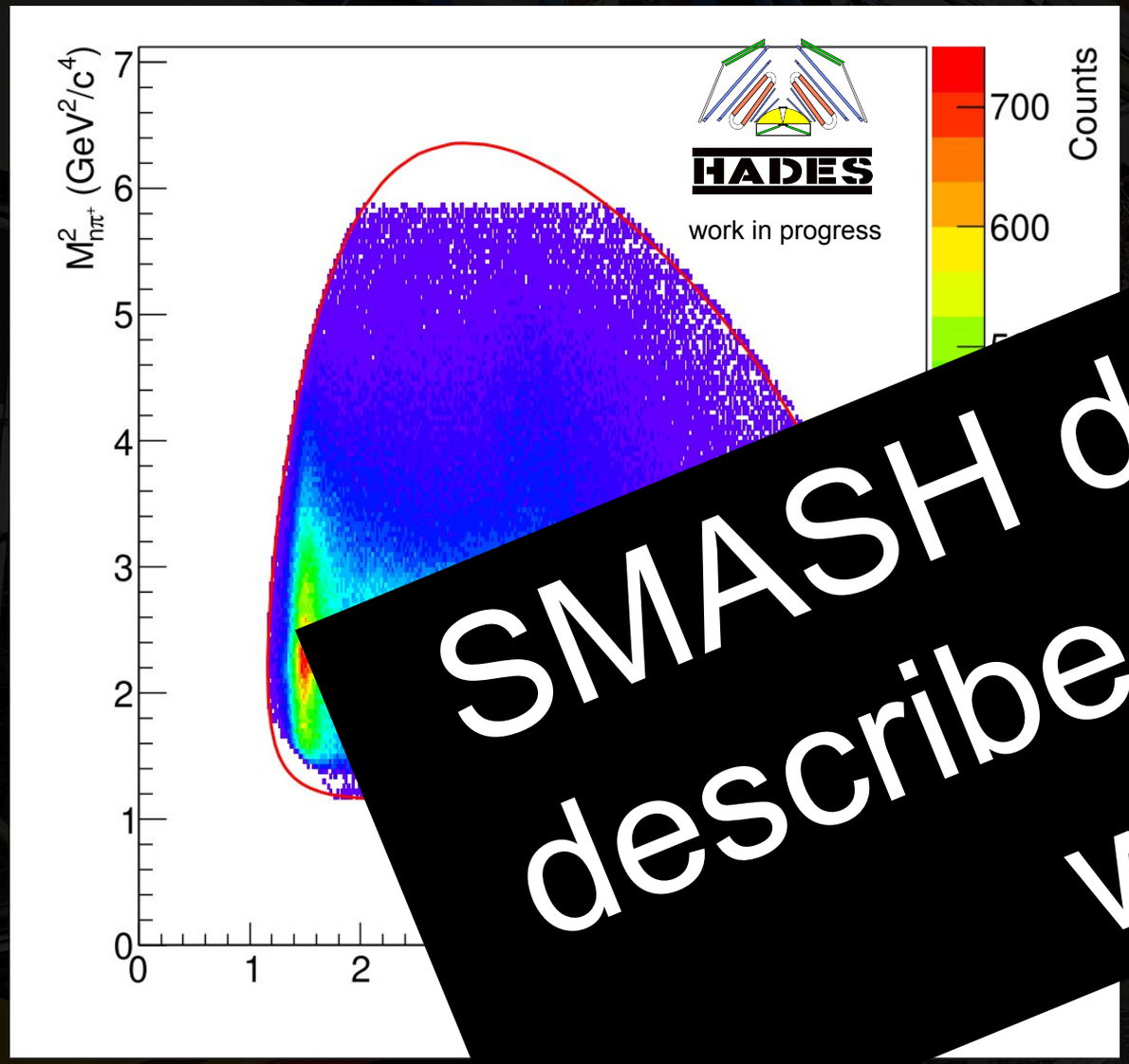

SMASH does not describe the data well

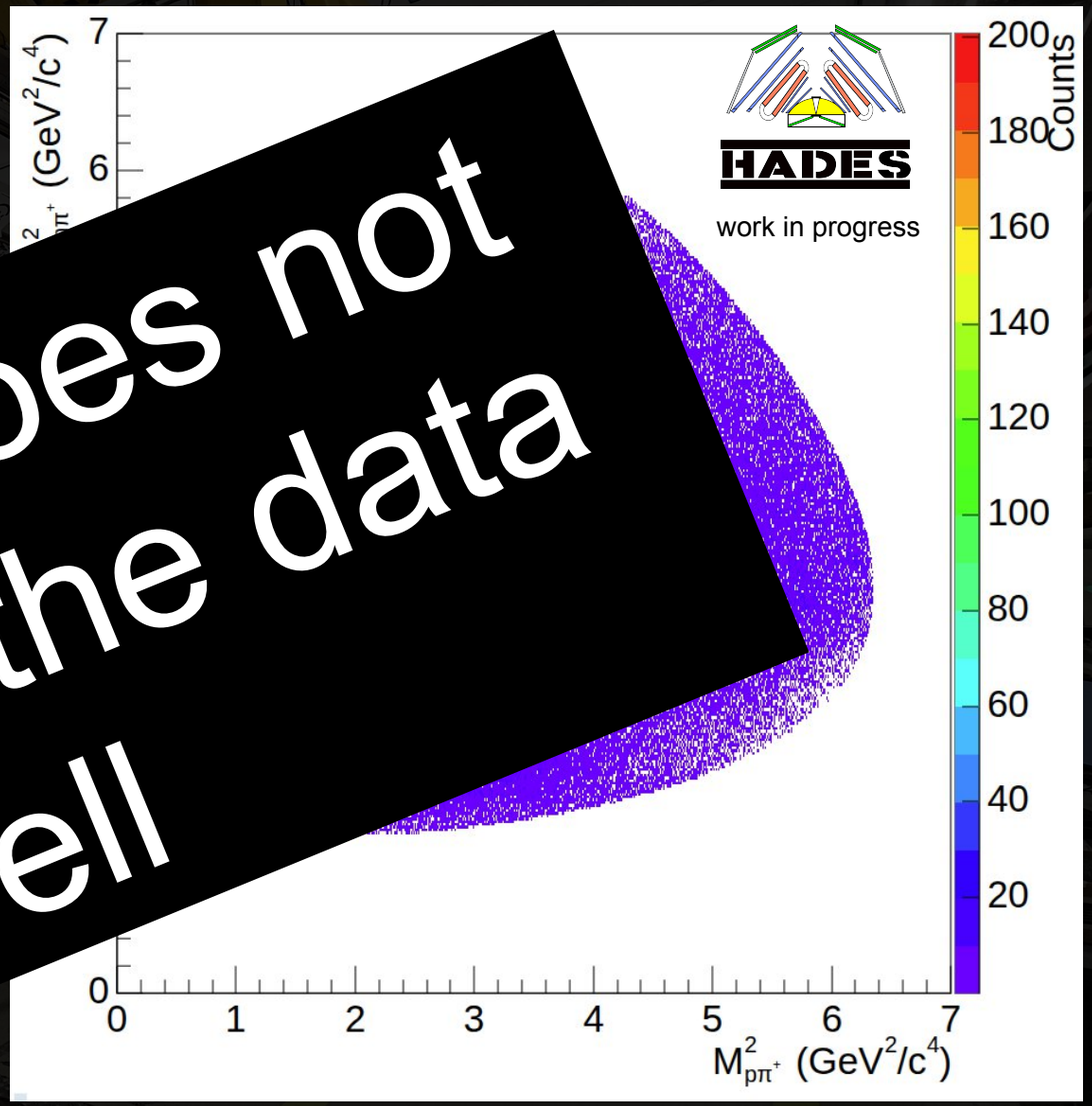

SMASH

$pp \rightarrow pp\pi^0$

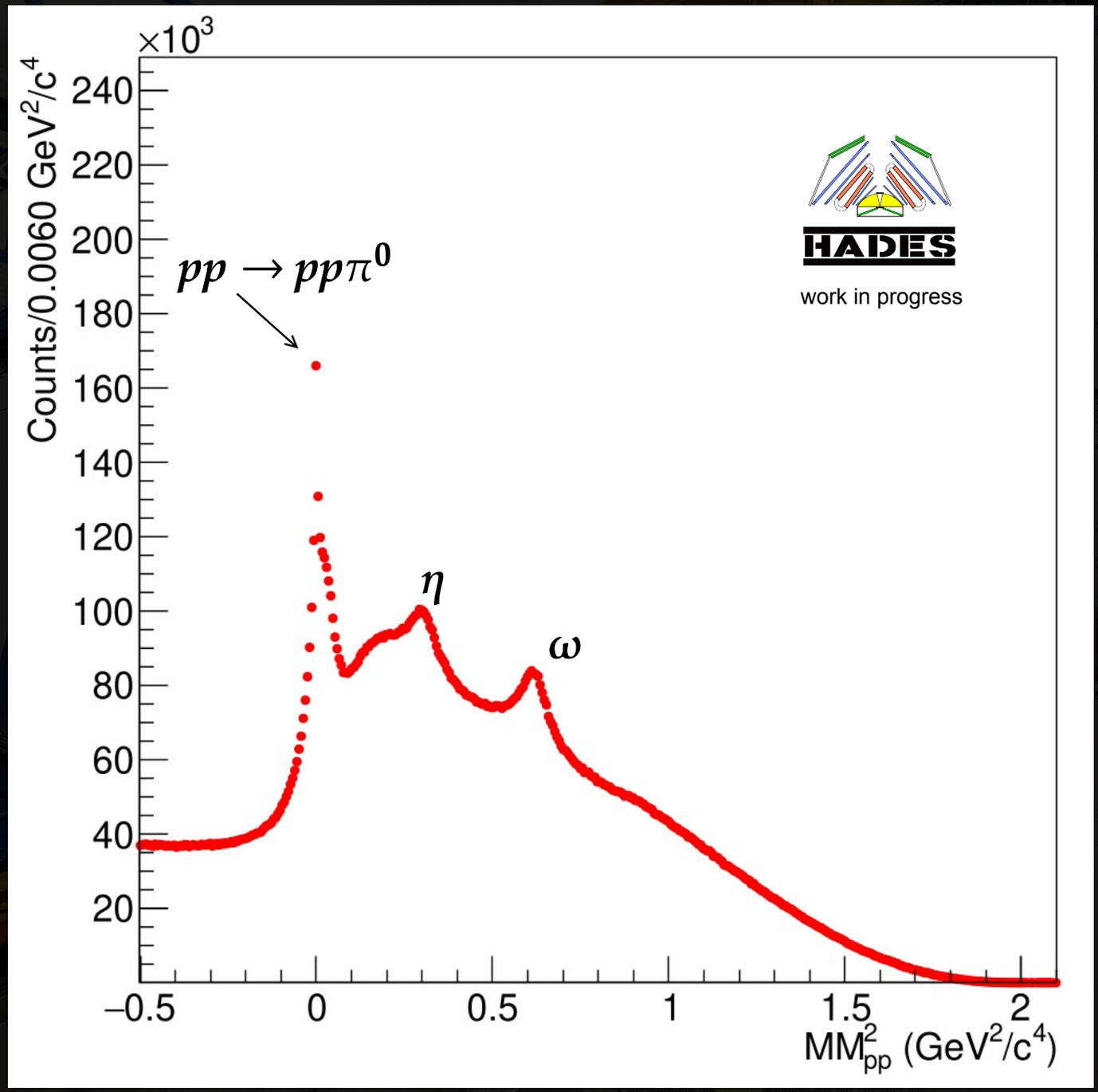

work in progress

Elastic Cut

- Inelastic events are selected by applying cuts based on the expected kinematics of elastic scattering.

$$\Delta\phi = |\phi_1 - \phi_2| = 180^\circ$$

$$\tan\theta_1 \times \tan\theta_2 = \frac{1}{\gamma_{CM}^2}$$

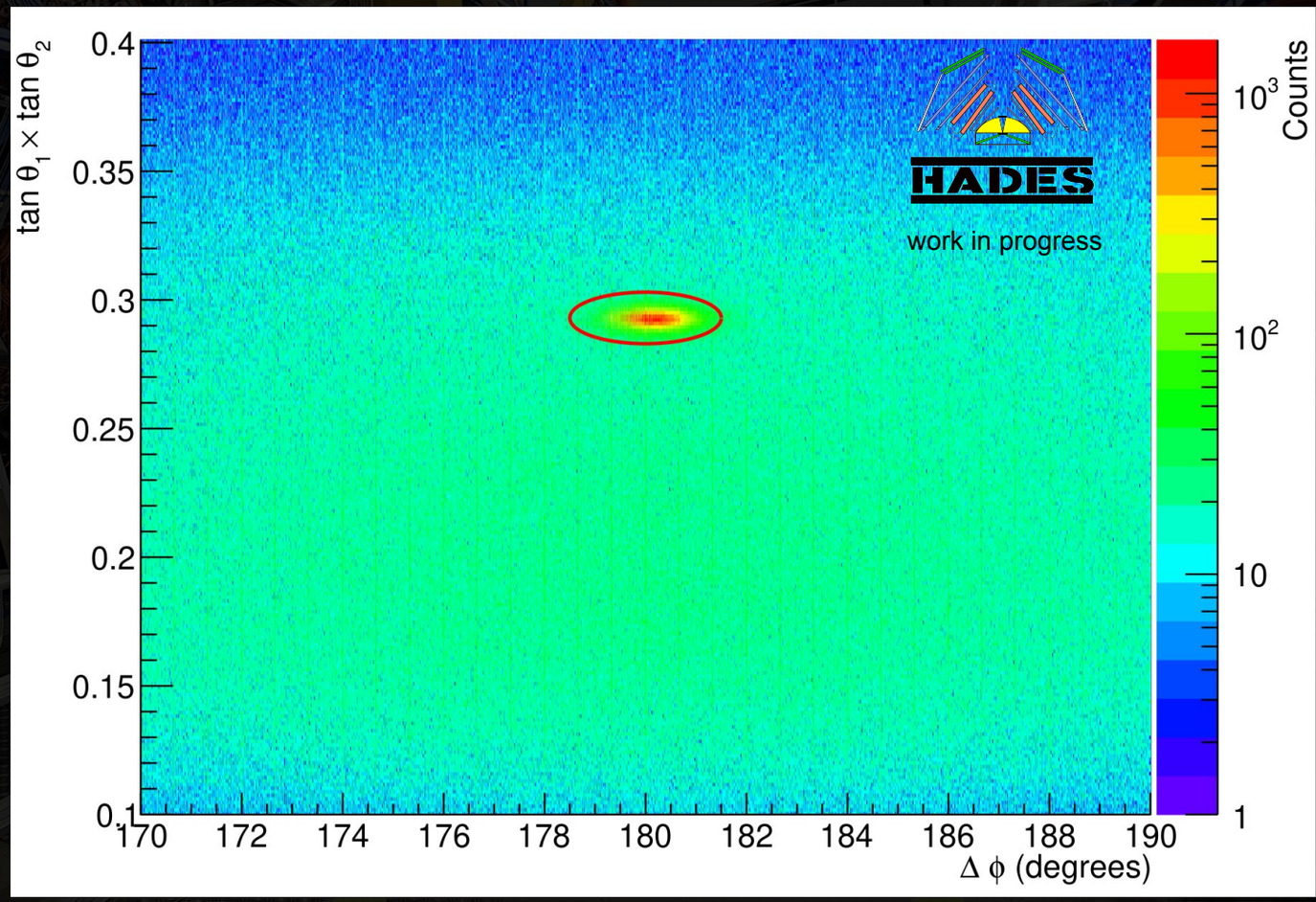

$pp \rightarrow pp\pi^0$

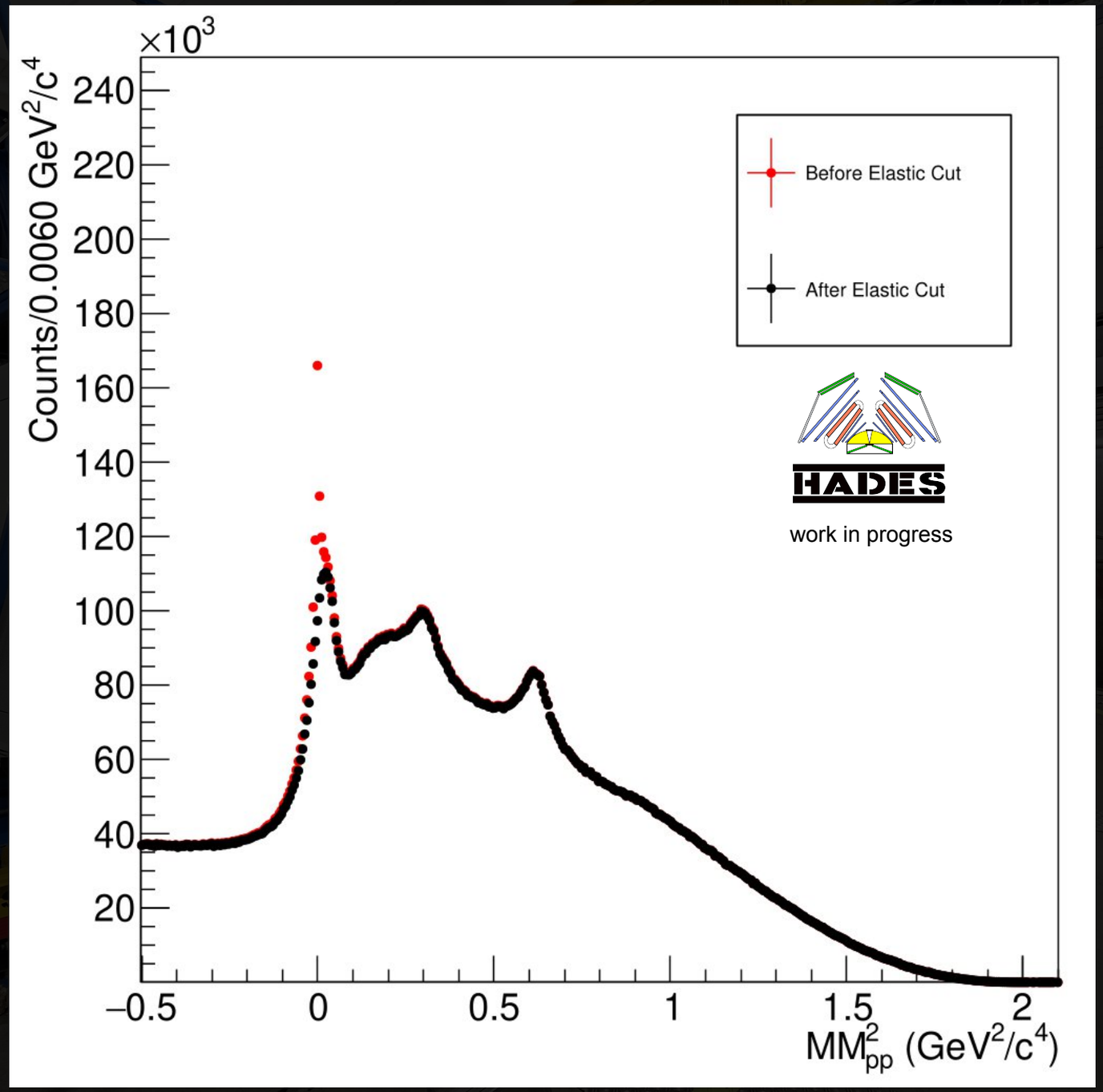

$pp \rightarrow pp\pi^0$

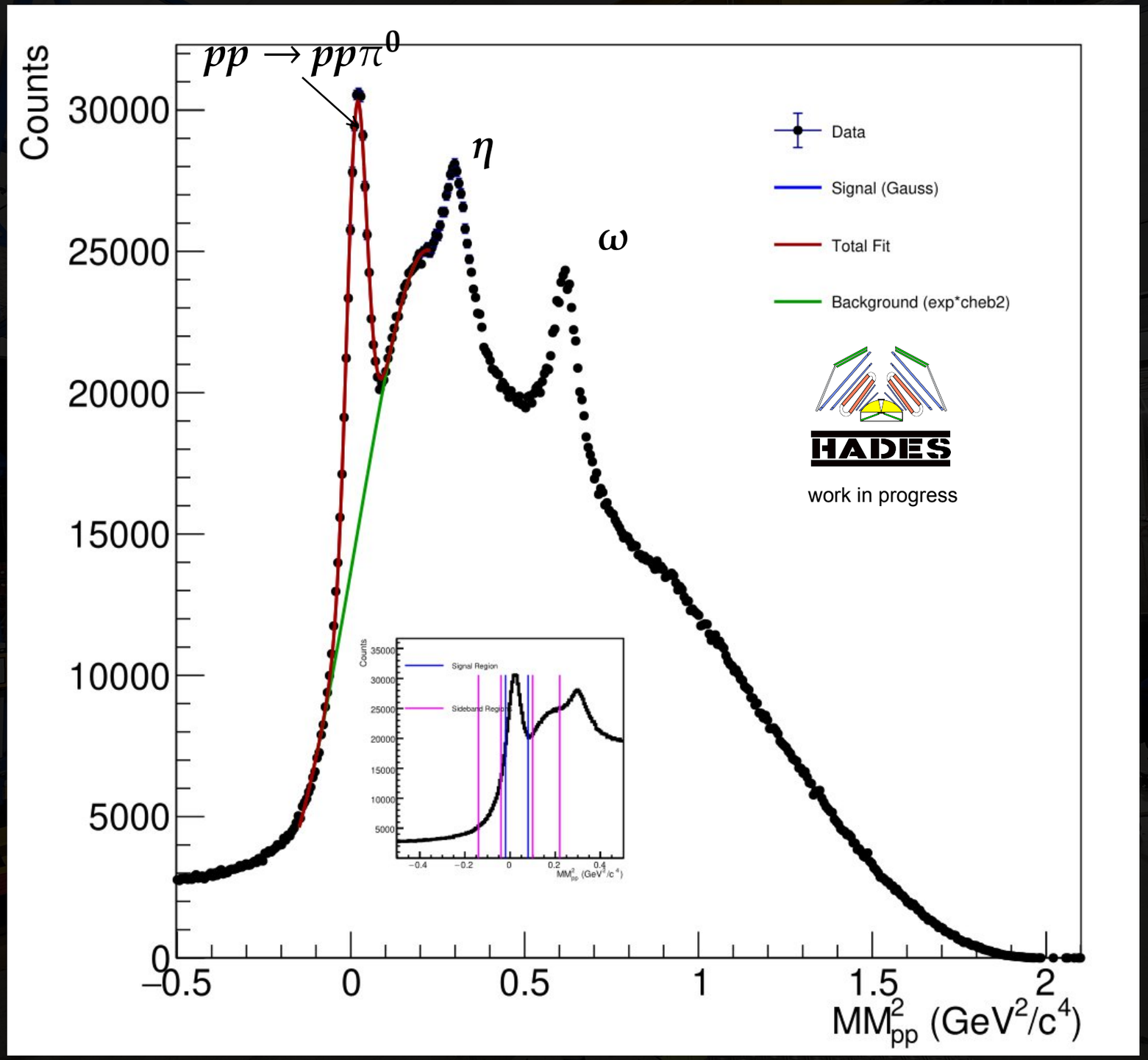

$pp\pi^0$ Dalitz Plot

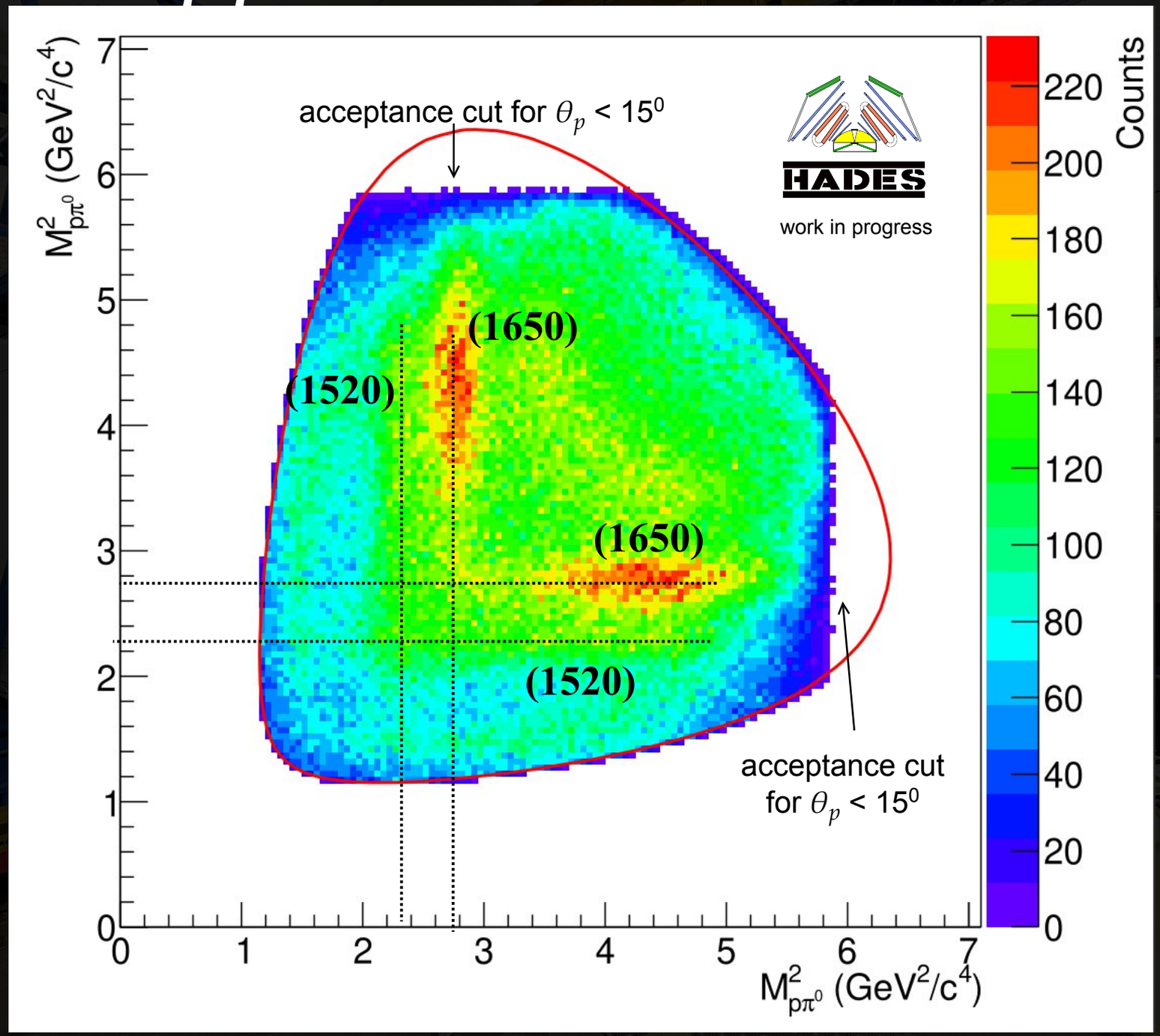

$pp\pi^0$ Dalitz Plot

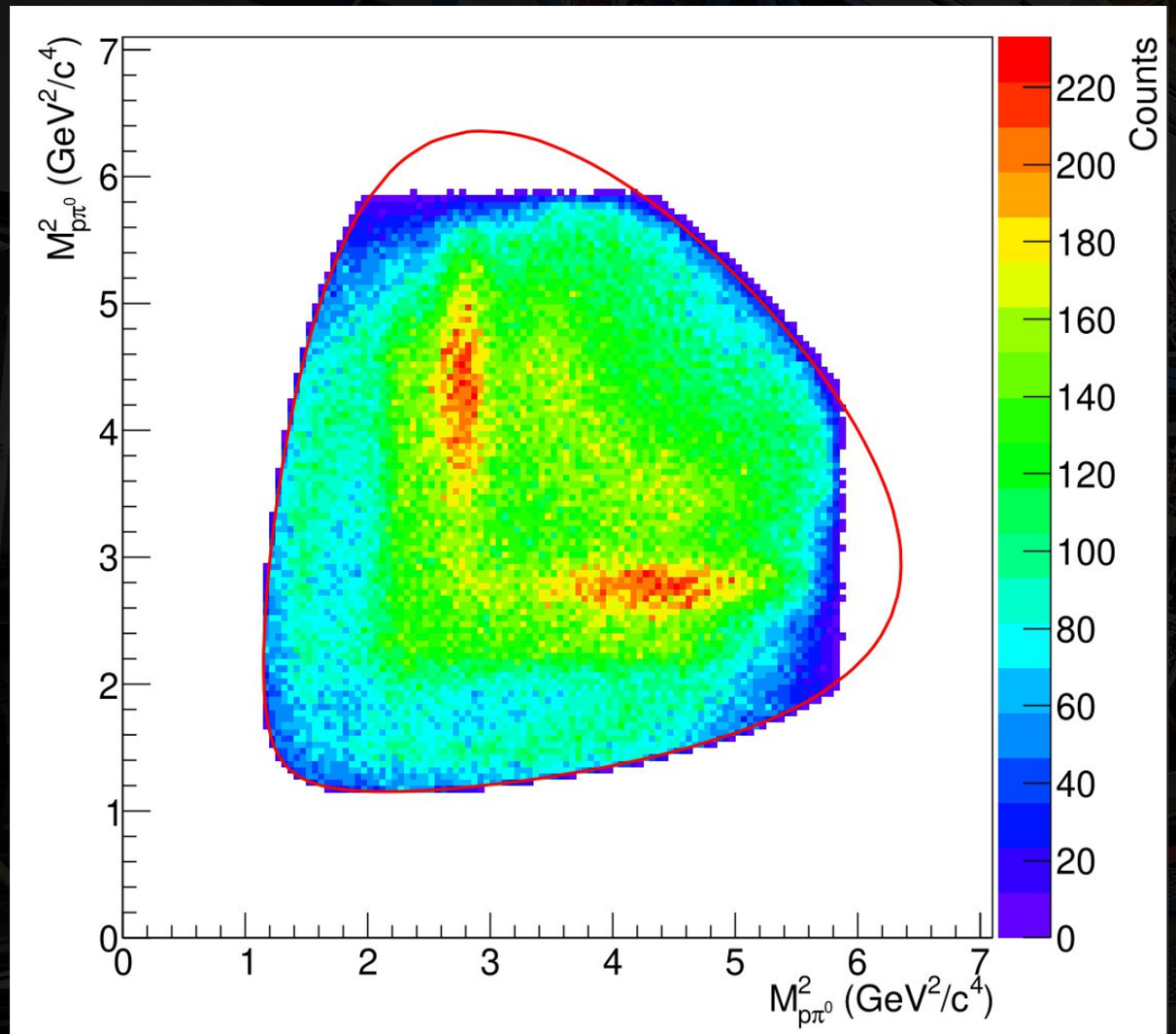

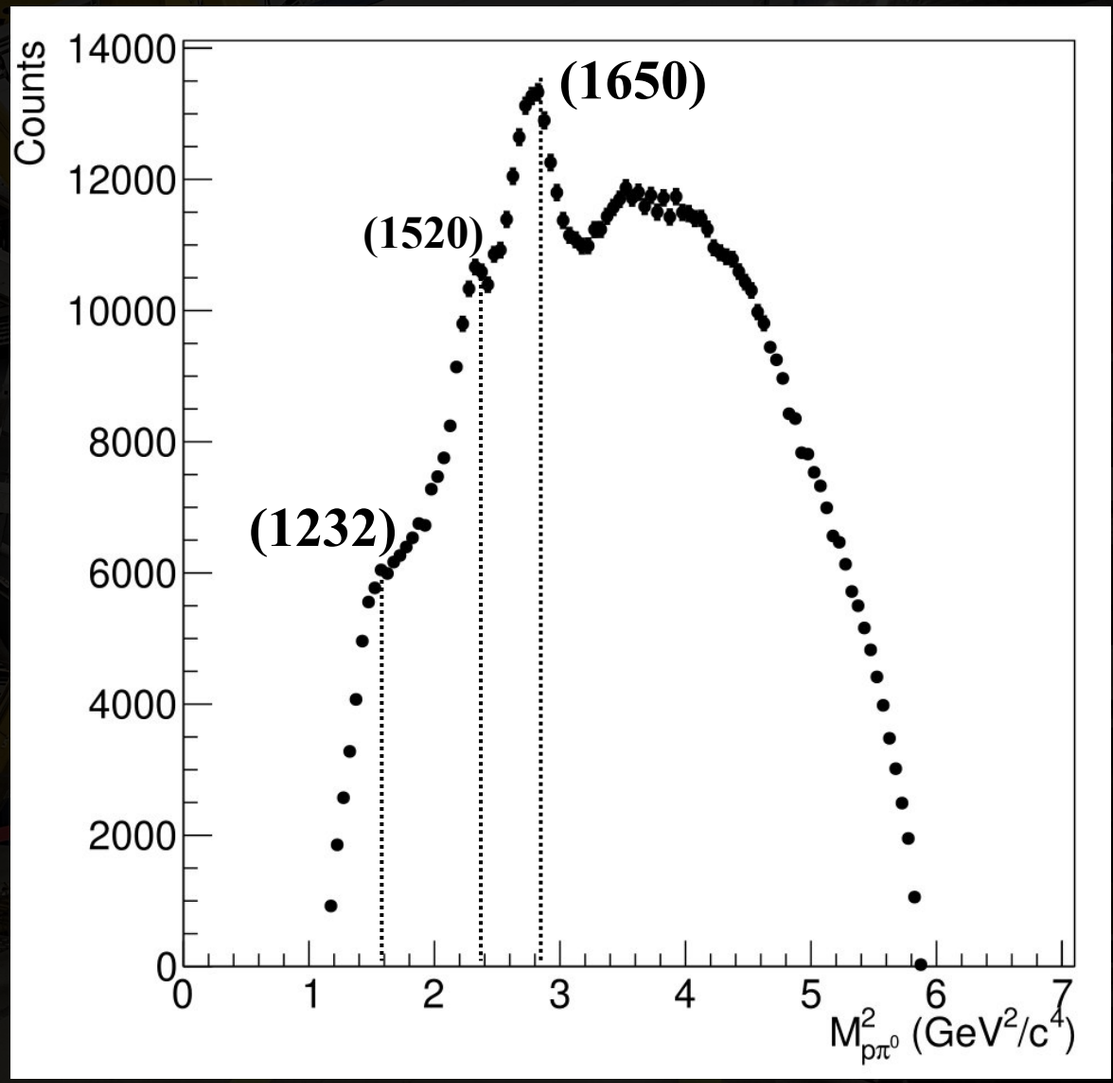

$\frac{\sigma(pp \rightarrow pn\pi^+)}{\sigma(pp \rightarrow pp\pi^0)}$

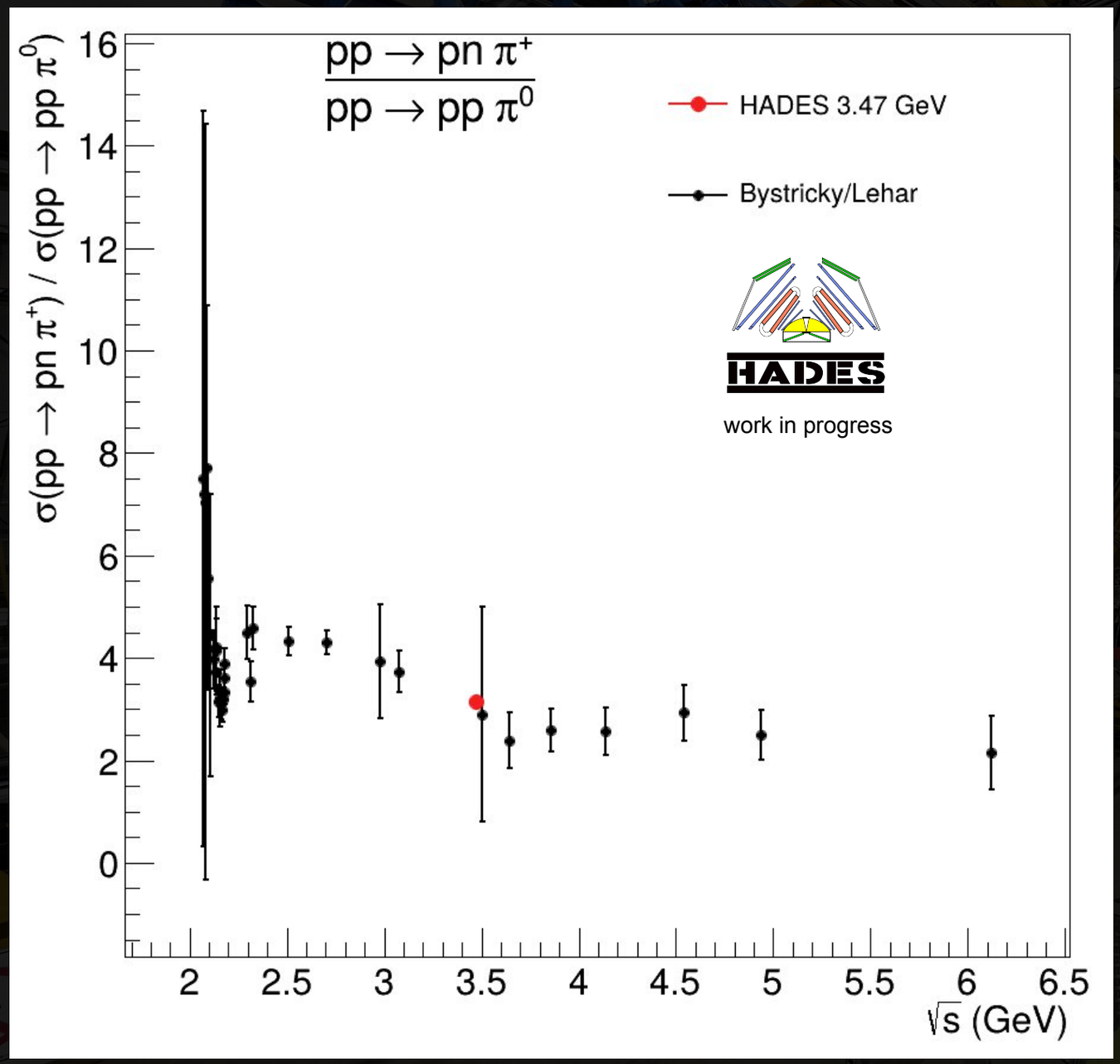

$$\frac{\sigma(pp \rightarrow pn\pi^+)}{\sigma(pp \rightarrow pp\pi^0)} = 3.14 \pm 0.005\ (stat)$$

The decreasing cross-section ratio reflects the transition from Δ(1232)-dominated pion production to increasing contributions from higher-mass baryon resonances.

Missing Mass Resolution

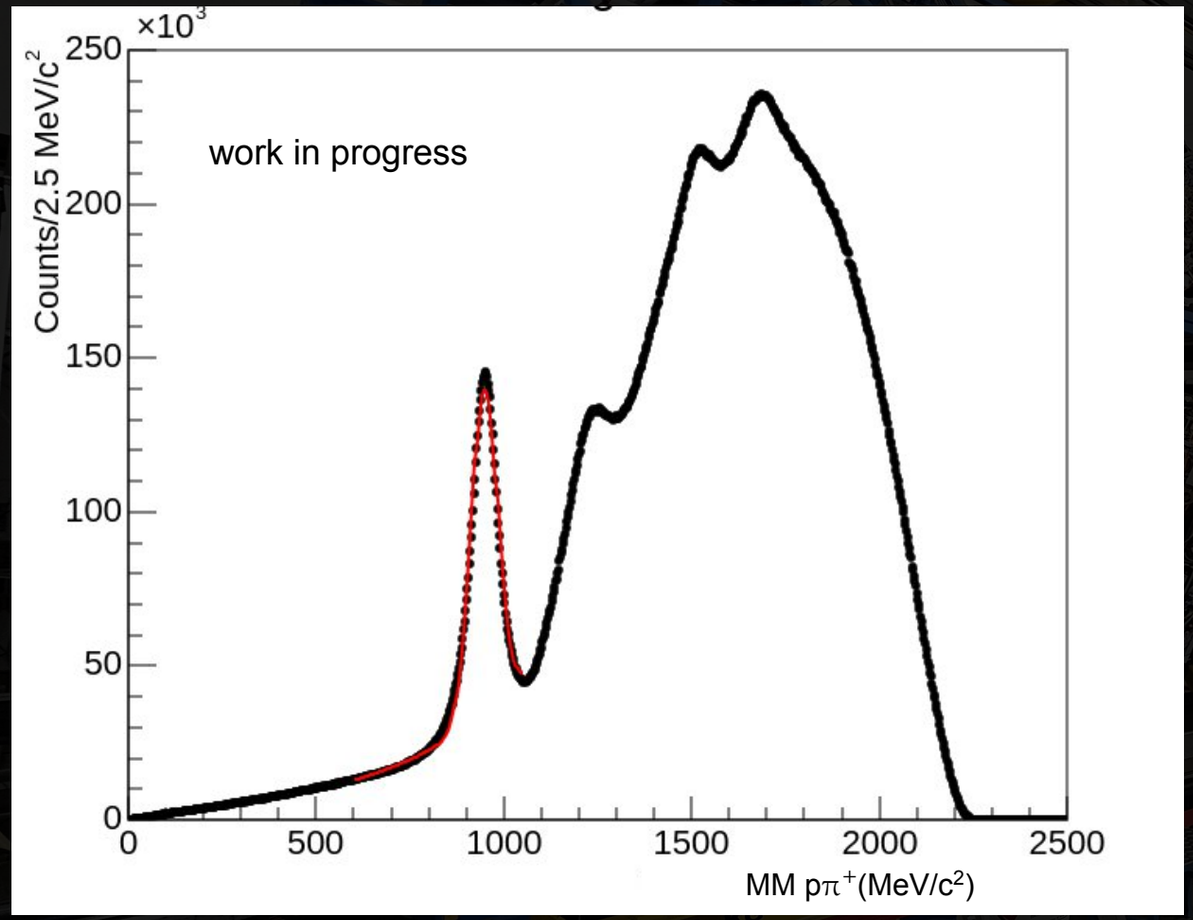

Neutron Peak Resolution ~ 35 MeV/c^2

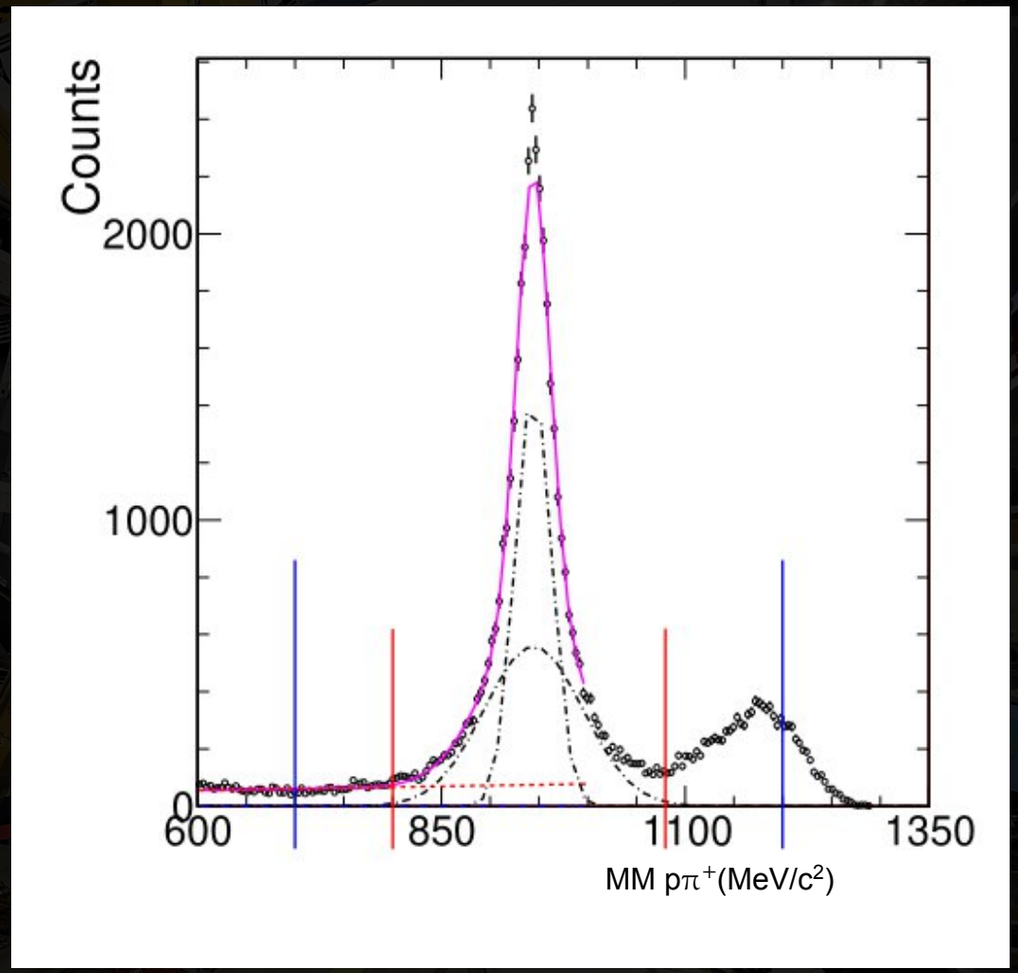

pp at T = 1.25 GeV
T. Liu, PhD Thesis 2010.

Neutron Peak Resolution ~ 12 MeV/c^2

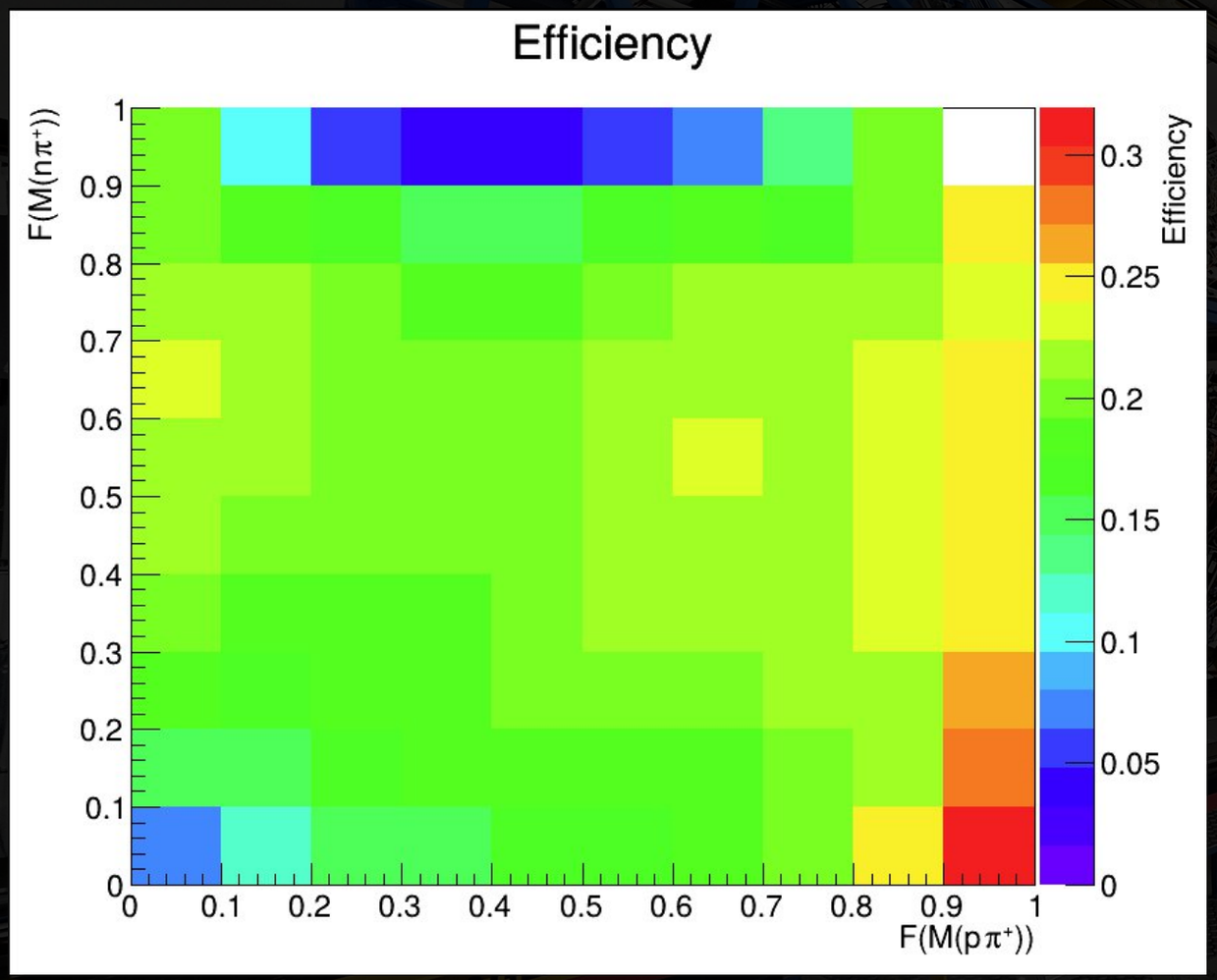
Efficiency
F(M(nπ⁺))
1
0.9
0.8
0.7
0.6
0.5
0.4
0.3
0.2
0.1
0
0
0.1
0.2
0.3
0.4
0.5
0.6
0.7
0.8
0.9
1
F(M(pπ⁺))
Efficiency
0.3
0.25
0.2
0.15
0.1
0.05
0

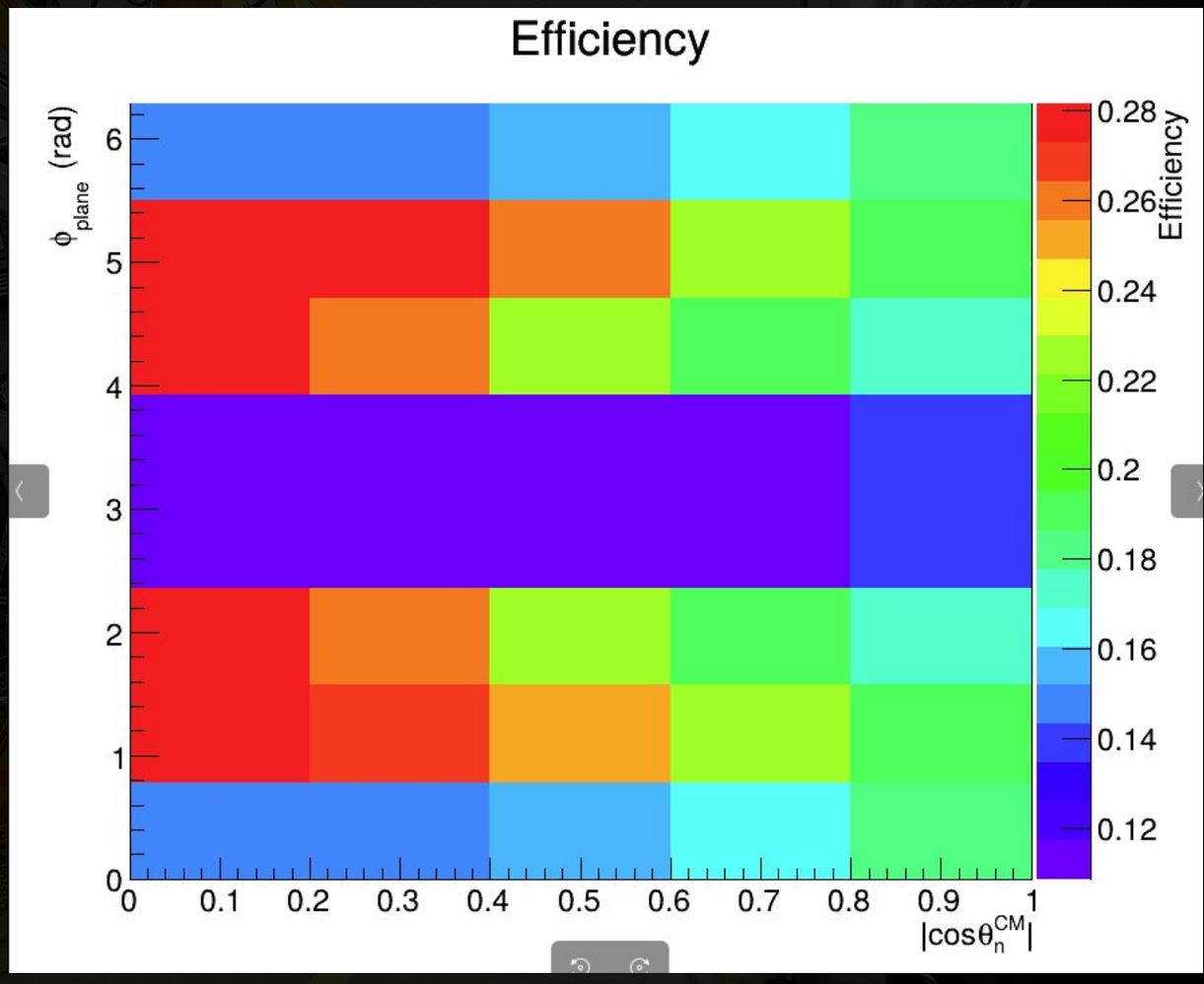
Efficiency
ϕ_{plane} (rad)
6
5
4
3
2
1
0
0
0.1
0.2
0.3
0.4
0.5
0.6
0.7
0.8
0.9
1
$|\cos\theta_n^{CM}|$
Efficiency
0.28
0.26
0.24
0.22
0.2
0.18
0.16
0.14
0.12

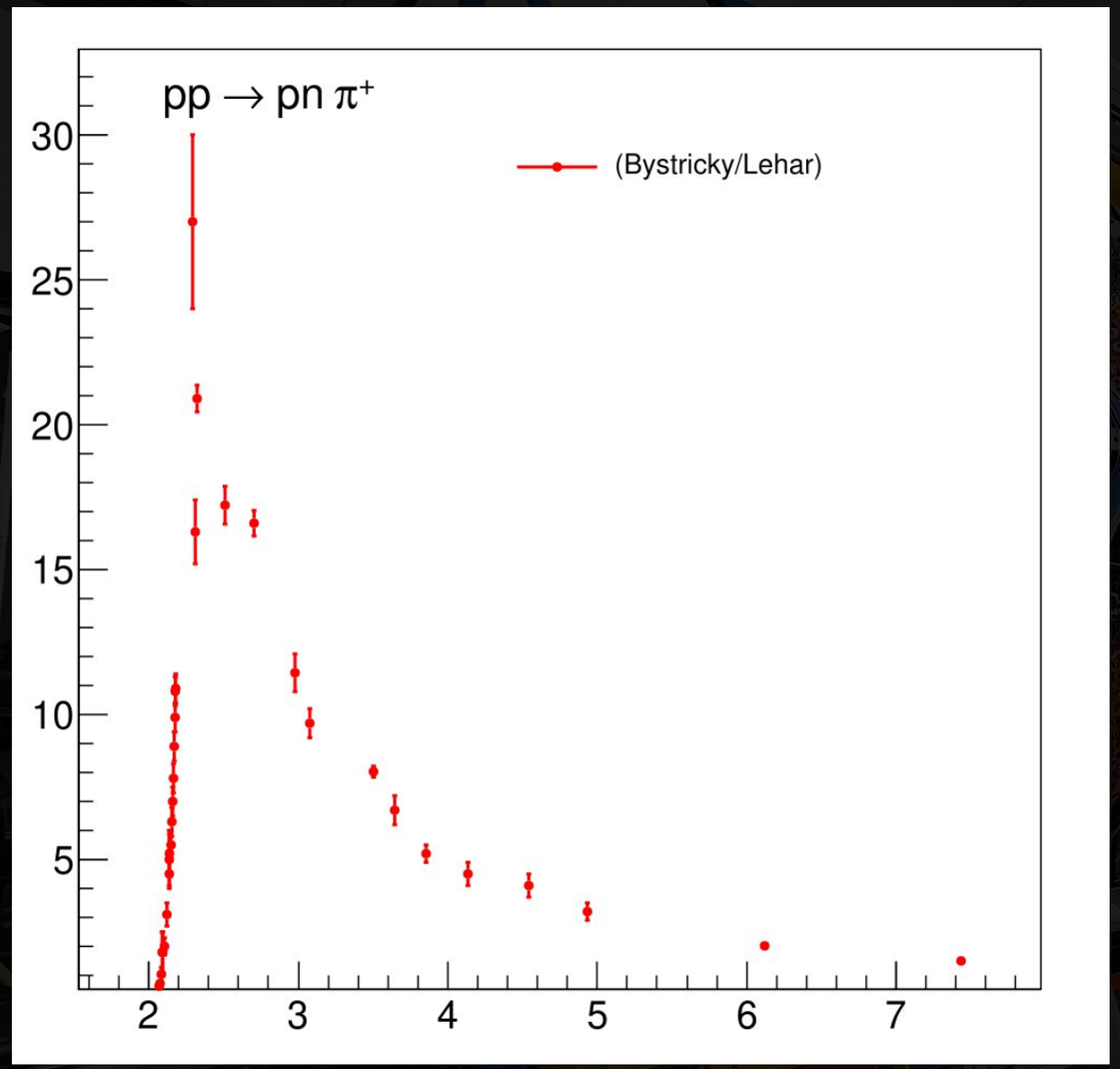
pp → pn π+
(Bystricky/Lehar)
30
25
20
15
10
5
2
3
4
5
6
7

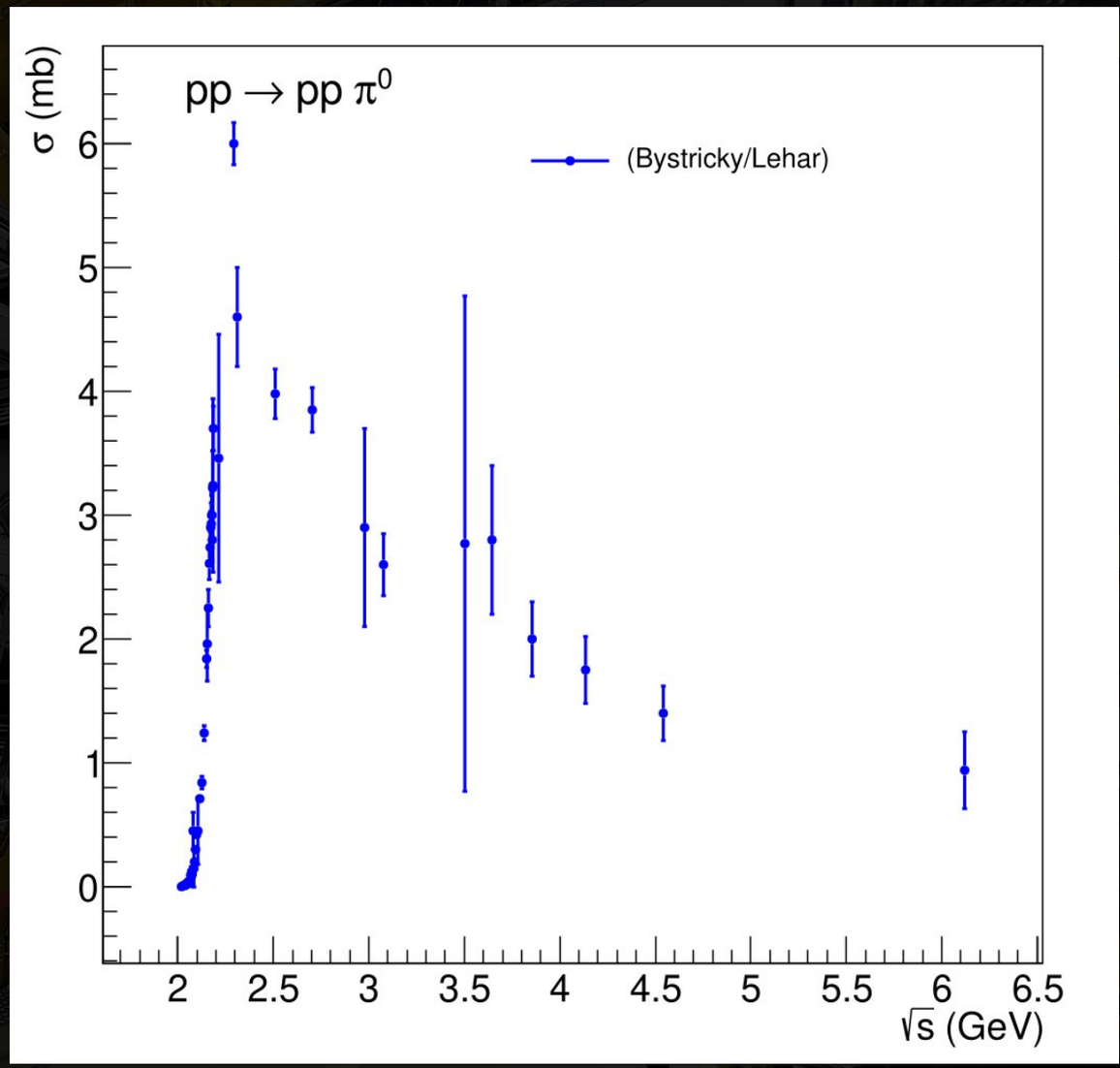
pp → pp π0
(Bystricky/Lehar)
σ (mb)
6
5
4
3
2
1
0
2
2.5
3
3.5
4
4.5
5
5.5
6
6.5
√s (GeV)

$M^2_{p\pi^+}$ vs t_2

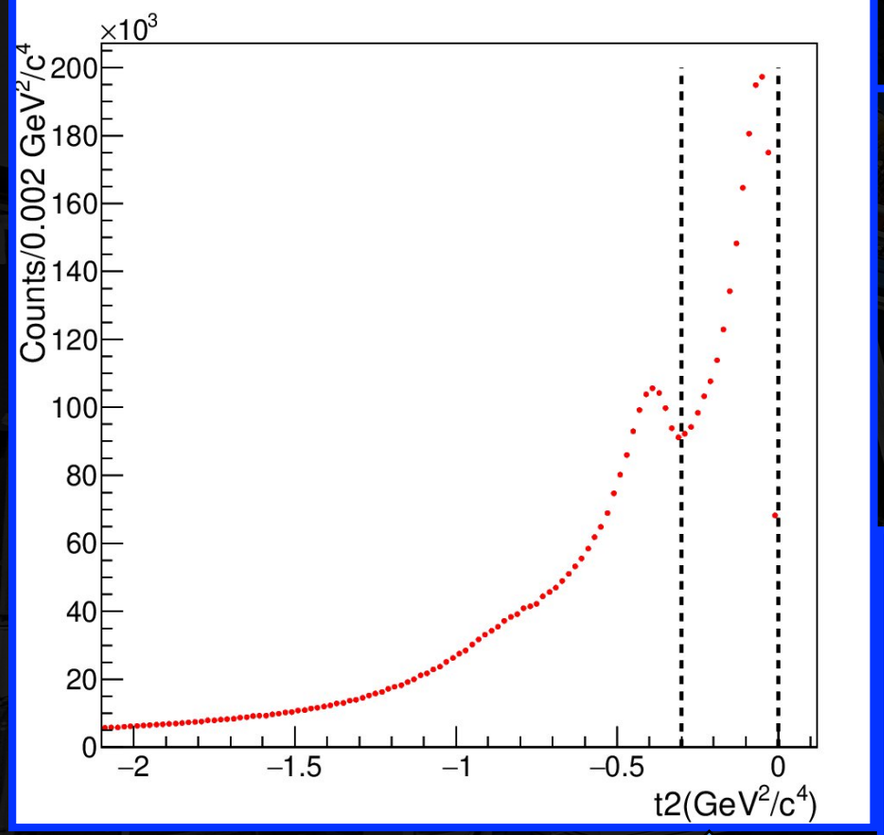

Y projection

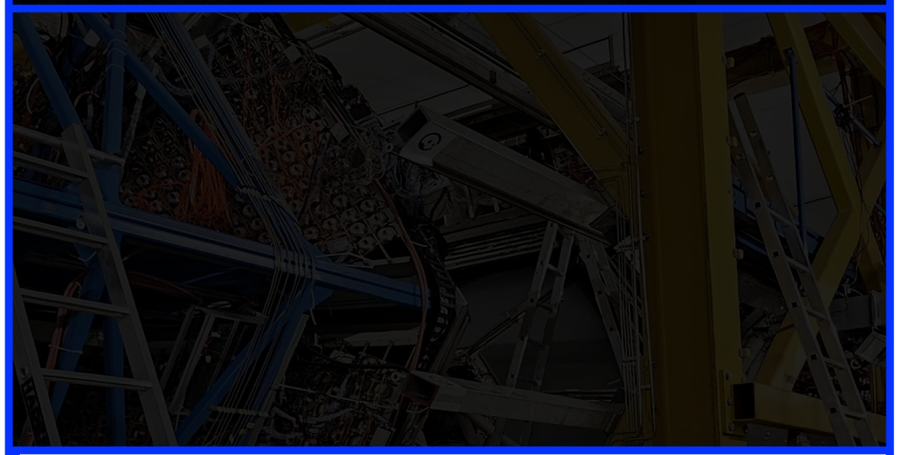

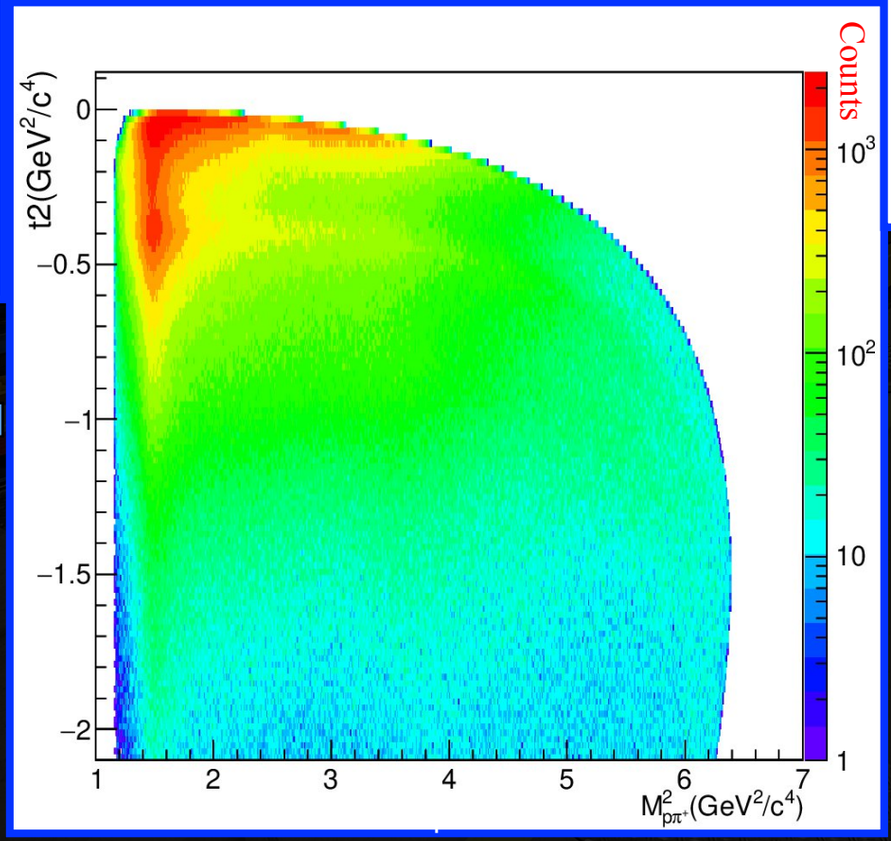

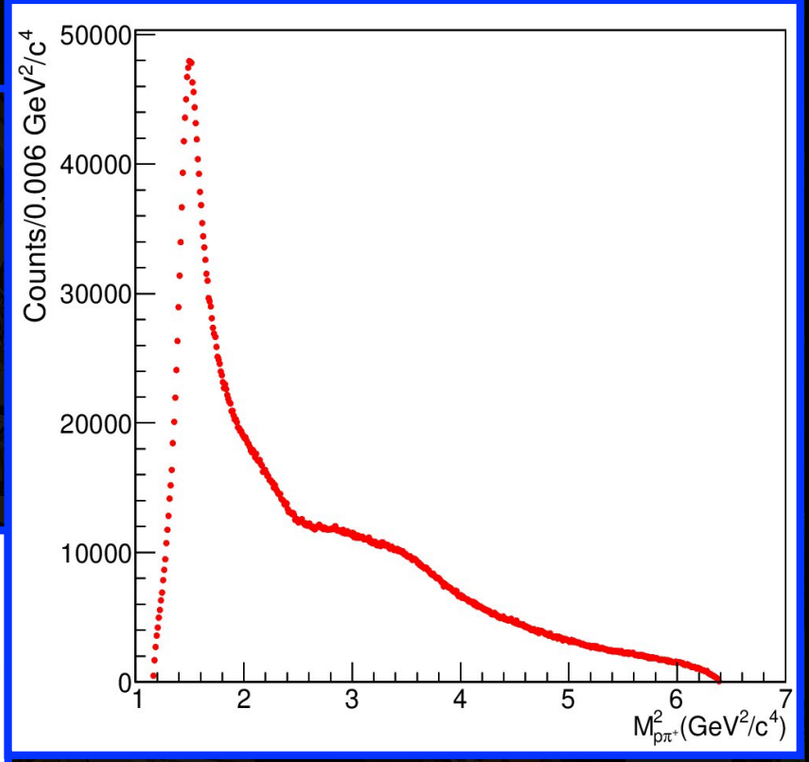

X projection